50272-101

PB92176924

REPORT DOCUMENTATION PAGE	1. REPORT NO.	2.

4. Title and Subtitle

Acoustic Emission Monitoring of Dump Points

5. Report Date
04-10-92

6.

7. Author(s)
Jeffrey A. Aldinger

8. Performing Organization Rept. No.

9. Performing Organization Name and Address
Twin Cities Research Center
5629 Minnehaha Avenue South
Minneapolis, MN 55417-3099

10. Project/Task/Work Unit No.

11. Contract(C) or Grant(G) No.
(C)
(G)

12. Sponsoring Organization Name and Address

Bureau of Mines
U.S. Department of the Interior
Washington, DC 20241

13. Type of Report & Period Covered

14.

15. Supplementary Notes

16. Abstract (Limit: 200 words) The U.S. Bureau of Mines investigated the feasibility of acoustic emission monitoring as a means of determining the stability of dump points at mine stockpiles and waste dumps. The goal was to devise a dump point stability monitoring methodology using inexpensive hardware and simple, straightforward analytical procedures. A small scale test facility was constructed for testing model dump points, with loading provided by a caster mounted on a shaft which moved both vertically and horizontally. The acoustic emissions generated in the soil were picked up by piezoelectric accelerometers. The acceleration data were analyzed for amplitudes, ring-down count rates, energy rates and frequency spectra. Stationary load tests were conducted on stable and unstable slopes. The results of dynamic load tests simulating a truck backing to the slope edge were dependent on waveguide location. Most of the waves detected by the transducers originated from tire and soil surface interaction. Since that noise could not be differentiated from slope instability, the goal of this study was not achieved. Although beyond the scope of this study, the use of more extensive instrumentation and signal processing may enable differentiation of acoustic emissions caused by tires versus slopes, thereby permitting unstable slope identification.

17. Document Analysis a. Descriptors

b. Identifiers/Open-Ended Terms

acoustic emission monitoring
mine dump points
slope stability
surface mining

c. COSATI Field/Group 08/09, 08/10

18. Availability Statement

Unlimited release by NTIS

19. Security Class (This Report)
unclassified

21. No. of Pages
79

20. Security Class (This Page)
unclassified

22. Price

FINAL

Open File Report

Acoustic Emission Monitoring of Dump Points

Jeffrey A. Aldinger
Mining Engineer
U. S. Bureau of Mines
Twin Cities Research Center

CONTENTS

ILLUSTRATIONS

ILLUSTRATIONS-Continued

ILLUSTRATIONS-Continued

TABLES

UNIT OF MEASURE ABBREVIATIONS USED IN THIS REPORT

c/min	counts per minute
c/s	counts per second
°C	degree Celsius
dB	decibel
dB/ft	decibel per foot
ft	foot
g	acceleration due to gravity
Hz	hertz (cycles per second)
hr	hour
in	inch
in^2	square inch
in^3	cubic inch
kHz	kilohertz
lb	pound
min	minute
mm	millimeter
ms	millisecond
mV	millivolt
pct	percent
psig	pound per square inch, gauge
s	second
t	ton
t/ft^2	ton per square foot
V	volt
V^2/Hz	square volt per hertz
V^2/s	square volt per second

ACOUSTIC EMISSION MONITORING OF DUMP POINTS

By Jeffrey A. Aldinger[1]

ABSTRACT

The U. S. Bureau of Mines investigated the feasibility of acoustic emission monitoring as a means of determining the stability of dump points at mine stockpiles and waste dumps. The goal of this study was to devise a dump point stability monitoring methodology using inexpensive hardware components and simple, straightforward analytical procedures. A small scale test facility was constructed for testing model dump points made of a sand and gravel mixture. Loading was provided by a rubber tired caster mounted on a shaft which moved both vertically and horizontally by hydraulic cylinders. The acoustic emissions generated in the soil were picked up by piezoelectric accelerometers and the output signals saved with a digital waveform recorder.

The acceleration data was analyzed for amplitudes, ring-down count rates, energy rates and frequency spectra. Stationary load tests were conducted near the slope edge (an unstable loading) and on stable soil away from the edge. The results of dynamic load tests simulating a truck backing to the slope edge were dependent on waveguide location. Most of the waves detected by the transducers appear to have originated from tire and soil surface interaction and not the instability of the slope. Since noise from tire and soil surface interaction could not be differentiated from slope instability, the goal of this study was not achieved. Although beyond the scope of this study, the use of a more extensive instrumentation network and more elaborate signal processing protocols may enable differentiation of acoustic emissions caused by tires versus slopes, thereby permitting identification of unstable slopes by this method.

[1]Mining Engineer, Twin Cities Research Center, U.S. Bureau of Mines, Minneapolis, MN.

INTRODUCTION

The U.S. Bureau of Mines investigated the use of acoustic emissions as a method to monitor dump point stability on mine stockpiles and waste dumps. This project was part of a research program aimed at reducing dump point accidents involving mobile mining equipment. The potential for accidents near mine dump points exists because the mobile equipment is operating near the edge of slopes. Stockpiles and waste dumps are typically unstable because they are constructed of unconsolidated material, are constantly changing with the addition or removal of material, and are subject to weather changes (*1*)[2].

From 1983 to 1987, an average of 20.6 dump point accidents per year were reported in the coal and metal/nonmetal surface mining industries (*2*). About 80 pct of the accidents involved haulage trucks. Although these accidents are infrequent, they are severe and result in numerous injuries and fatalities. Dump point accidents are fatal 10.7 pct of the time, compared to only 0.6 pct of the time for non-mobile equipment accidents (*2*). Dump point accidents result in an average of 67 lost work days, compared to 37 lost work days for all other surface, mobile mining equipment related accidents (*2*). The stability of the dump point is a major factor in many of these accidents. Slope failure was the primary or contributing cause in 58 pct of the dump point accidents (*2*).

Acoustic emission (AE) monitoring was first studied in the late 1930's by two Bureau of Mines researchers, Obert and Duvall (*3,4*). They discovered that stressed rock pillars in deep hard rock mines emitted micro-level sounds. Much research has been done since then on rock samples in the laboratory and in situ testing in both surface and underground mines. Numerous mines are now using AE (sometimes called microseismic activity) monitoring, mostly on a developmental basis, to locate unstable or overstressed rock (*5,6*). The results are used to locate mine areas that should be closed off or to take preventative measures to strengthen an underground opening or stabilize a slope.

The first reported field work on AE monitoring of slope stability in soils was published by Beard in 1961 (*7*). In 1967, Cadman and Goodman published the first report on a laboratory study of AE in soils (*8*). They studied landslide noises by tilting a small model slope until failure occurred. Detailed studies of the AE properties of soils were begun in 1972 at Drexel University (*9*). Most AE studies in soils have concentrated on the stability of dams and embankments. These studies have shown a correlation between the AE activity rate and the stability of a slope with a known background noise rate. The focus in these studies has been the long term stability of statically loaded slopes or slopes with no external load. This report presents research on dynamically loaded slopes, as encountered on mine stockpiles and waste dumps.

The origin of AE activity is not completely understood, but it is believed to be related to the release of strain energy occurring during the deformation and failure of materials (*10,11*). Acoustic emissions

[2]Italic numbers in parentheses refer to items in the list of references preceding the appendix at the end of this report.

generated in soils are probably related mostly to the shear strength components within the soil, such as sliding and rolling friction, degradation, dilation and perhaps some cohesion (*12*). This strain energy is released in the form of an elastic wave, which radiates out from the source and can be detected by AE monitoring equipment.

Testing for this research was done predominantly on small scale models in the laboratory. Previous experience has shown that full scale testing is expensive, time consuming and difficult to control. The purpose of these tests was to determine whether AE monitoring could be used to determine the stability of mine stockpiles and waste dumps. The knowledge gained could then be used by mine operators to alert the equipment operators of unsafe conditions, thereby reducing the number of dump point accidents occurring in the field.

BACKGROUND ON ACOUSTIC EMISSION MONITORING SYSTEMS

The elastic strain waves emanating from a soil undergoing deformation can be detected with an accelerometer, velocity transducer, microphone, or pressure transducer. Piezoelectric accelerometers are preferred in soils because of their sensitivity and generally flat frequency response. The frequencies emitted by most types of soils vary from about 250 Hz to 8,000 Hz (*13,14*). Both granular and cohesive soils produce AE, but granular soils are more emissive (*13*).

Acoustic Emission waves are attenuated quite rapidly through soil. The amount of attenuation is dependent on the frequency, the soil, and the distance between the AE source and the transducer. Attenuation through soil and mine wastes ranges from 1 dB/ft to 200 dB/ft (*12,15*). Thus, the accelerometer must be near the AE source or the AE wave transmitted to the transducer through a medium which has less attenuation. Because it is inconvenient and expensive to bury accelerometers in the soil near the anticipated or potential failure zone, AE waves are normally transmitted to the accelerometer through a metal rod or waveguide. The attenuation of elastic waves through a steel rod is three to four orders of magnitude less than through soil (*12*). Acoustic emissions can be transmitted through a steel wave guide without serious degradation of the wave, when compared to the soil alone (*16*). Burying a steel rod in soil increases the attenuation through the rod, but the attenuation is still significantly less than through the soil alone (*16*). In addition, a waveguide buried in the ground provides a volume of soil sensitive to AE pickup that is 30 times larger than an accelerometer on the surface with no waveguide (*16*). Waveguides are typically pushed into the soil with an accelerometer attached to the exposed end. The closer the waveguides can be placed to the zone of AE generation in the soil, the better the accelerometer signals will be.

A preamplifier is needed to amplify the millivolt signals generated by the accelerometer and is often an integral part of the accelerometer. A coaxial cable is used to transmit the signals to a location where the data can be processed and analyzed. In field testing the cables may be hundreds of meters long. Band pass filters are commonly used to eliminate the low and high frequency noises from the data. The signal is then amplified to a level at which it can be recorded for future analysis or sent to a counter or oscilloscope for immediate analysis.

Placing the amplifier behind the filters is preferred, because this further increases the signal level for later processing (*9*).

Acoustic emission field data is typically recorded on magnetic tape. The tape is played back in the laboratory through a counter to obtain the total AE event counts or ring-down counts exceeding a chosen voltage threshold. Cumulative ring-down counts or count rates are the most commonly used methods to quantify the data. Other methods of analysis include the determination of frequency, amplitude, pulse rise time, pulse length, energy, signal to noise ratio, and signal source location.

EQUIPMENT AND MATERIALS

SMALL SCALE MODELING

A small scale model of a dump point was constructed to provide an inexpensive and controllable environment in which to perform the AE testing. The slope loading system was designed to simulate the rear wheels of a dump truck backing up to the edge of a dump point. The slope and load system were not designed to be a precise scale down of an actual dump point, but to be a convenient place to begin learning the fundamental relationships between slope stability and AE response.

Soil

The soil used in the small scale dump point tests was a brown, predominately sand and gravel mixture. Bentonite clay was added to the sand and gravel mixture to give the soil some cohesion. The cohesion in the soil allowed the soil to support a larger load, which produced more dramatic slope failures in the small scale testing. Less than one pct of this material was silt or clay sized particles (fig. 1). About 27 pct of the material was gravel, i.e., greater than 2-mm particle diameter. The coefficient of uniformity, d_{60}/d_{10}, was 4.9, where d_{60} and d_{10} are the particle sizes at which 60 pct and 10 pct, respectively, of the sample was finer (*17*). This indicates that the soil was a well graded sand and gravel mixture. The angle of repose was about 35 degrees when the material was dry. This material was used because its range of grain sizes and subangular grains produced significant AE (*18,19*). A poorly graded white sand was found to produce AE amplitudes twelve times smaller than the well graded gravel/sand/clay mixture.

Sand Box and Load System

A 2-ft by 2-ft by 3-ft plywood box, with one glass side, was built to contain the soil during testing (see fig. 2). This box and the load frame were placed on a 65-in by 73-in by 0.75-in plywood base, which was isolated from the floor by rubber and felt matting. Soil loading was provided by two-way hydraulic cylinders, one 2.5-in bore by 6-in stroke cylinder pushing downward and one 2-in bore by 12-in stroke cylinder providing the horizontal movement. The vertical cylinder was mounted on a carriage, which was pushed by the horizontal cylinder along a pair of parallel horizontal shafts and linear bearings (fig. 3). A vertical linear bearing mounted below the carriage provided a guide for the shaft

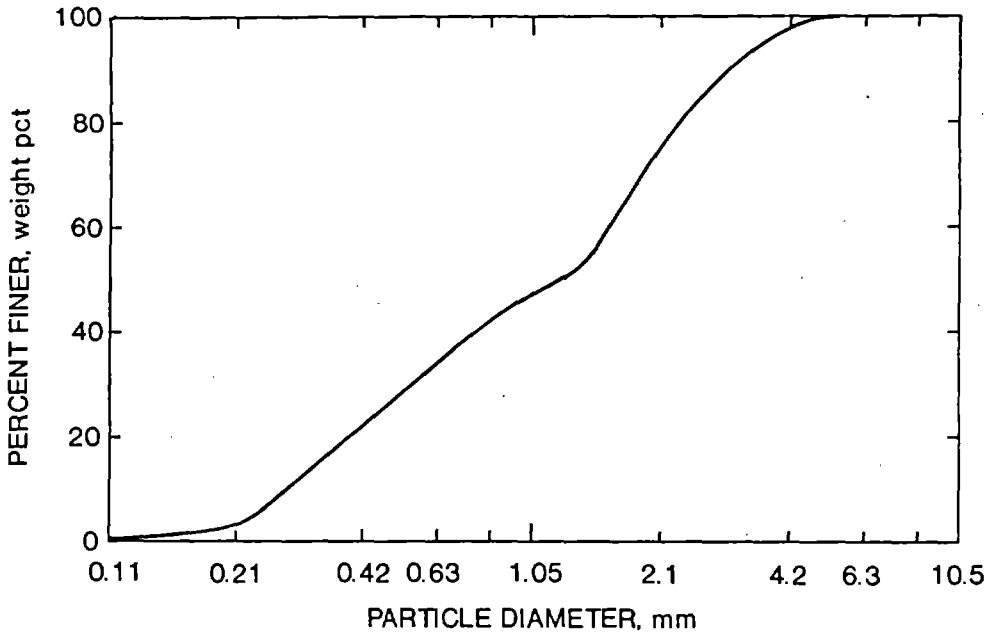

Figure 1.--Grain size distribution of soil used in small scale modeling.

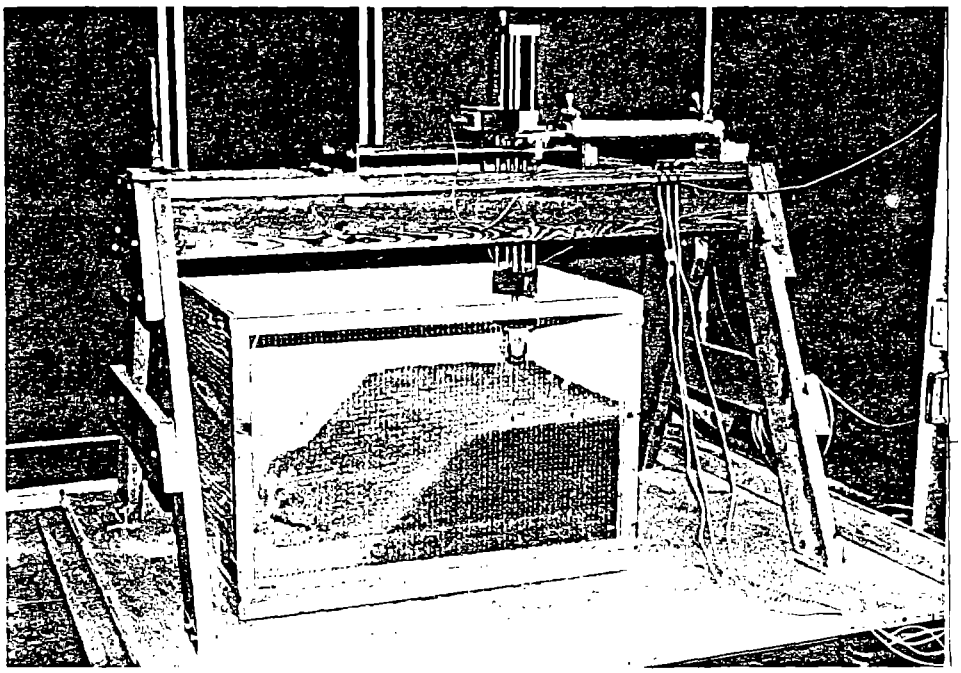

Figure 2.--Small scale test box and load frame.

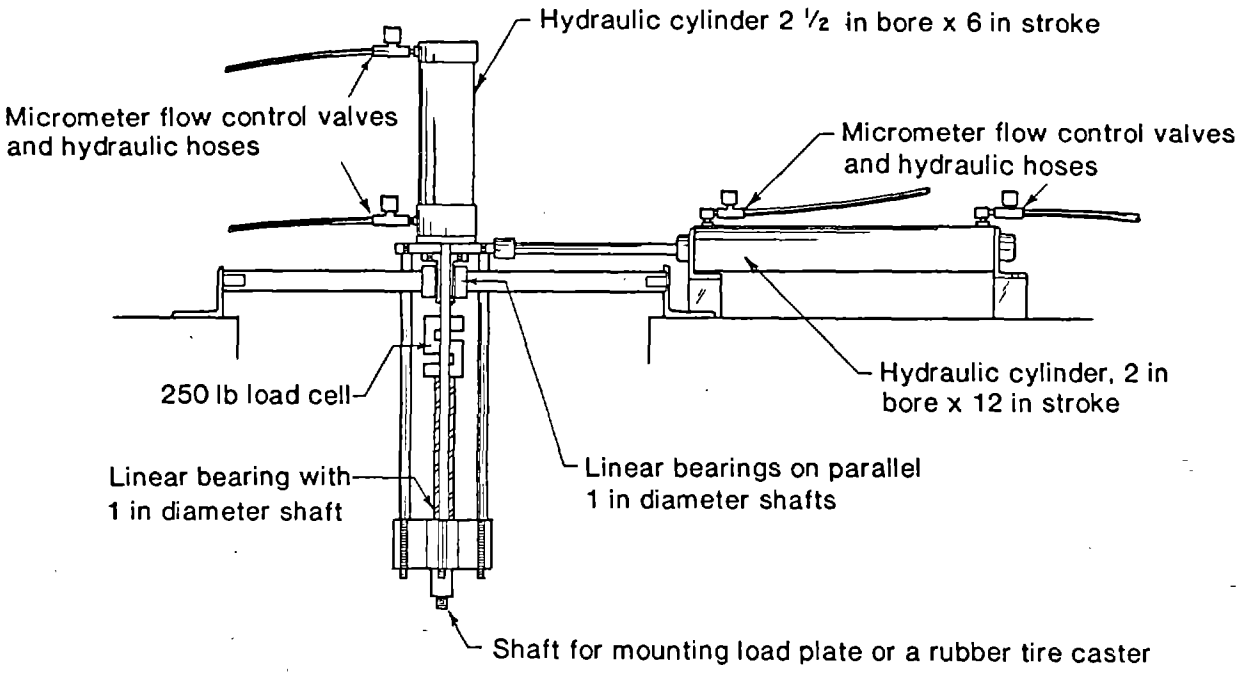

Figure 3.--Schematic diagram of hydraulic load system.

extending from the vertical cylinder. The end of the vertical shaft pushed on the soil with either a flat load plate (4 in^2 or 9 in^2) or a solid rubber wheel simulating a truck tire (fig. 4). The tires were casters, either single (1.3-in wide, 3.5-in dia.) or dual (1.8-in wide, 2.5-in dia.) wheeled. The dual wheel caster was used for the majority of the tests. The load system was mounted above the sand box on a large wooden sawhorse-like frame (37-in high, 63-in long). A slot cut in the top of the sawhorse allowed clearance for the vertical cylinder to pass through and the horizontal cylinder to push sideways. The frame was moved by hand to position the load inside the box. C-clamps held the sawhorse to the base during a test to prevent the frame from moving.

The cylinders providing the load were hydraulic, but powered by compressed air. A compressed air source of 80 psig was filtered and regulated before going to a 45-in^3 air-over-oil reservoir. Air entered the top of the reservoir while oil flowed out the bottom. Each hydraulic cylinder required two reservoirs, one for the inlet and one for the outlet. The system had a maximum regulated pressure of about 65 psig, providing up to 250 lb of vertical force on the soil. Four-way pneumatic valves controlled the direction of the hydraulic cylinders.

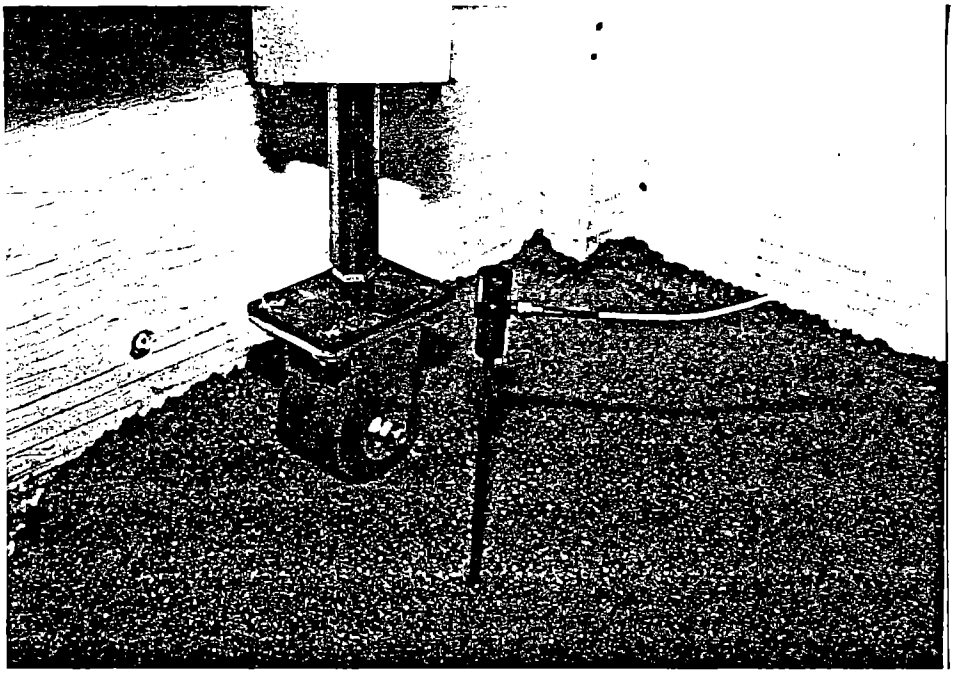

Figure 4.--Close up view of rubber tire caster and waveguide/ accelerometer.

An "S" type strain gauge load cell with a 250-lb capacity was mounted in the middle of the vertical load rod (fig. 3). Excitation and signal conditioning for the load cell were provided by three Action Instrument[3] modules. Output was read on a digital panel meter or could be output to the digital waveform recorder along with the accelerometer data. A Celesco cable displacement transducer with a 20-in stroke tracked the vertical movement of the load rod as load was applied. Action Instrument modules were used for signal conditioning, while excitation was provided by a Fluke model 382A voltage/current calibrator. Output was read on a digital panel meter mounted on the control panel along with the pneumatic controls.

Acoustic Emission Monitoring Equipment

High sensitivity accelerometers were needed to detect the weak AE waves generated by the soil. Acoustic emissions in the box were detected by Columbia model 306-H piezoelectric accelerometers with voltage sensitivities ranging from 105 to 112 peak mV per peak g. The frequency response was 0.2 Hz to 5000 Hz. The accelerometers were stud mounted on a 0.5-in diameter by 0.75-in long steel rod. A 0.2-in dia., 15-in long steel waveguide was screwed into the other end of the

[3]Reference to specific products does not imply endorsement by the U.S. Bureau of Mines.

mounting cylinder (see fig. 4). All threaded connections were coated with a thin layer of high vacuum, stop cock grease to act as a couplant (*20*). A 10-ft long coaxial cable connected the accelerometer to a Kistler model 5004 charge amplifier. The amplifiers had 6.8-kHz low pass filters and were set for 40 dB of amplification. Amplifier output was sent to an Ithaco model 4212 electronic band pass filter, which was usually set for 200-Hz high pass and 6300-Hz low pass filtering. A maximum of three accelerometers were used at any one time.

Signal output from the accelerometer/amplifier/filter was captured on a DSP Technology Inc. digital waveform recorder mounted in a electronics rack (fig. 5). Data were saved to disk for future analysis and could be plotted for immediate viewing, such as shown in figure 6. DSP software was used to convert the data from DSP format to Asyst format and then transfer it to a floppy disk. Asystant data analysis software on an IBM or IBM compatible personal computer was used to perform time and frequency domain analysis of the data (*21*).

FIELD TESTING

Field testing was conducted to determine whether AE generated by haulage trucks on actual stockpiles and waste dumps were of sufficient amplitude to be detected. The same Columbia accelerometers used in the laboratory were used for field testing. The waveguide was a half inch diameter, two piece steel rod 80-in long, joined in the center by a threaded coupling. A 30-ft shielded coaxial cable connected the

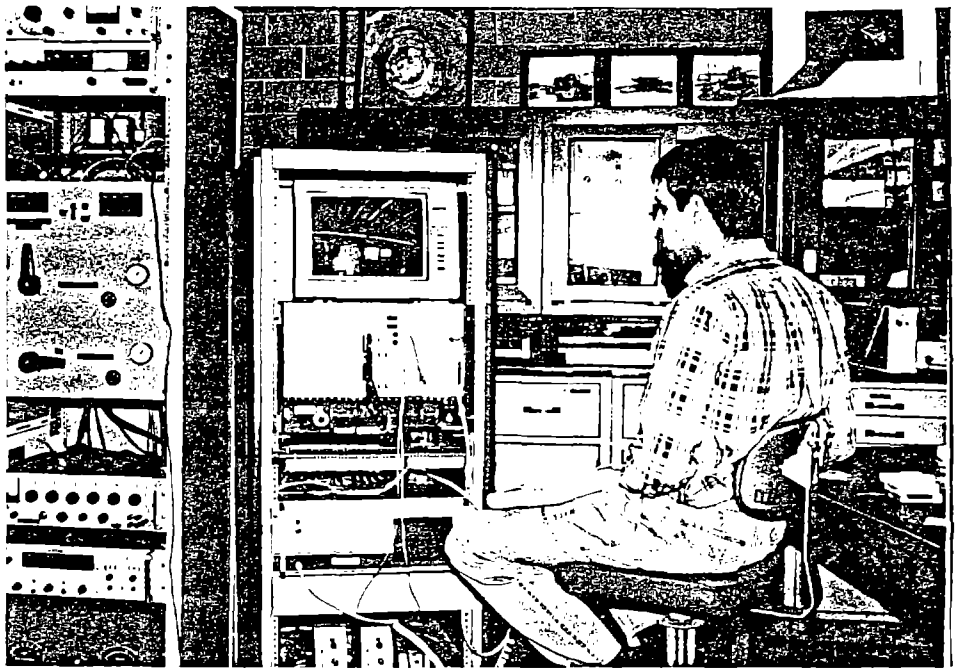

Figure 5.--Digital waveform recorder and computer.

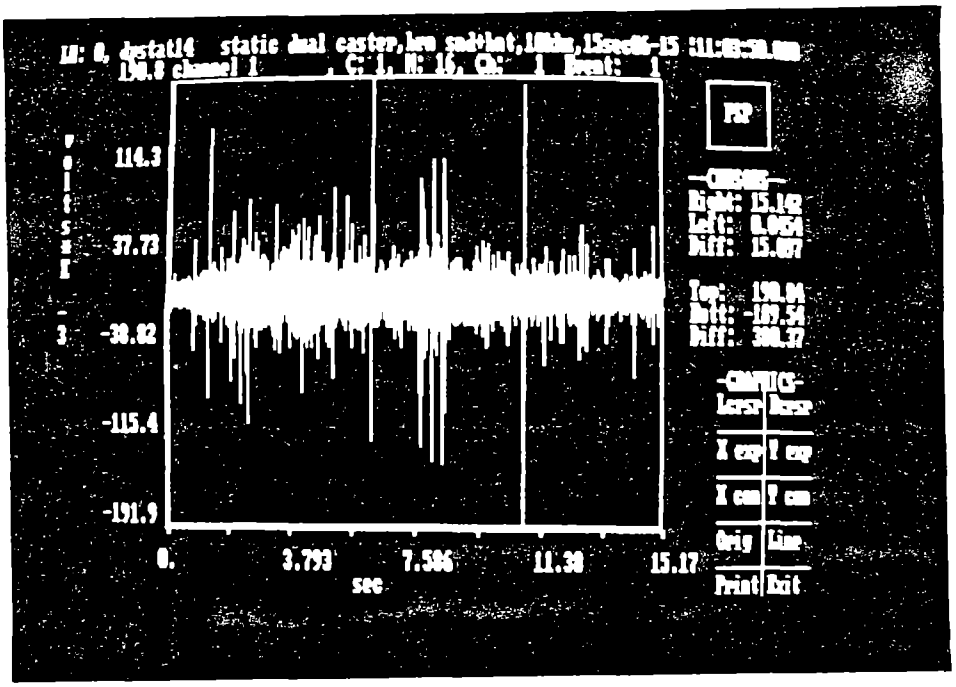

Figure 6.--Typical voltage versus time display from digital waveform recorder.

accelerometer to the amplifier. A battery powered Endevco model 2721A charge amplifier was used. Amplifier output was viewed on a Leader LBO-315 battery powered, portable oscilloscope.

Field testing was conducted at a limestone quarry in August 1989. This testing was done as an adjunct to a field trip to collect acceleration data on haulage trucks backing to the crests of stockpiles and waste dumps. The test area was a stockpile of crushed limestone, which was washed and screened to minus 1 in. The stockpile was about 16-ft tall and had an angle of repose of about 34 degrees. Caterpillar and Euclid 35-t rear dump haulage trucks were dumping crushed stone over the edge of the berm (fig. 7).

EXPERIMENTAL PROCEDURES

SMALL SCALE MODELING

The soil was prepared by adding water and mixing by hand until the soil began to stick together when balled up in hand (4 to 6 pct water). The box was normally about one third full of soil. Slopes were built up by successively adding and compacting layers of soil. Each fresh layer of soil was first troweled with a scrap 2 X 2 board to level and settle the soil. Compaction was done by hand with a tamping rod having a 5-in^2 steel plate on the end and also by slapping the 2 X 2 board on the surface to obtain a smooth surface. When the slope reached the desired height, a smooth and level surface was formed on top. The slope face was allowed to form at the natural angle of repose as the layers were

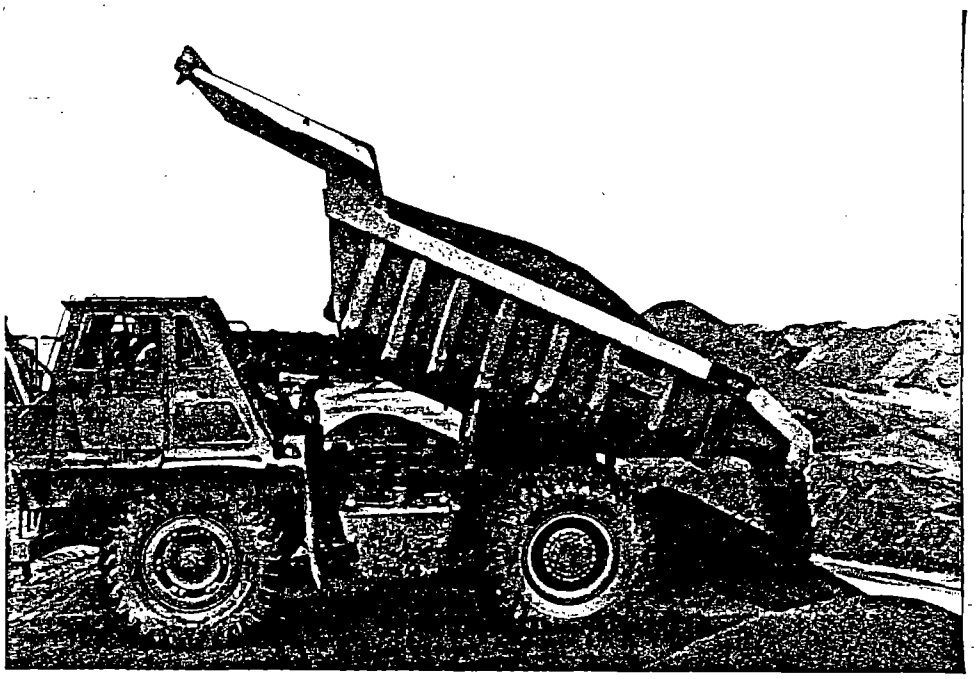

Figure 7.--Haulage truck dumping crushed stone over edge of dump point.

added. The slope was steepened past the angle of repose in some cases to create an unstable condition. Waveguides were pushed horizontally into the face of the slope or vertically into the top. Waveguides were placed at different distances and depths from the point of loading to determine the attenuation through the soil and to determine the best waveguide position. The waveguides were not placed down slope from the load, because soil falling on the waveguide and accelerometer would produce signals much greater than any AE generated within the soil.

The waveform recorder had four channels, but two or three channels were used during most tests to help conserve recorder memory. The recorder sampling rate was 10,000 points per second on each channel. A higher sampling rate consumed the waveform recorders' memory too fast, while a lower sampling frequency would produce aliasing (*22*). Sampling time varied from 4 s for stationary loads to 25 s for some dynamic loads. The largest sample that could be recorded was about 30 s.

After each test, the load frame and accelerometers/waveguides usually had to be repositioned. Up to nine stationary load tests and three dynamic load tests were run for each slope constructed. A penetrometer reading was taken for each slope with a Soiltest CL-700A pocket penetrometer. This compressive strength reading (t/ft^2) gave a relative measure of the degree of compaction of the slope. The moisture content of the soil was determined by sampling soil, weighing it, drying it overnight at 105° C and reweighing the sample.

Stationary Loading

Stationary loading refers to the procedure where the load pressure was gradually increased at a single, fixed point. Stationary load testing was conducted prior to the more complex dynamic load testing, where the moving tire creates significant noise. One way to apply the stationary load was with a flat plate. This was used only while the test procedures were being developed. In later testing, a single or dual wheel caster was mounted on the load rod, providing a more representative model of an actual dump point loading. This stationary load method was used for loadings less than 5 in from the crest of the slope (assumed an unstable loading) and loadings 12 to 15 in away from the crest (assumed stable). These load positions were used throughout this study to differentiate between a stable and an unstable slope.

The soil was preloaded with a small load, such as 10 lb, to reduce the shock loading of the soil. Without this preloading, the tire, suspended above the soil, would contact the soil surface as the tire began to move, thus creating a large amount of noise. The vertical hydraulic cylinder was engaged in the down position and the digital waveform recorder triggered to start the test. The vertical hydraulic cylinder control valve was left open so that the tire continued to move downward with increasing load until maximum pressure was reached. The air pressure regulator was set before the test to produce different loading rates and maximum loads. The higher the air pressure, the faster the load was applied to the soil and the higher the maximum load obtained. Most tests were conducted with the air pressure set at 40 or 45 psig, which provided the best slope failures. In addition, the exhaust flow from the vertical hydraulic cylinder was adjusted with a micrometer flow control valve to vary the load rate.

To better model an unstable slope, a series of tests were conducted with the toe of the slope removed (soil removed from the base of the slope). Removing the toe of a stockpile or waste dump is one of the most common causes of dump point accidents (*2*). This practice severely reduces the bearing capacity of the slope. In most of these tests, the toe of the slope was removed immediately prior to the start of data recording. The toe was removed one inch at a time by scraping the soil away with a metal plate. Then the test was conducted as described above for the other tests. The data recorder was usually turned on after removing the toe, because the disturbance created while removing the toe produced a large amount of noise and lengthened the test. This required a sample time greater than the data recorder's memory could handle. A couple of tests were conducted with the data recorder running during toe removal, resulting in limited data recorded after toe removal.

Dynamic Loading

The other type of loading was the dynamic load, in which the load wheel moved across the surface of the slope toward the crest. This load simulated a truck backing up to the edge of a dump point. A "constant" load was placed on the wheel by adjusting the air regulator (increasing the air pressure) before the test until the desired load was obtained. This load was determined from previous experience and by evaluating the

degree of compaction of the soil. The largest load that the soil would be able to support was usually chosen. The load did not actually stay constant, because of surface irregularities and the tire's tendency to plow into the soil when underway. Immediately before the test, the control valve for the vertical cylinder was placed in the downward "on" position and allowed to stabilize. Time zero for the test was when the horizontal cylinder and waveform recorder were triggered on.

The load wheel was typically started 10 to 15 in from the slope crest. As the wheel progressed towards the slope crest, the soil surface began to crack and eventually fail. As the slope failed, the wheel could not keep up with the moving soil block. Thus, in some tests the vertical cylinder pressure was increased manually as the slope began to fail. This was thought to be a better simulation of a truck falling over the edge of a slope, but also added a variable load into the test data. The dynamic load tests were video taped in the later stages of the research. Without a video tape, it was difficult to correlate the visual events with the AE data. A few dynamic load tests were run with the toe of the slope removed. The procedure for removing the toe was similar to that described above for the stationary load tests.

Data Analysis

Data analysis procedures were similar for both stationary and dynamic load tests. Amplitude (voltage) versus time was plotted from the DSP software for each test. These plots provided a first look at the data and indicated whether the test was run correctly and the data was worth saving for analysis. Video tapes of the dynamic load tests were played back to get the time at which the soil started to move and crack on the surface, when the slope failed, and when the load was passing a waveguide. These times were then correlated to the AE data.

Acoustic emission data analyses consisted predominately of determining the average amplitudes, ring-down count rates, energy rates, and power spectral densities (PSD). These were obtained with Asystant software on a personal computer (PC). The raw data was transferred from the DSP recorder to a PC. Asystant segments the data into data sets of up to 8192 data points (0.8192 s at 10-kHz sampling rate). The amplitude, count and energy data were segmented into 0.25-s portions. Larger data sets used up too much memory, while smaller data sets lengthened processing time. Power spectrum and fast Fourier transformation (FFT) analysis was done with 0.2048-s data sets. This was the data set length closest to 0.25 s which still had an even power of two points, as required by Asystant's FFT operations. The AE data was processed with a user function in Asystant's file processor. Details of the user functions are given in the appendix.

Amplitude data of both positive and negative voltages were averaged to reduce the effect of any large spurious signals. Ring-down count rates were based on a 40-mV threshold, which was determined to be about twice the maximum background noise level. Ring-down counting is the number of times the output voltage exceeds a threshold value (*20,23*). An amplitude distribution was plotted for some tests. This information was obtained by changing the threshold in the ring-down count function to determine the number of counts at different amplitude voltages (*24*).

Some event counting was tried, but the numerous overlapping events made the data difficult to analyze. Energy rates were calculated by squaring the voltage and integrating over time (*25,26*).

A user function (algorithm) was written within Asystant to determine how frequency varied with time. This function calculates the average frequency of the 100 largest PSD's over a 0.2048-s interval (see appendix). Averaging the frequency in this manner tended to smooth the frequency versus time plot and reduced the effects of spurious noises (*22*). This data was used to observe frequency changes as the slope began to fail. All the AE data was plotted versus time and compared to the visual events noted during the test or playback of the video tape.

In addition to the AE data, the load cell output was also saved on one channel of the waveform recorder. Load cell data was transferred to floppy disk for analysis with Asystant, just as the AE data was. The data was first converted to voltage, then averaged and finally converted to load in pounds. Load cell data was then plotted against the AE data.

FIELD TESTING

The site for AE field testing was the dump point of an active crushed limestone stockpile. The AE monitoring equipment was set up to the side of the active dumping area, inside the berm at the crest of the slope (fig. 8). The equipment was moved as dumping progressed, to stay near the active dumping area. The waveguide was pounded into the slope with a sledge hammer at different locations and orientations.

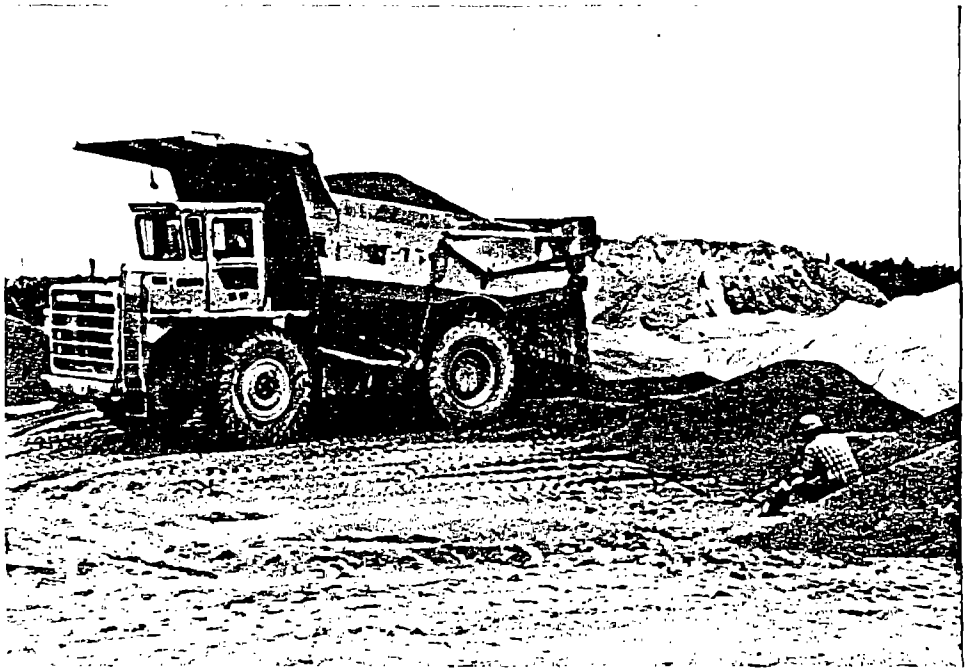

Figure 8.--Acoustic emission monitoring at dump point crest.

The waveguide was usually driven into the ground at a 30-45 degree angle because the length of the waveguide made it difficult to drive in the rod vertically. A threaded steel cap was placed on the end of the waveguide while being driven into the ground. The cap was then removed and the accelerometer threaded onto the waveguide. A 30-ft coaxial cable connected the accelerometer to the amplifier and kept the operator a safe distance from the haul truck.

A strong wind was found to be causing a rather high level of background noise. A cloth glove was taped over the accelerometer and the coaxial cable buried slightly to reduce the wind noise (*27*). Signal amplitude readings were taken from the oscilloscope as the haul truck backed up to the dump point and also while dumping its load. The distance from the nearest tire tracks to the waveguide was paced off and recorded after the truck left the area. The oscilloscope was turned off after each dump cycle to conserve the limited battery life of slightly more than an hour. A picture was taken of the slope to obtain an accurate measure of the slope height.

EXPERIMENTAL RESULTS

SMALL SCALE TESTING

Analysis of AE signals throughout this study has shown that average amplitude, count rates and energy rates are comparable to one another. Average amplitudes were easiest and fastest to calculate and thus were used most frequently. In general, when a comparison is made with average amplitudes, the same trend will be true for ring-down count rates or energy rates. Figure 9 shows the close correlation between average amplitude, count rate and energy rate. Energy rates correlate to average amplitudes better than count rates. This is expected because energy is calculated as the square of the voltage integrated over time, where voltage is a direct measure of the amplitude. Count rate plots look somewhat different when the count rates are small (low amplitudes), because the count rate may be zero and the plot will look more erratic because of the automatic scaling of the Y-axis with Asystant. A count rate plot with a maximum of 5 counts will look more erratic than a plot with a maximum count of 100. In these cases the average amplitude and energy plots look smoother because these values never go completely to zero and may be real numbers. This difference is due to the way that counts are determined, i.e. the threshold level must be reached for a ring-down count (integer) to be tabulated.

Accelerometer and Load System Noises

The background noise levels of the accelerometers, cables, amplifiers, and filters were found to have an average maximum amplitude of 17 mV, but ranging from 11 to 20 mV. A threshold level of twice the maximum background noise, 40 Mv, was chosen for calculating the ring-down count rates. The background noises were generally significantly smaller in magnitude than the AE signals generated during slope failure testing. The PSD plot of the sensor background noises, figure 10, shows that the noise levels were highest at frequencies less than 200 Hz;

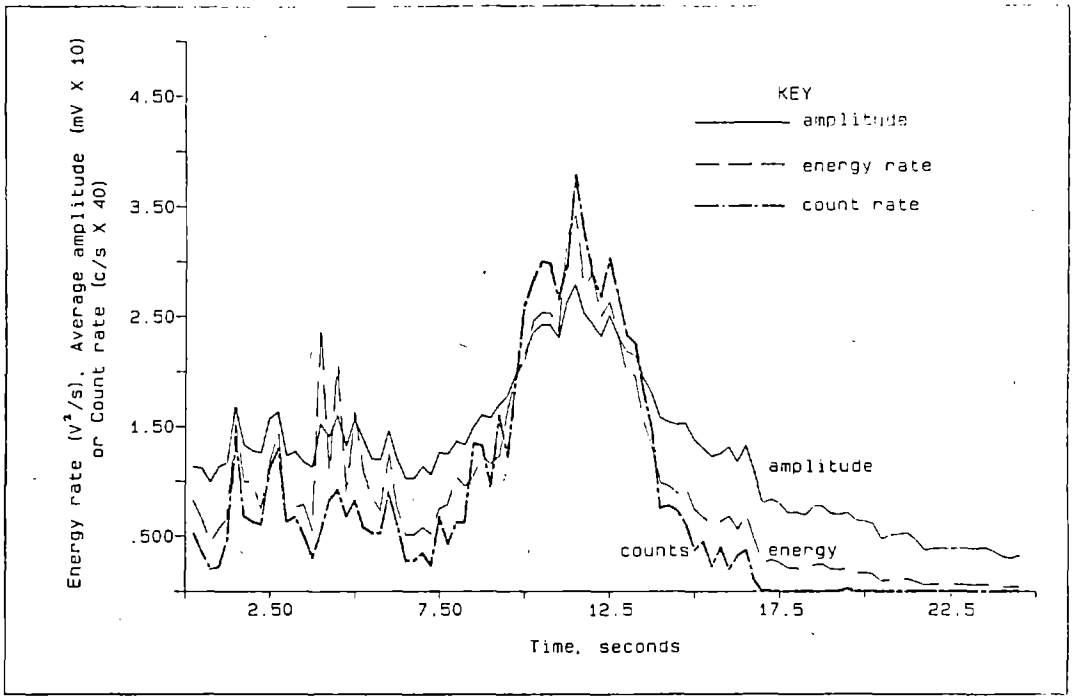

Figure 9.--Comparison of average amplitude, ring-down count rates, and energy rates.

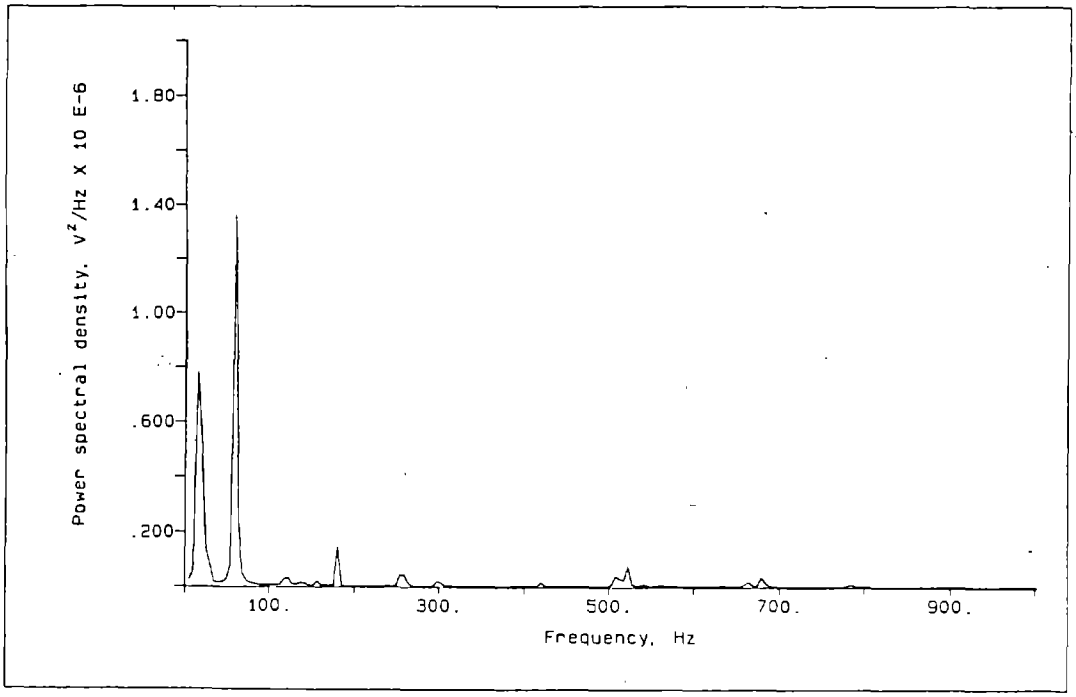

Figure 10.--Power spectral density of sensor background noise, unfiltered.

particularly at 15, 60, and 180 Hz. Frequencies above 1000 Hz are not shown because the PSD's were very small in that frequency range. Because of the 60 and 180 Hz peaks, this noise is assumed to be from electrical sources. As a result of this analysis, most subsequent testing was done with the high pass filter set at 200 Hz.

Figure 11 shows the PSD plot of the background noise after 200-Hz high pass filtering and 6300 Hz low pass filtering. This is essentially the same as figure 10, but the spikes less than 200 Hz have been reduced and the scale expanded to show the smaller spikes at frequencies above 200 Hz. Frequencies above 2000 Hz are not shown because of their small power spectrums. The largest noise spike occurs at 508 to 522 Hz, with smaller spikes at 259, 298, 420, 679, 786, and 1050 Hz. The PSD at 180 Hz was reduced significantly compared to the unfiltered spectra. A 200-Hz high pass filter attenuated the 180 Hz noise sufficiently so that it was no longer significant. The background noise tended to be slightly stronger when the soil was dry, but the frequency content did not change.

Most of the noise produced by the hydraulic/pneumatic load system came from the operation of the pneumatic, directional control valves. The noise generated by the horizontal valve depended on the direction of travel. Retraction strokes, or reversing from an extension stroke to a retraction stroke, created the most noise. Valve noise also varied with the amount of load on the tire or load plate. The highest noise levels were obtained at low loads, because the pressure differential in the pneumatic system was greatest and thus there was more pressure

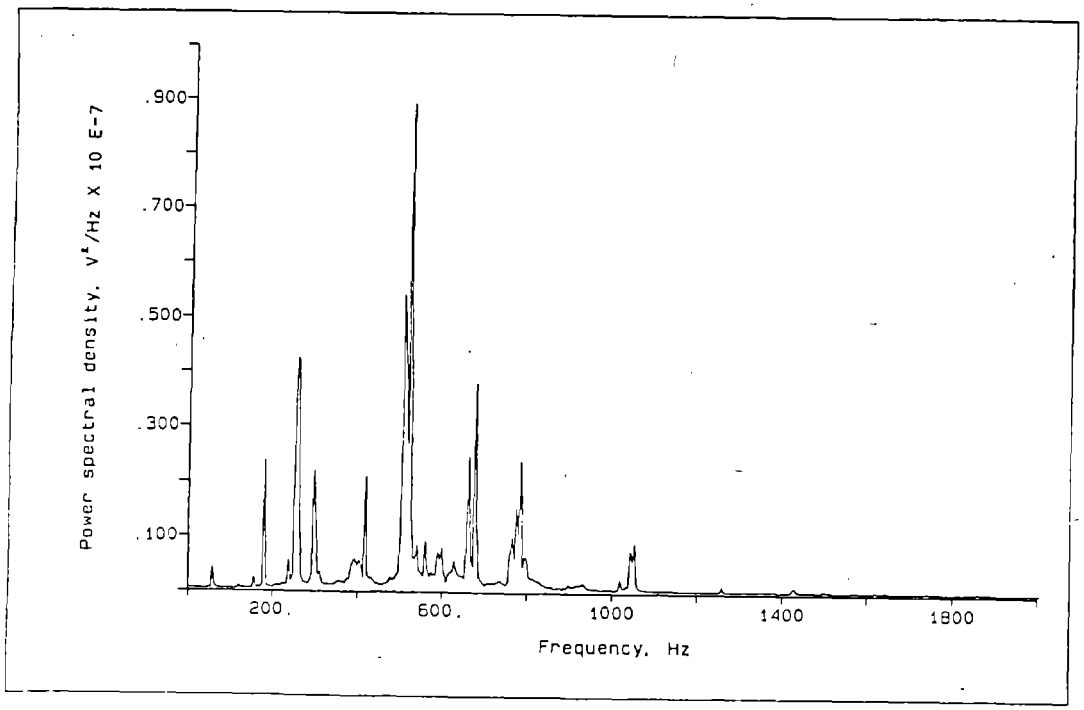

Figure 11.--Power spectral density of sensor background noise, band pass filtered at 200 Hz and 6300 Hz.

equalization and relief noise created by the valve. When a flat steel load plate was mounted on the load rod, load system noise transmitted to the soil was up to ten times greater than when a tire was mounted on the rod. This was probably due to the damping effect of the rubber tire. These pneumatic valve noises were avoided during testing by not starting the data recorder until after the valve had been opened.

After elimination of valve operation noise, the load system was found to be a significant noise source. Several tests were run with an accelerometer mounted in the side of the solid rubber caster tire. These tests were conducted without the tire coming into contact with any objects, i.e., the tire ran above the soil while suspended in air. Horizontal cylinder motion was found to produce an average noise about eight times that of the vertical cylinder motion (98 mV versus 12 mV). With both the vertical and horizontal cylinders operating, the average amplitude (62 mV) was less than the horizontal noise but more than the vertical noise. Horizontal cylinder noise peaked at 93 Hz while the vertical cylinder noise peaked at 88 and 200 Hz. With both cylinders running, the noise peaked at 88 Hz (fig. 12).

All of the significant noises were less than 200 Hz and were filtered out by the high pass filter. The vertical cylinder noise at 200 Hz was not attenuated by the 200-Hz high pass filter, but this noise was of low enough amplitude that it did not interfere during signal analysis. By the time this noise was transmitted through the soil to the waveguide, it was reduced significantly because of soil attenuation. This indicates that there was less noise generated by the load system during stationary load tests than during dynamic load tests. These noises were insignificant when compared to the AE generated in the soil.

Signal Attenuation

The attenuation of AE through soil is very high, as discussed earlier in the report. Even at the short distances dealt with in this study, attenuation through the soil can have a significant effect on signal strength and content. The effect of soil attenuation on signal amplitude was investigated at several different frequencies. Attenuation coefficients were determined by measuring the amplitudes of noises created in the soil at various distances from the noise source (*28*). Attenuation increased as the frequency increased (fig. 13). The soil was very dry (0.3-pct water), so these attenuations represent a worse case scenario. Koerner, et al, report that attenuation decreases as the soil moisture increases (*18,19*). Thus, most of the testing done here had coefficients of attenuation less than those shown in figure 13. Attenuation coefficients were not determined for other soil moistures.

Some AE signal attenuation studies were conducted in conjunction with the dump point stability testing. As expected, the attenuation increased with increased distance between the AE source (load tire) and waveguide. Table 1 shows how the average amplitude, count rate and energy rate indices decrease with increasing tire to waveguide distance. This data gives the reader a general idea of how the AE signals are attenuated with distance under typical test conditions. This data is from a stationary load located 8 in from the slope edge, soil moisture 3.9 pct and band pass filtering at 500 Hz and 6800 Hz.

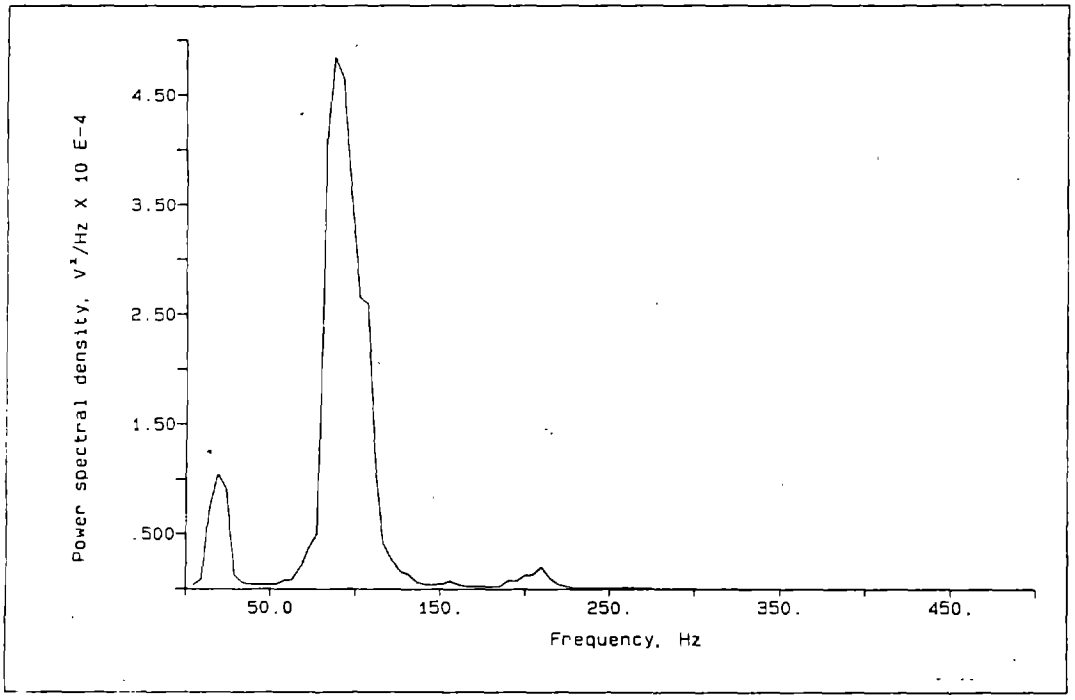

Figure 12.--Power spectral density of hydraulic load system, combined vertical and horizontal motions.

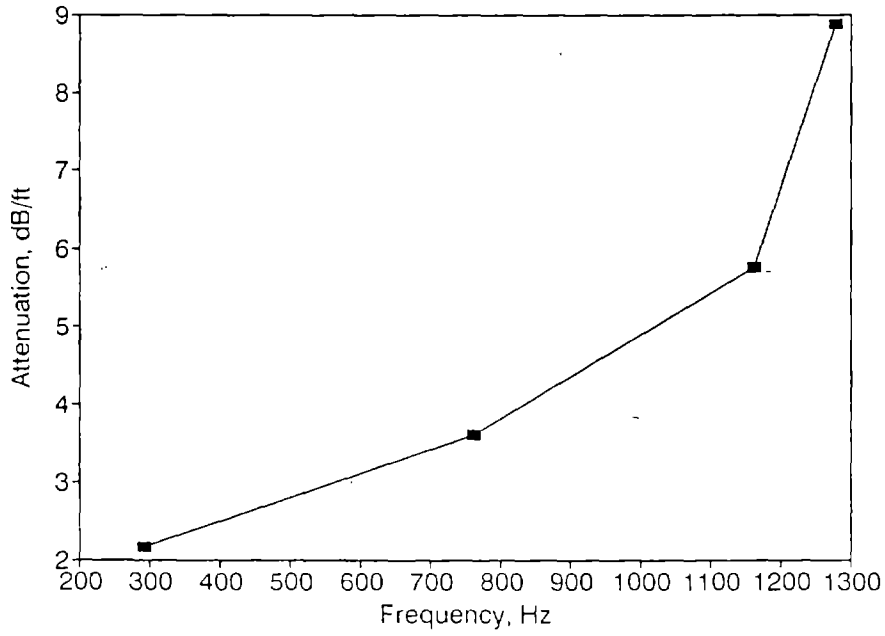

Figure 13.--Influence of frequency on attenuation coefficient.

Table 1.--Signal strength versus distance

Waveguide to Tire Distance	Amplitude	Count Rate	Energy Rate
4 in	35 mV	205 c/s	25.1 V^2/s
9 in	27 mV	98 c/s	13.9 V^2/s
15 in	15 mV	22 c/s	3.7 V^2/s

These same test data show how the attenuation increases as frequency increases. At frequencies of 500-1000 Hz, there is very little attenuation at the distances encountered in the test box (fig. 14). Above 1000 Hz, the amplitudes decrease as the distance between the source and the sensor increases. At each distance, the amplitudes decreased rapidly from a peak in the 650-1250 Hz frequency range. The maximum amplitude frequency shifted to higher frequencies as the distance from source to sensor decreased. The power spectrum amplitude at the higher frequencies drops about two orders of magnitude for a waveguide 15 in from the source compared to one only 4 in away.

A closer look at individual AE events shows the same result when looking at the effect of attenuation on the frequency content. Figure 15 shows the amplitude (A & B) and PSD plots (C & D) for a single large event as received by two different accelerometers located 9-in apart. This data is from a stationary load test with the load placed 12 in from the edge of the slope (test STAT 1, table 2). The peak amplitude in figure 15 B is about 2 dB less than that of figure 15 A. This indicates a 2.7-dB/ft attenuation coefficient, agreeing with figure 13, for a signal of about 500 Hz. The high frequency components in figure 15 C have been reduced by attenuation in figure 15 D. The test numbers

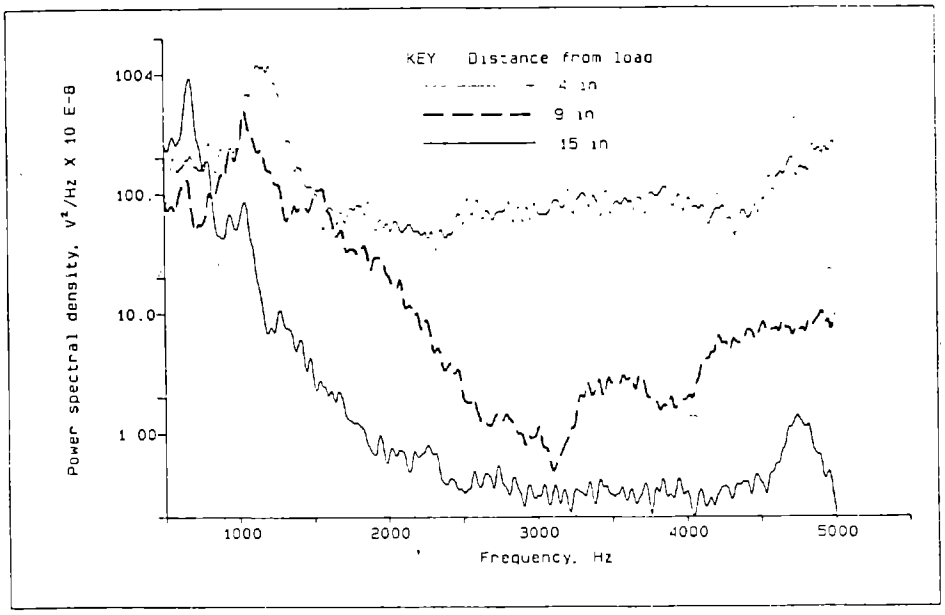

Figure 14.--Power spectral density change with distance from stationary load.

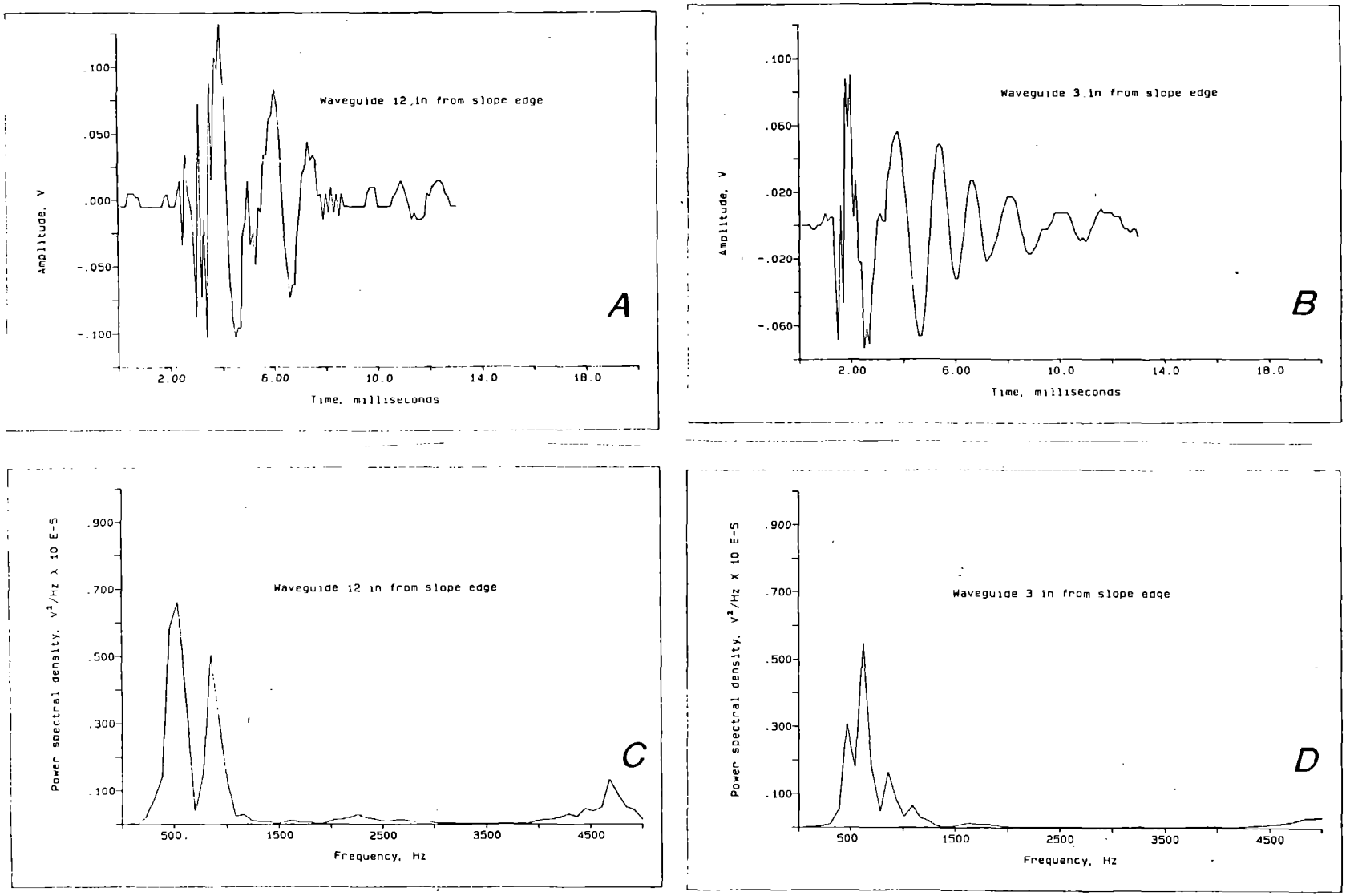

Figure 15.--Amplitudes (A&B) and power spectral densities (C&D) of AE signal at waveguide distances of 3 in and 12 in from slope edge, load 12 in from slope edge.

Table 2.--Stationary load test data

Test Number	Dist to edge of slope, in		Amplitude mV		Count rate [1]c/s		Energy rate V^2/s		[2]Peak freq	[3]Frequency Hz		Soil moist	Soil comp	Vertical load	
	tire	wave	avg	max	avg	max	avg	max	Hz	avg	max	[4]pct	[5]t/ft^2	[6]psig	[7]flow
STAT 1.1	12	3	2.3	5.2	0.84	20	0.12	0.9	513	693	899	2.3	2.1	45	2
STAT 1.3	12	12	5	6.2	4.6	32	0.36	1.1	874	2066	2632	2.3	2.1	45	2
STAT 2.1	3	3	5.6	7.8	4.3	26	0.6	1.2	698	697	889	2.3	2.1	45	2
STAT 2.3	3	12	7.1	9.5	6.4	30	0.84	1.8	738	663	743	2.3	2.1	45	2
STAT 3.1	12	3	3.7	4.8	1.4	16	0.28	0.7	513	561	628	2.3	2.1	45	2
STAT 3.3	12	12	5.6	6.9	4.7	36	0.6	1.3	513	1585	3159	2.3	2.1	45	2
STAT 4.1	12	3	19	28	150	316	6.2	13	557	624	682	5	0.4	45	4
STAT 4.3	12	12	29	42	222	364	15.1	30	591	672	1078	5	0.4	45	4
STAT 5.1	3	3	23	32	267	480	8.8	17	693	691	762	5	0.4	45	4
STAT 5.3	3	12	13	17	6.2	20	2.9	4.8	693	627	698	5	0.4	45	4
STAT 6.1	3	3	26	35	291	436	11.3	20	591	630	661	5	0.4	45	4
STAT 6.3	3	12	12	17	8.1	44	3	5.1	776	692	740	5	0.4	45	4
STAT 7.1	12	3	6	9.9	1.1	36	0.8	3.9	596	562	633	4.7	0.6	30	2
STAT 7.3	12	12	9.7	13	4.5	20	1.3	3.4	610	782	1199	4.7	0.6	30	2
STAT 8.1	3	3	6.2	9.8	2.2	36	0.72	3.3	664	664	737	4.7	0.6	30	2
STAT 8.3	3	12	9.2	11	0.64	20	1	2.3	615	640	704	4.7	0.6	30	2
STAT 9.1	12	3	12	18	46	108	3	7.4	615	577	716	4.7	0.6	30	4
STAT 9.3	12	12	14	20	25	76	3.5	7.1	586	669	887	4.7	0.6	30	4
STAT 10.1	3	3	17	23	140	244	5.2	12	679	664	710	4.7	0.6	30	4
STAT 10.3	3	12	13	15	2.9	20	2.2	4.4	645	600	660	4.7	0.6	30	4
STAT 11.1	12	3	12	18	48	128	2.8	7.4	552	615	988	4.7	0.6	30	5.9
STAT 11.3	12	12	16	21	72	168	4.4	7.6	903	1111	1785	4.7	0.6	30	5.9
STAT 12.1	3	3	18	25	174	336	5.6	12	571	645	818	4.7	0.6	30	5.9
STAT 12.3	3	12	13	16	5.4	28	2.3	4	894	807	881	4.7	0.6	30	5.9
STAT 13.1	12	3	1.9	2.7	0.08	4	0.08	0.3	664	683	1115	4.7	0.6	15	4
STAT 13.3	12	12	5.8	8.8	0.88	24	0.68	5.2	254	1258	1651	4.7	0.6	15	4
STAT 14.1	3	3	6.3	8.6	5.4	44	0.76	1.8	664	646	701	4.7	0.6	15	4
STAT 14.3	3	12	9	9.9	0.52	16	0.96	1.5	796	808	892	4.7	0.6	15	4
STAT 15.1[8]	2	2	7.8	21	57	264	1.9	8.7	806	1008	2427	3.5	1	45	1.5
STAT 16.1	3	3	7.8	9.3	5.7	28	1	1.7	664	635	695	5	0.4	45	2
STAT 17.1	12	12	6.2	8.3	3.1	28	0.64	1.4	1055	782	982	3.6	0.5	15	4
STAT 18.1	7	7	6.1	7.2	1.2	20	0.6	1.5	981	961	2584	3.6	0.5	15	4
STAT 19.1	3	3	5.9	7.3	1.7	16	0.6	1.1	552	728	1108	3.6	0.5	15	4
STAT 20.1	4	4	3.2	4	0	0	0.16	0.2	503	880	1308	6.1	0.4	10	4
STAT 20.2	4	4	3.1	4.1	0	0	0.16	0.2	503	1034	1393	6.1	0.4	10	4
STAT 21.1	4	4	3.7	4.4	0.4	8	0.24	0.4	503	845	1123	6.1	0.4	12	4
STAT 22.1	4	4	4.4	5.6	1.4	12	0.36	0.7	933	860	1094	6.1	0.4	14	4
STAT 23.1	4	4	3.8	5.1	1.1	12	0.28	1	1026	897	991	6.1	0.4	16	4
STAT 23.2	4	4	4.7	6.2	2.1	20	0.4	1.3	898	836	967	6.1	0.4	16	4
STAT 24.1	4	4	4.2	5.5	1.1	12	0.28	0.8	503	856	1010	6.1	0.4	18	4
STAT 25.1	4	4	5.3	8.6	4.6	40	0.56	1.9	864	886	1212	6.1	0.4	20	4
STAT 26.1	4	4	5.1	7	2.8	20	0.48	1	840	867	1116	6.1	0.4	22	4
STAT 27.1	4	4	4.2	5.8	1.8	16	0.32	0.7	850	880	1692	6.1	0.4	24	4
STAT 28.1	[9]12	12	6	9.9	3.6	52	0.6	2.7	1260	1458	2730	1.7	>4.5	40	2.5
STAT 28.3	[9]12	12	5	9.5	6.8	52	0.56	3.4	1543	1877	2844	1.7	>4.5	40	2.5
STAT 29.1	[9]3	3	8	14	26	76	1.6	5	957	849	1297	1.7	>4.5	40	2.5
STAT 29.3	[9]3	3	9	13	41	76	2	8.2	1001	920	1028	1.7	>4.5	40	2.5

[1]Ring-down count rate (40 mV threshold).
[2]Average peak frequency.
[3]Average frequency of 100 strongest power spectrums.
[4]Percent soil moisture.
[5]Compressive strength of soil from pocket penetrometer.
[6]Vertical cylinder air pressure.
[7]Vertical cylinder micrometer flow control valve setting (5.9=max. flow).
[8]Load was flat plate (9 in^2), all other tests were dual tire caster.
[9]Waveguide 4-in to the side of tire, all other tests 6-in.

in table 2 and all following tables include a decimal point, and a number 1 to 4, which indicates the channel number of that test.

Waveguide Orientation

The orientation of the waveguide (vertically into the top of the slope or horizontally into the slope face) was found to affect the reception of AE signals. Tests were conducted to determine which waveguide placement produced the best results. The average amplitude plot of a dynamic load test shows the relationship between horizontal and vertical waveguide signal strength (fig. 16). The results were not always consistent, but in general the vertical waveguide produced larger amplitude signals than a horizontal waveguide buried an equal distance below the load. For this reason and because a vertical waveguide was a more convenient placement, vertical waveguides were used for the remainder of the testing. Also, horizontal waveguides buried below the surface are not practical for field work at active dump sites.

An observation made in the late stages of this research may have important implications for future work in this area. An amplitude distribution comparing vertical and horizontal waveguide placements was plotted (fig. 17). These plots show the distribution of signal amplitudes by obtaining ring-down counts at different threshold levels. The X-axis shows the threshold level expressed as dB, referenced to 1 mV. Both waveguide positions have approximately the same number of total ring-down counts (20,000 +/- 100) at a 10-dB threshold. But, at

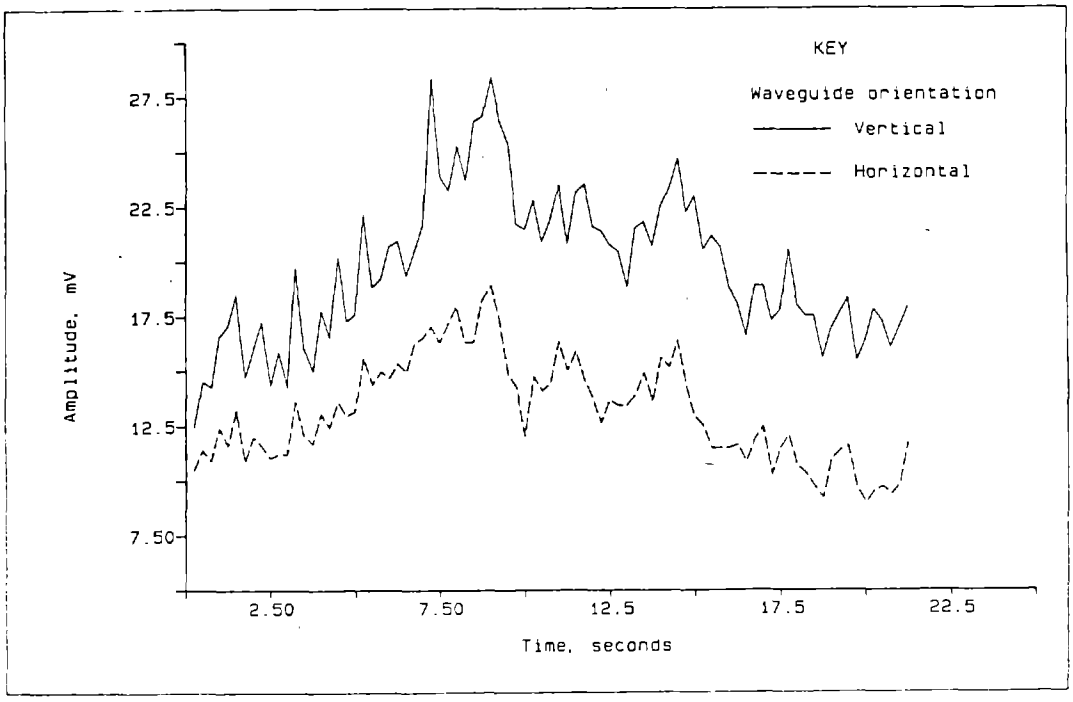

Figure 16.--Horizontal and vertical waveguide signal strengths.

the 40-mV threshold (32 dB) used throughout most of this study, the vertical waveguide has a much higher total count, 5336, versus 2174 counts for the horizontal waveguide. The amplitude distribution for the vertical waveguide (fig. 17 A) is skewed more towards the higher amplitudes than the horizontal waveguide (fig. 17 B).

Most of the waves being picked up by the transducer are probably being generated by the tire on the soil surface. The horizontal waveguide buried in the soil detects these emissions at a lower amplitude than the vertical waveguide, which has a direct surface path to the tire. Thus, a waveguide buried below the surface may detect less tire generated noise while being more sensitive to AE generated within the soil when using a voltage threshold. But, this may not be a practical placement for a waveguide on an active stockpile or waste dump. For this reason, the buried waveguide was not used for subsequent testing, because the goal was to develop a technique in the lab which was practical for field use.

Stationary Load Tests

Stationary load tests were conducted before the dynamic load tests to provide a basis for the dynamic load testing. The information learned here was then applied to the more complex case of a dynamic load. But even with a stationary load, in many cases it was difficult to determine whether the signals received by the transducer were caused by the tire compacting the soil or from the soil beginning to move and fail. Stationary load tests were conducted at different slope edge to load wheel distances. Distances less than 5 in from the slope edge were considered an unstable loading, because loads in that region caused slope failures. Distances greater than 10 in were considered a stable loading. Distances of 3 and 12 in from the slope edge were used most often for unstable and stable loads, respectively. Distances between 5 and 10 in were not used much, because it was uncertain whether this was a stable or unstable loading of the slope.

In all stationary load tests, one of the waveguides was placed 4 or 6 in to the side of the load tire, at the same distance from the edge of the slope as the center of the tire. The 6 in distance was used in most tests; the 4 in distance was used only in the early stages of testing. The distance from the tire to the waveguide was measured from the center of the tire. Figure 18 is a schematic sketch of the stationary load test setup, showing the locations of the load tire and waveguides for both stable and unstable loadings. Another accelerometer was sometimes placed the same distance to the side of the tire, but 9 in closer or further away from the edge of the slope. In the case of a load at 12 in from the slope edge, the second waveguide was placed 3 in from the edge, in the same spot where the waveguide would be if that test was a loading 3 in from the slope. Conversely, the second waveguide would be placed 9 in further from the slope edge when loading near the slope edge. This arrangement allowed one stable and one unstable slope loading to be completed by simply repositioning the tire. Another waveguide position used was the same distance from the edge of the slope as tire, but 12 in from the side of the tire instead of 6 in from the tire.

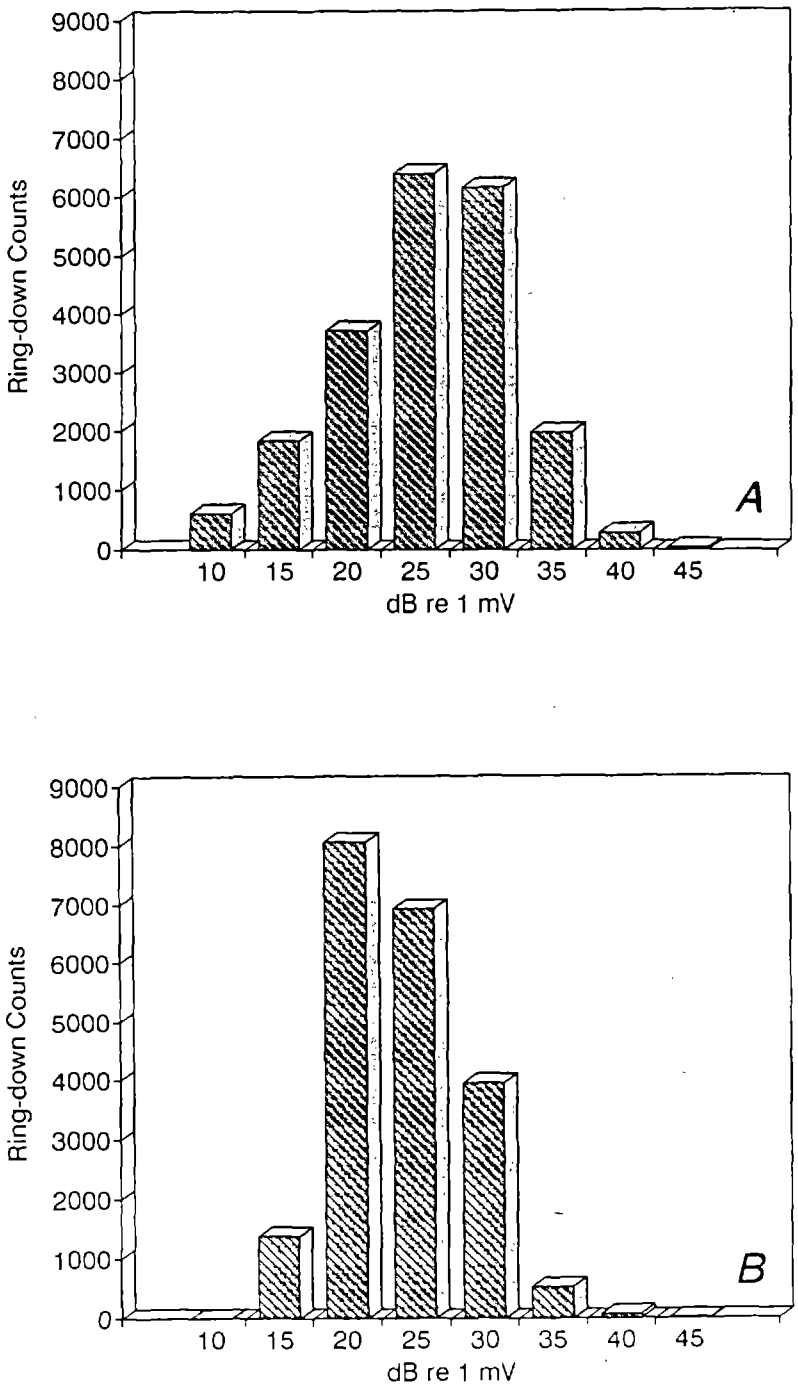

Figure 17.--Amplitude distributions of vertical (A) and horizontal (B) waveguides.

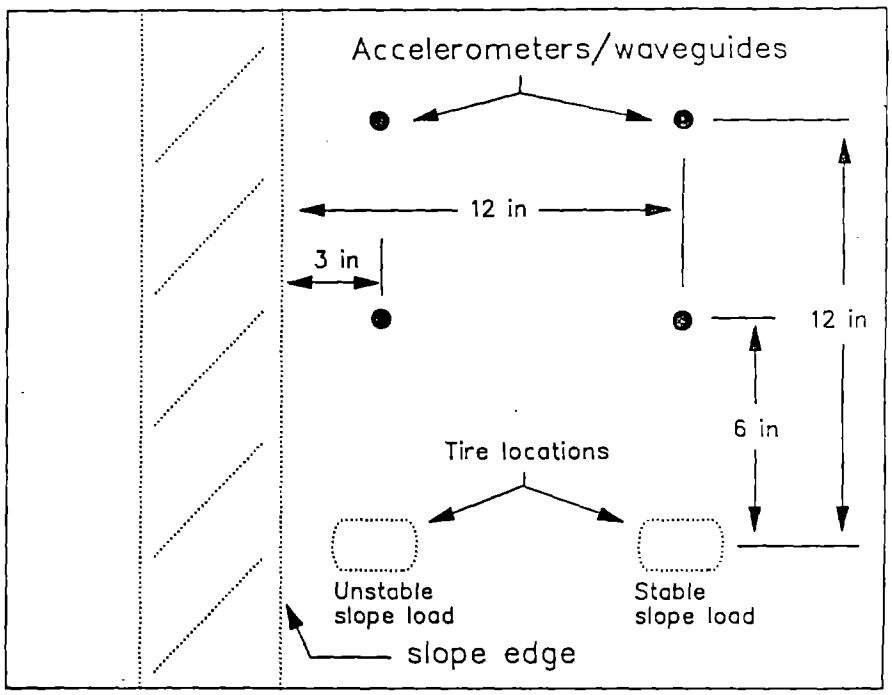

Figure 18.--Schematic diagram of stationary load test layout.

Load Rate/Magnitude

The rate and magnitude of the load applied to the soil was found to affect the amplitude of the AE signals produced. Load magnitude was controlled by the vertical cylinder air pressure. The higher the air pressure, the larger the load placed on the soil. Load rate was controlled by a combination of air pressure and the exhaust flow control valve on the vertical hydraulic cylinder. During stationary load tests the load was increasing throughout the test. The loads shown in the figures and discussed in the text are the resultant loads on the soil and not the applied load. This resultant load was controlled by the air pressure and flow rate of the load system and also by the resistive force (strength) of the soil.

The load plot for stable loadings 12 in from the slope edge is different than it is for unstable loadings 3 in from the slope edge. Figure 19 shows a typical load curve for these two cases. The load curve at 3 in from the slope is generally fairly linear while the curve for 12 in loadings is parabolic. The load plots at 12 in are parabolic because the load quickly reached the bearing capacity of the soil and then increased at a slower rate as the load continued to move downward. This appears to be elastic deformation early in the test, followed by plastic deformation as the load increases. The bearing capacity of the

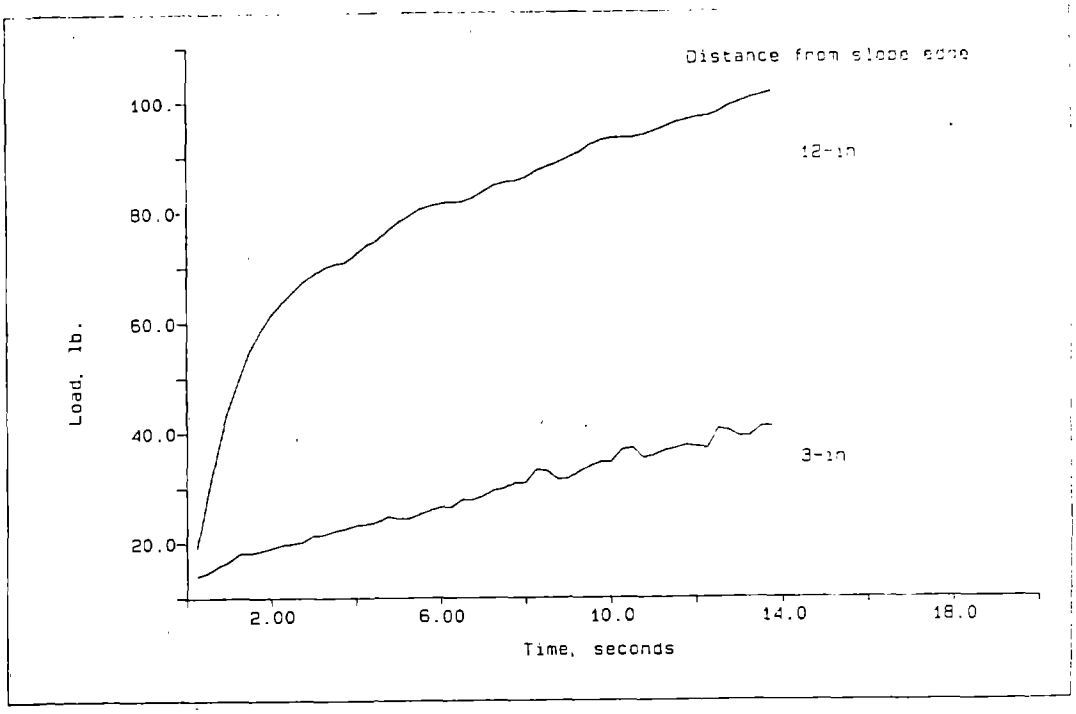

Figure 19.--Typical stationary load cell outputs at 3 in and 12 in from slope edge.

soil was exceeded in many cases, causing a small localized failure immediately under the tire. At 3 in from the slope, the soil appeared to deform plastically, the load tire meeting a relatively constant resistive force as it moved deeper, even as the slope was failing. Thus the curve is trending linearly but with small scale deformations causing oscillations along the way.

For equal vertical cylinder settings, the resulting load was higher at the 12-in distance than at 3 in, because the soil could not support as heavy a load near the edge as it could away from the edge. The cylinder pressure affects how high the final load will be. The flow rate of the hydraulic fluid affects the steepness of the curves, with higher flow rates producing steeper load curves. Only in the case of a major slope failure did the load decrease significantly during the test. This happened when the soil was very dry and compact and the failure was sudden, more like that of a rock than a soil slope.

Load magnitude (vertical cylinder air pressure) had a significant effect on the AE signal strength between different tests. Figure 20 shows that as the regulated air pressure increases from 15 psig to 45 psig, the average amplitude increases. The micrometer flow control valve was set at 4.0 for these tests. The same trend holds for both stable loadings away from the slope edge (fig. 20 A, and table 2, tests STAT 4,9,13) and loadings near the slope edge (fig. 20 B, and table 2,

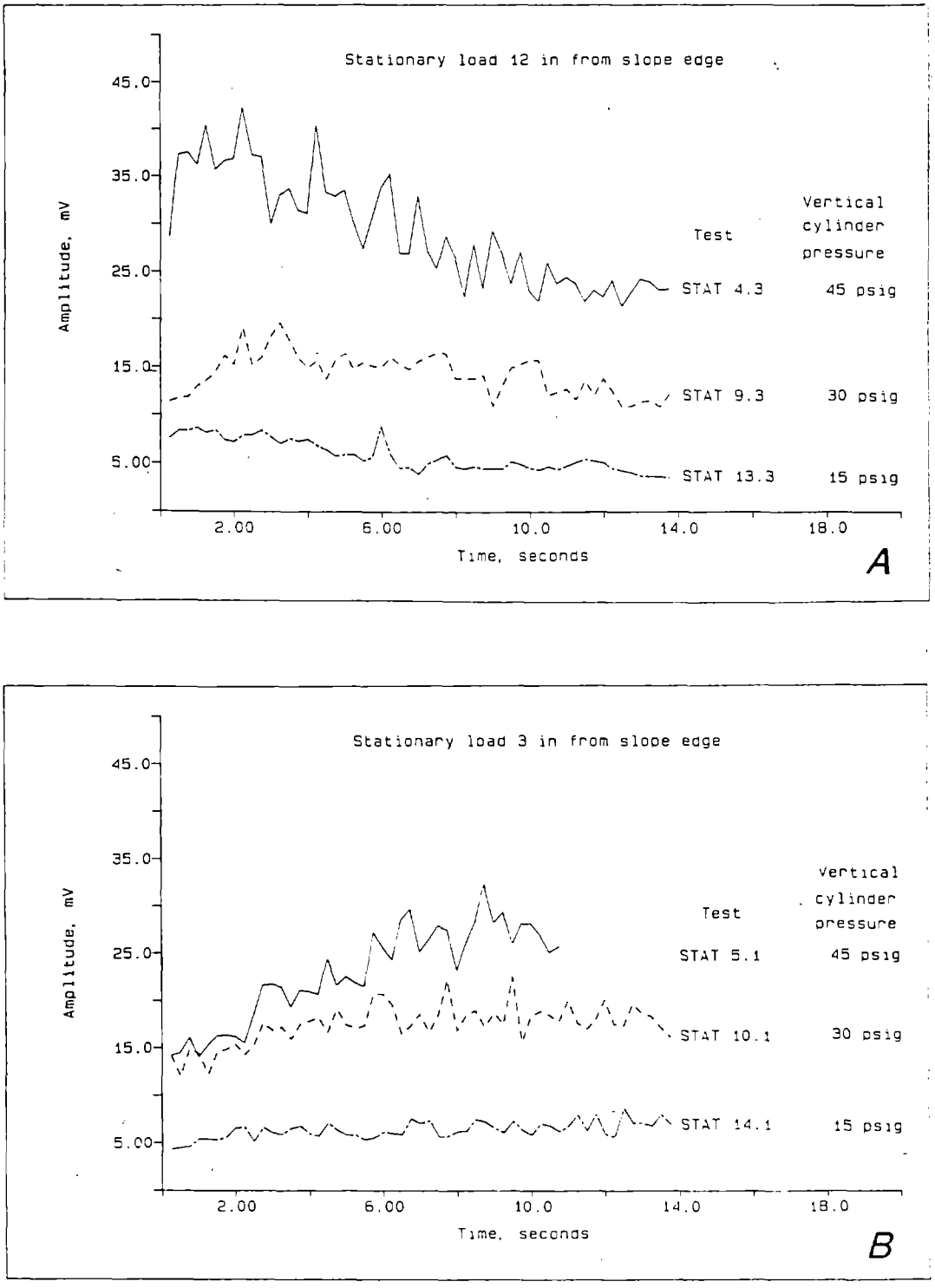

Figure 20.--Effect of load pressure on stationary load amplitudes at 12 in (A) and 3 in (B) from slope edge.

tests STAT 5,10,14). In all of these tests the waveguides were placed vertically into the top of the soil, 6 in to the side of the load. This trend of increasing AE with load magnitude is consistent throughout the stationary load tests, whether looking at amplitudes, ring-down counts or energy rates. This is also consistent with the results of other researchers (*4,9,13,14,18,19,29*). When loading near the crest of the slope, a 15-psig air pressure was found to be too small to produce a slope failure. At this pressure, surface cracks just began to form at the edge of the slope; slope failure was just beginning. An air pressure of at least 30 psig was found to produce a slope failure under most slope/soil conditions.

This trend of increasing AE signal strength with increasing load is clearly seen from the data in table 3. This is selected table 2 data that has been sorted first with all similar load and waveguide positions grouped together, secondly by increasing load pressure, and finally by increasing load rate (vertical cylinder flow rate). In nearly every test the AE signal strength increases as the load increases. There are a few exceptions, mainly in the count rate data, which tend to be more erratic than the amplitudes or energy rates. The general trend does not hold true for tests STAT 9.1 and 11.1, for example (table 3). The amplitude and energy rate at a flow setting of 4 was slightly less than that at 5.9, but this is a very small difference, and not statistically significant considering the variability of the data.

Acoustic emission signal strength also tended to increase as the rate of loading increased, i.e., as the flow control valve was opened. The difference in AE signal strength is not as great between increasing flow rates as it is between increasing load pressures. Thus the average amplitude plots are not as cleanly separated and occasionally intersect, as shown in figure 21. The plots show average amplitude increasing as the vertical cylinder flow control valve was opened from 2.0 to 5.9 on the valve micrometer (5.9 was the maximum flow setting). Data is shown for a stable stationary load placed 12 in from the slope edge (fig. 21 A, tests STAT 7,9,11) and an unstable loading 4 in from the edge (fig. 21 B, tests STAT 8,10,12). See table 2 for additional data on these tests. These plots have been smoothed using Asystant to make the plots less confusing because of undulating and crisscrossing lines.

Test STAT 15.1 is an example of a stationary load test near the crest of the slope. This test is an exception because it so clearly shows the relationship between load and AE signal strength (fig. 22 A). It is quite evident from this plot when the slope was failing. Most tests do not exhibit as pronounced a difference in prefailure and failure signal strengths. This test was conducted with a flat load plate on the end of the vertical load rod instead of the caster, and also had a slower flow rate (1.5 micrometer setting). The large area of the load plate (9 in^2) created a large slope failure and large AE's, while the low loading rate slowed down the slope failure. Amplitude rose slowly as the load increased and then increased rapidly as the slope began to fail, at the peak of the load plot. Amplitude continued to rise as the slope failed, finally reaching a peak and falling slightly. The load began to drop as the slope failed because the

Table 3.--Selected stationary load test data sorted by waveguide position and load

Test number	Dist. to edge of slope, in		Avg amplitude	Count [2]rate	Energy [3]rate	Soil		Vertical load	
	tire	[1]waveguide	mV	c/s	V^2/s	[4]moist pct	[5]comp t/ft^2	[6]psig	[7]flow
STAT 14.3	3	12	9	0.52	0.96	4.7	0.6	15	4
STAT 8.3	3	12	9.2	0.64	1	4.7	0.6	30	2
STAT 10.3	3	12	13	2.9	2.2	4.7	0.6	30	4
STAT 12.3	3	12	13	5.4	2.3	4.7	0.6	30	5.9
STAT 2.3	3	12	7.1	6.4	0.84	2.3	2.1	45	2
STAT 6.3	3	12	12	8.1	3	5	0.4	45	4
STAT 5.3	3	12	13	6.2	3.9	5	0.4	45	4
STAT 19.1	3	3	5.9	1.7	0.6	3.6	0.5	15	4
STAT 14.1	3	3	6.3	5.4	0.76	4.7	0.6	15	4
STAT 8.1	3	3	6.2	2.2	0.72	4.7	0.6	30	2
STAT 10.1	3	3	17	140	5.2	4.7	0.6	30	4
STAT 12.1	3	3	18	174	5.6	4.7	0.6	30	5.9
STAT 2.1	3	3	5.6	4.3	0.6	2.3	2.1	45	2
STAT 16.1	3	3	7.8	5.7	1	5	0.4	45	2
STAT 5.1	3	3	23	267	8.8	5	0.4	45	4
STAT 6.1	3	3	26	291	11.3	5	0.4	45	4
STAT 17.1	12	12	6.2	3.1	0.64	3.6	0.5	15	4
STAT 13.3	12	12	5.8	0.88	0.68	4.7	0.6	15	4
STAT 7.3	12	12	9.7	4.5	1.3	4.7	0.6	30	2
STAT 8.3	12	12	14	25	3.5	4.7	0.6	30	4
STAT 11.3	12	12	16	72	4.4	4.7	0.6	30	5.9
STAT 1.3	12	12	5	4.6	0.36	2.3	2.1	45	2
STAT 3.3	12	12	5.6	4.7	0.6	2.3	2.1	45	2
STAT 4.3	12	12	29	222	15.1	5	0.4	45	4
STAT 13.1	12	3	1.9	0.08	0.08	4.7	0.6	15	4
STAT 7.1	12	3	6	8.1	0.8	4.7	0.6	30	2
STAT 9.1	12	3	12	46	3	4.7	0.6	30	4
STAT 11.1	12	3	12	48	2.8	4.7	0.6	30	5.9
STAT 1.1	12	3	2.3	0.84	0.12	2.3	2.1	45	2
STAT 3.1	12	3	3.7	1.4	0.28	2.3	2.1	45	2
STAT 4.1	12	3	19	150	6.2	5	0.4	45	4

[1]Waveguide located 6 in to side of tire.
[2]Average ring-down count rate (40 mV threshold).
[3]Average energy rate.
[4]Percent soil moisture.
[5]Compressive strength of soil from pocket penetrometer.
[6]Vertical cylinder air pressure.
[7]Vertical cylinder micrometer flow control valve setting (5.9=max. flow).

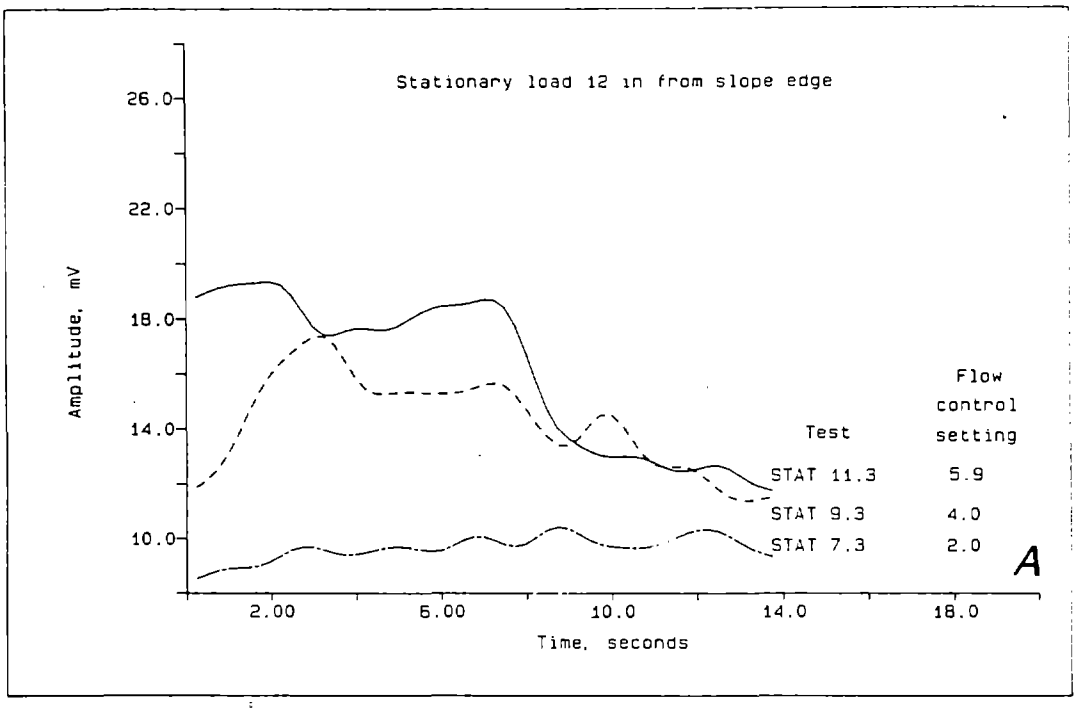

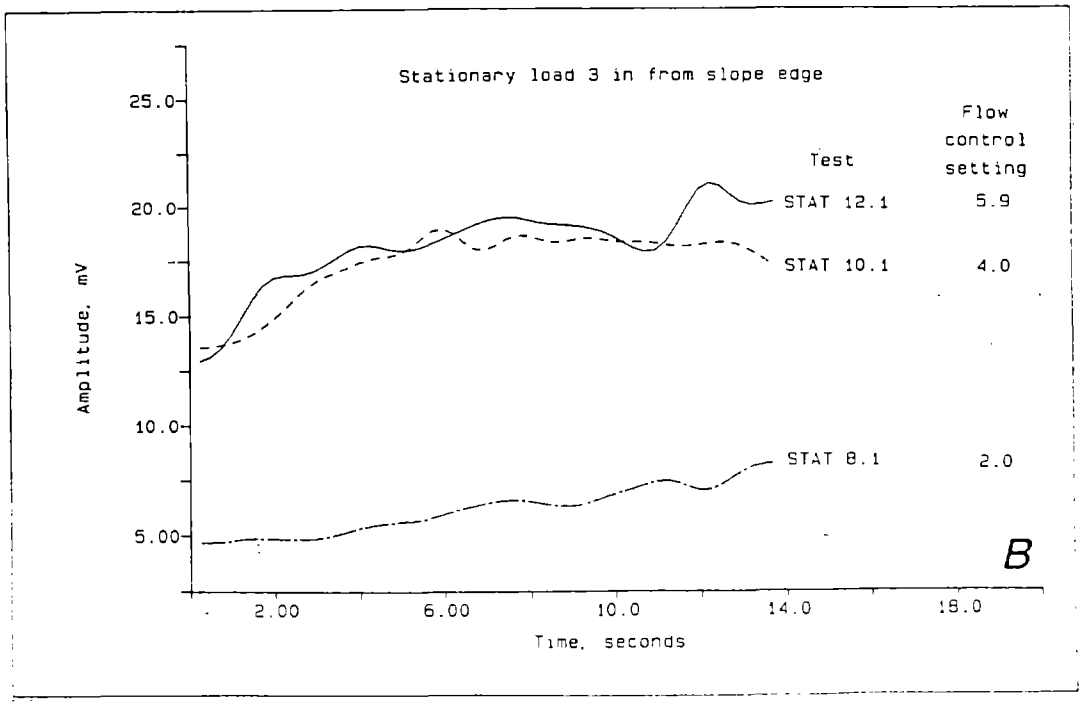

Figure 21.--Effect of flow rate on stationary load amplitudes at 12 in (A) and 3 in (B) from slope edge.

soil was giving way under the load and the load system could not keep up with the moving soil. This AE data (fig. 22 A) is similar to the type of response shown in the literature for statically loaded slopes or slopes with no external loads monitored over a long period of time (*4,9,13,14*).

Test Stat 15.1 also illustrates how frequency changed with load. Figure 22 B shows that the frequency tended to rise as the load increased and the slope became more unstable. The average frequency of the 100 largest power spectrums reached a maximum just before the slope began to fail, falls as the slope was failing, and then levels off. The line through the frequency plot is an averaged or smoothed value of the average frequency. The rise in average frequency with increasing load was not necessarily typical for all stationary load tests, but the drop in frequency at the time of failure did occur in most tests, both stationary and dynamic loads.

The average frequency of the 100 strongest power spectral amplitudes were plotted for each test and their general trends studied. For a stable slope, the frequency tended to drop as the load increased only 7 pct of the time. Sixty seven percent of the time, frequency was essentially unchanged and 27 pct of the time, the frequency rose with an increasing load. These percentages changed for loads near the slope edge, to 15 pct decreasing, 35 pct constant and 45 pct increasing. This stationary load test data shows that there is no clear trend in frequency as the load increases.

Soil Moisture/Compressive Strength

In this study soil moisture and soil compressive strength have a strong inverse relationship to one another. This is due to the way a dry slope was constructed. A dry slope refers to a slope that was constructed with a wet soil and then allowed to dry over a period of time before slope failure testing was initiated. A slope with a high moisture content was freshly constructed. The clay didn't have a chance to dry out and bond the soil grains together, and thus it generally had a lower compressive strength (penetrometer reading). Some slopes were allowed to dry from 3 hr to a maximum of a week. Letting the slope dry allowed the clay in the soil to bond the soil grains together, thus increasing the compressive strength.

Tests were not specifically run to determine the effects of soil moisture. But, the effects of soil moisture can be seen from the test data available. In the few instances where a comparison can be made between different soil moistures, the results are not always clear. From table 4, tests TOE 1 versus TOE 5, the amplitudes, counts and energy all increased as the soil moisture decreased. These two tests are from the toe removal test data, but are instances when there was 0-pct removal of the toe. The opposite trend is seen when comparing test STAT 2.1 against test STAT 16.1 or STAT 19.1 to 14.1 (table 3). In this case the moist slope has higher AE levels than the drier slope. Another observation shows that soil moisture has little or inconsistent effects on the AE; compare tests STAT 17.1 and 13.3 in table 3. Tests STAT 17 and

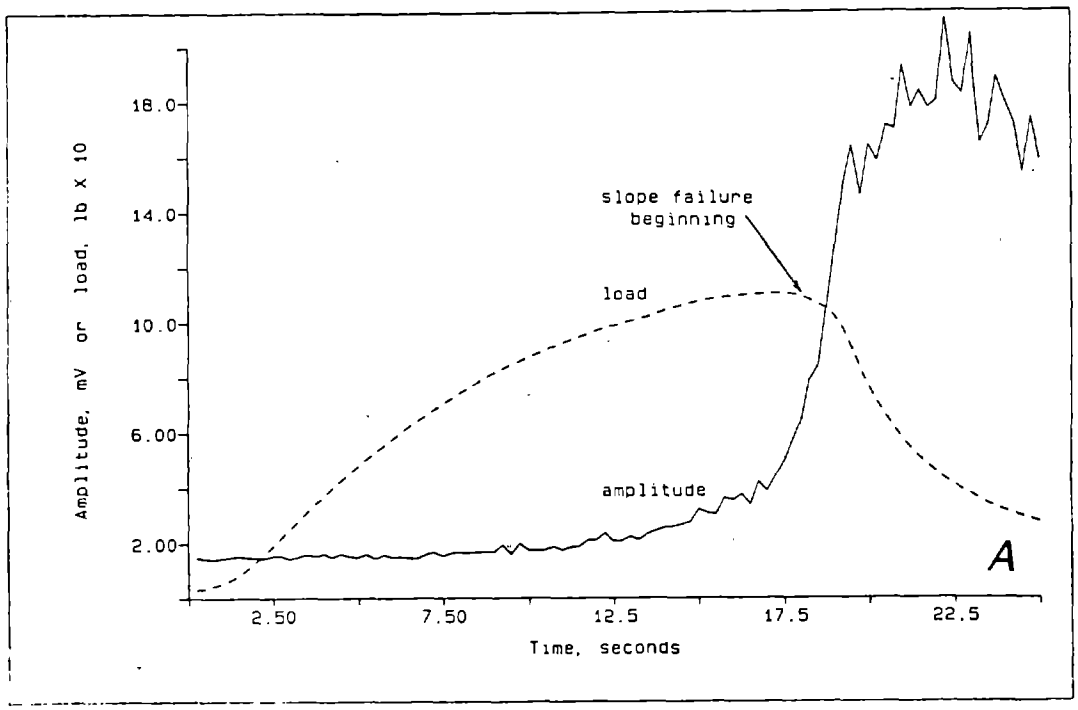

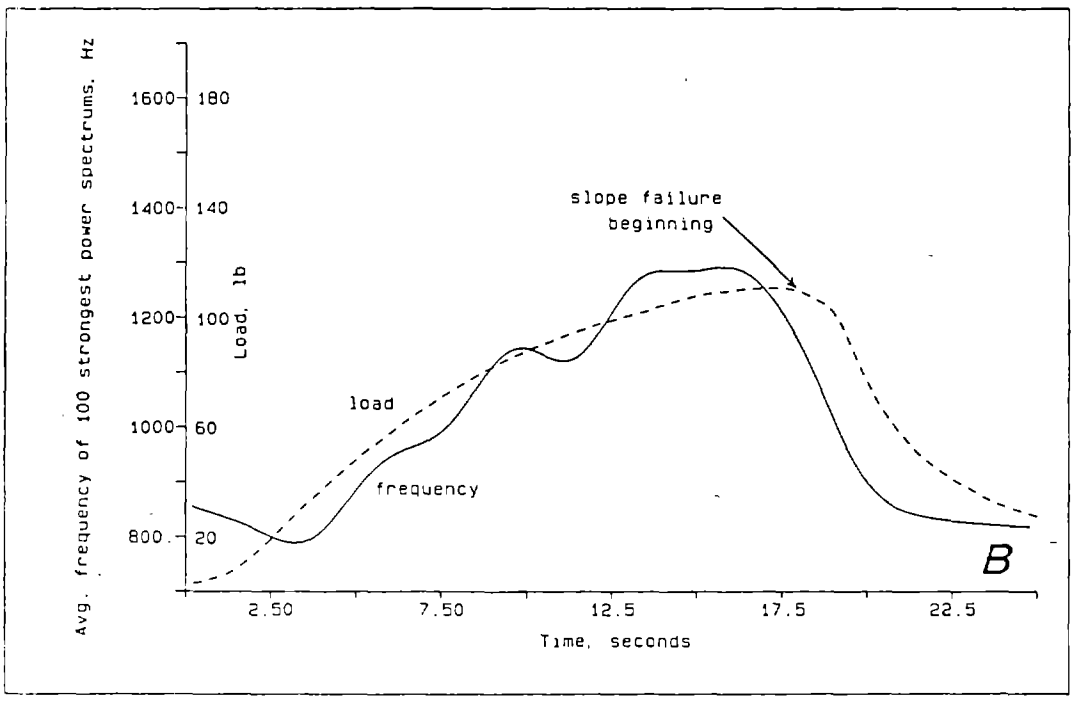

Figure 22.--Average amplitude (A) and frequency (B) compared to load for stationary, flat plate load.

Table 4.--Toe Removal test data

Test number	Dist. to slope	Amplitude mV		Count rate [1] c/s		Energy rate V^2/s		Frequency [2] Hz		Soil moist	Soil comp	Toe loadout	Vertical load	
	in	avg	max	avg	max	avg	max	avg	max	[3] pct	[4] t/ft^2	pct	[5] psig	[6] flow
TOE 1	4.5	3.6	4.4	0.6	8	0.2	0.44	843	1064	5.8	0.5	0	10	5.9
TOE 2	4.5	3.5	8	0.4	12	0.2	0.96	909	1146	5.8	0.5	11	10	5.9
TOE 3	4.5	3.2	3.6	0	0	0.16	0.2	914	1233	5.8	0.5	22	10	5.9
TOE 4 [7]	4.5	5	45	13	620	0.4	16	708	906	5.8	0.5	33	10	5.9
TOE 5	3	4.3	5.7	2.9	20	0.28	0.52	782	883	3.6	0.8	0	10	5.9
TOE 6	3	4	5.2	0.44	20	0.28	0.76	790	1089	3.6	0.8	10.5	10	5.9
TOE 7	3	3.4	4.9	0.56	12	0.2	1.3	863	1188	3.6	0.8	21.1	10	5.9
TOE 8	3.5	6.1	7.1	0.36	8	0.6	0.76	589	903	3.5	0.4	0	15	4
TOE 9	3.5	6.6	8.7	2.2	16	0.72	1.3	658	858	3.5	0.4	11	15	4
TOE 10	3.5	6.6	9.8	6.8	32	0.8	1.8	647	711	3.5	0.4	22	15	4
TOE 11	4	5.6	7.5	1	16	0.56	1	737	823	6.2	0.4	0	12	4
TOE 12	4	5.4	6.5	1.2	20	0.48	0.84	778	916	6.2	0.4	11	12	4
TOE 13	4	4.7	5.6	0.32	4	0.36	0.56	727	849	6.2	0.4	22	12	4
TOE 14	4	4.9	8.4	0.76	8	0.4	1	799	887	6.2	0.4	33	12	4
TOE 15	5	3.6	4.9	0.44	12	0.2	0.64	990	1374	5.9	0.5	0	10	5.9
TOE 16	5	3.1	4.1	0.2	8	0.16	0.4	1090	1431	5.9	0.5	11	10	5.9
TOE 17	5	3.1	4.4	0.04	4	0.16	0.28	1097	1532	5.9	0.5	22	10	5.9

[1] Ring-down count rate (40 mV threshold).
[2] Average frequency of 100 strongest power spectrums.
[3] Percent soil moiture.
[4] Compressive strength of soil from pocket penetrometer.
[5] Vertical cylinder air pressure.
[6] Vertical cylinder micometer flow control valve setting (5.9=max. flow).
[7] Toe removed during test. Toe removed immediately before all other tests.

STAT 19 had soil moistures of 3.6 pct and compressive strengths of 0.5 t/ft^2. The compressive strength was lower than other slopes with comparable soil moistures because this slope (same slope for both tests) was constructed with a drier soil than was used in the other tests. Tests STAT 13 and STAT 14 had soil moistures of 4.7 pct and compressive strengths of 0.6 t/ft^2. Overall the signal strengths are quite similar between these four tests, regardless of the soil moisture. This could be due to the similarities in compressive strengths, which may have a larger effect on the AE's generated than the soil moisture.

At first glance, table 3 data indicates that a slight increase in AE signal strength generally occurs as the soil moisture increases or the soil compressive strength decreases. This might suggest that there is a correlation between increasing soil moisture/decreasing compressive strength and increasing AE signal level. But, these trends also hold true for increasing load rates, as described in the previous section. Thus it can not be clearly stated that this effect is due to moisture content/soil compressive strength or load rate.

Soil compressive strength generally had the opposite affect on AE signal strength as soil moisture does. This is because of the inverse relationship between these two soil parameters. The net result of the effect of soil compressive strength on AE signal strength is the same as

for soil moisture, i.e., there is no clear trend evident from the data.

A soil that has a low compressive strength is more likely to flow and move when stressed, and thus may emit more AE's than a stronger soil. Also, the attenuation of signals through soil decreases as the soil moisture increases (*18,19*). This may explain why signal strength might tend to increase as the moisture content increased and the compressive strength decreased. It is also noted from the literature that emission rates from soils tend to decrease as the water content increases, which would have an opposite effect from that above (*13*). No clear observations in regard to the effects of soil moisture/compressive strength on the AE signal strength can be made from the stationary load data. This is not unexpected, because these tests were not designed specifically to determine the effect of soil moisture on the AE signals.

Stable versus Unstable Loading

The main purpose of the stationary load tests was to determine the difference between the AE signals produced by stable slope loadings (away from edge) and unstable loadings (near edge). The results from these tests will then be used to help distinguish between a stable and unstable slope for the dynamic load tests. In most of the stationary load tests, the stable loading was done at a distance of 12 in from the slope edge, while unstable loadings were done at 3 in from the edge. The exception to this is for the toe load out tests, where the load was placed 3 to 5 in back from the edge.

Signal Strength

The general shape of the AE signal strength curves are different for stable and unstable slope loadings. This difference is probably due to the difference in the load curves for these two cases, as discussed in the previous section in reference to figure 19. A stable slope load typically produced one of three general patterns of emissions. The first is a sharply rising plot at the beginning of the test, then declining as the load rate decreases. The second pattern is a slowly decreasing plot and thirdly, a level trend with oscillations along the way. In only one case did the AE signal strength increase steadily throughout the test, though not at a steep angle.

Overall, the AE signal strengths tended to decrease as the test progressed 67 pct of the time. This is probably because the bearing capacity of the soil was usually exceeded in the stable slope tests. A small localized failure occurred directly under the load tire, relieving the stress built up in the soil. Once this occurred, the emissions tended to decrease or at least continue at the same rate. This localized failure caused some soil movement, but it was not a large enough movement to produce a significant amount of emissions. Thus, the net effect was generally a decrease in the AE signal levels.

An unstable slope loading 3 in from the slope crest produced an AE signal strength plot that is either level or steadily rising. In 80 pct of these tests the AE signal strength rose throughout the test. This may be explained by the following. First the stress built up in the soil, which should have caused the emissions to rise (*4,9,13,14,18,19,29*).

Then the soil began to fail and move, which caused more emissions (*8,9,12,27,30*). One would thus expect the emissions to have increased as the load increased near the edge of the slope and the slope became more unstable. The failure that occurred near the slope edge was much larger than the localized failure of the stable slope. This larger failure probably produced enough movement to create enough emissions to counteract any stress relief, which tends to reduce the emissions.

The unstable slope emissions tended to be stronger than those of a stable slope, with all other slope and load conditions being constant. In approximately 60 pct of the tests the signal strength was higher near the slope edge than away from it. The average amplitude plot in figure 23 is a typical example of this. This plot shows test STAT 9.3 loading 12 in from the edge and STAT 10.1 loading 3 in from the slope edge. These curves have been smoothed to make them easier to distinguish. But, not all tests produced higher AE signal strengths near the slope edge. Table 2 lists several tests that produced the opposite trend; see tests STAT 4 versus STAT 6, STAT 4 versus STAT 5, and STAT 7 versus STAT 8. In some cases one AE signal strength measure (such as amplitude) may indicate stronger AE near the slope edge while another signal strength

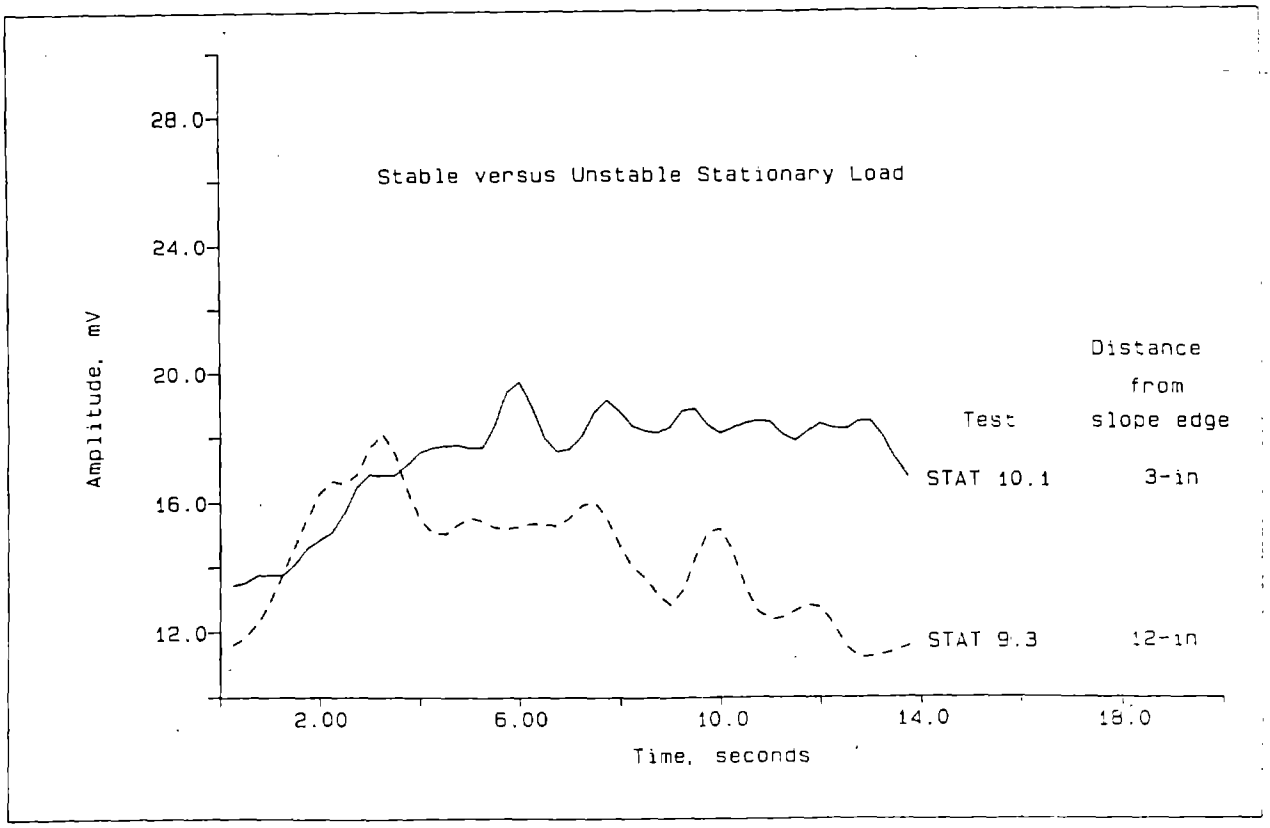

Figure 23.--Stationary load amplitudes at 3 in and 12 in from slope edge.

measure (such as ring-down count rate) may indicate the opposite. When making these comparisons one must remember to compare data from waveguides that were the same distance from the load tire and with similar loading conditions. Most of the comparisons made here are between tests with the load tire and waveguide 3 in from the slope edge and those with the load and waveguide 12 in from the edge. In these two cases the waveguides were the same distance from the tire but at different distances from the slope edge. One may also compare a test with the tire 3 in from the slope and the waveguide 12 in from the slope to a test with these waveguide and tire locations reversed. Though these data are included in the tables, the additional variable results in more complex data analysis, and precludes comparisons with other data sets.

The cumulative ring-down counts at a 3.2-mV or 10-dB threshold (total counts) were generally higher for a stable slope than for an unstable slope. But, the ring-down count rates (40-mV or 32-dB threshold) were generally higher near the slope edge. This apparent discrepancy is explained by a closer examination of the amplitude distribution plots. Figure 24 A shows the amplitude distribution for a stationary load 12 in from the slope edge, with a total count of 17,856 and an average 40-mV threshold count rate of 72 c/s (test STAT 11.3, table 2). Figure 24 B shows a load at 3 in from the edge, with a total count of 10,931 and an average count rate of 174 c/s (test STAT 12.1). The counts are skewed towards the lower amplitudes when loading away from the slope edge (fig. 24 A), but are skewed more towards the high amplitudes when loading near the edge (fig. 24 B). This difference results in more 40-mV threshold (32 dB) ring-down counts being obtained near the edge of the slope, and also the generally stronger average amplitudes and energies. The larger amplitude signals near the edge of the slope may be the result of the larger amount of soil movement taking place as the slope edge failed. Overall it appears that there was a greater tendency for the AE's to be stronger when loading near the unstable edge as compared to a load on more stable soil away from the slope edge.

Frequency Spectra

A closer look at the frequency domain may provide a clearer picture of the differences in loading on an unstable versus stable slope. The frequency spectra of some stationary tests were examined to compare the frequency content of a stable slope to an unstable slope loading. The PSD plots in figures 25 and 26 show the average spectra of the complete test from start to end. Figure 25 compares test STAT 7.3, a stable load, to test STAT 8.1, an unstable load. The unstable slope had a higher frequency peak than the stable slope (664 Hz versus 610 Hz). Figure 26 compares test STAT 11.3, a stable slope, to STAT 12.1, an unstable slope. In this case the unstable slope had a lower peak frequency than the stable slope (571 Hz versus 903 Hz), the opposite of those above. Both these cases were common and occurred nearly equally. A slight increase in the PSD in the frequency range of 4000 Hz to 5000 Hz for the stable slope was observed in all tests. This can be seen in figures 25 A and 26 A. This tendency is a little more noticeable in figure 26 A than in figure 25 A.

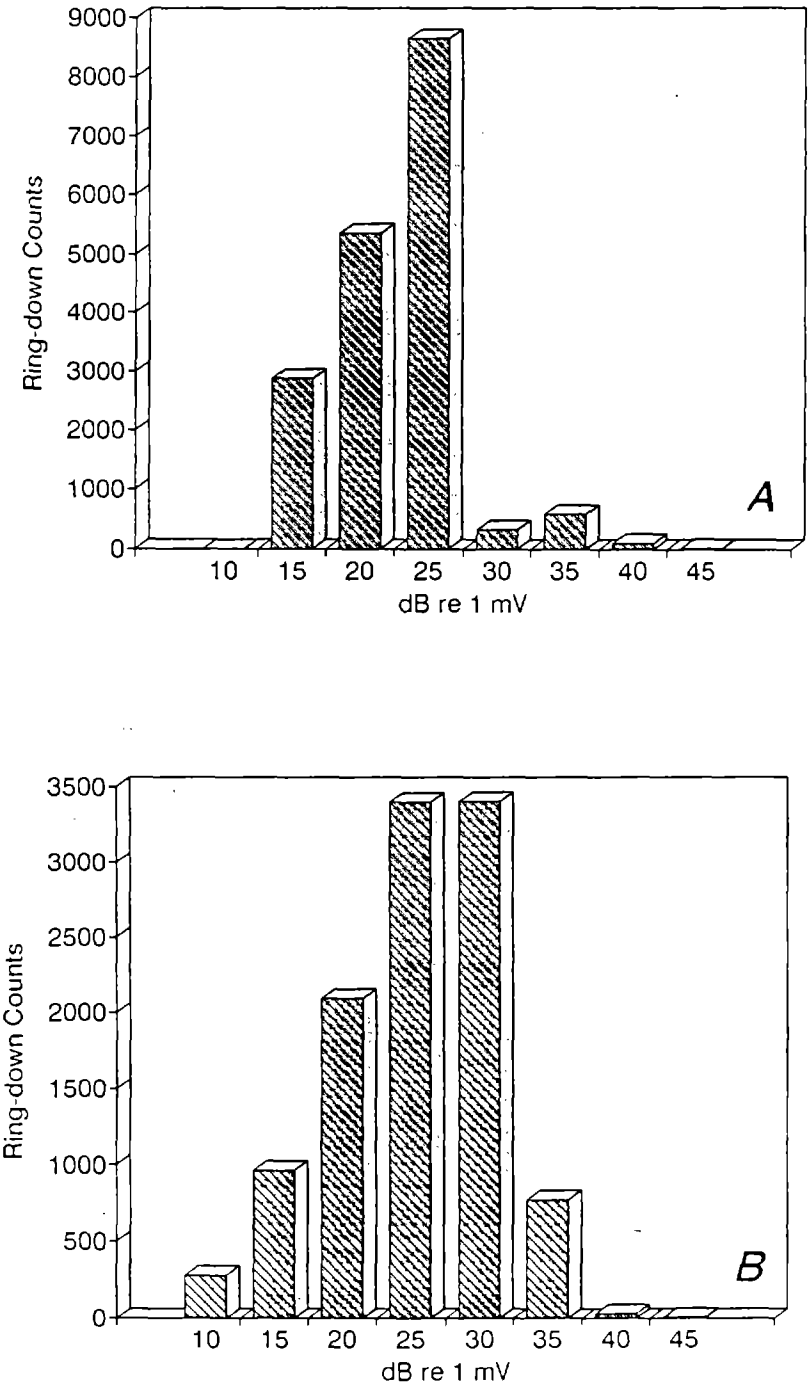

Figure 24.--Amplitude distributions of stationary loads at 12 in (A) and 3 in (B) from slope edge.

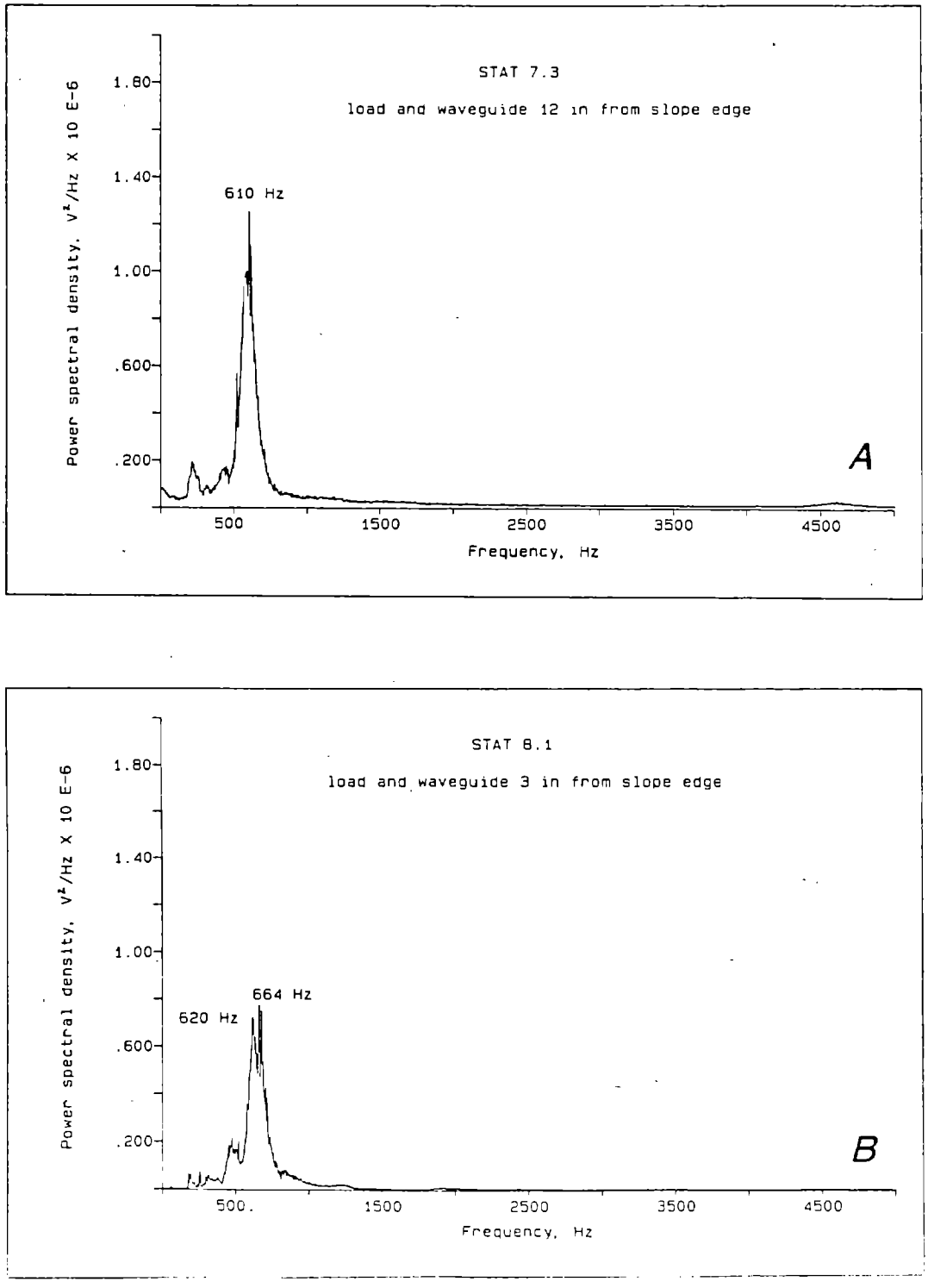

Figure 25.--Power spectral densities of stationary load tests STAT 7.3 (A) and STAT 8.1 (B), at 12 in and 3 in from slope edge, respectively.

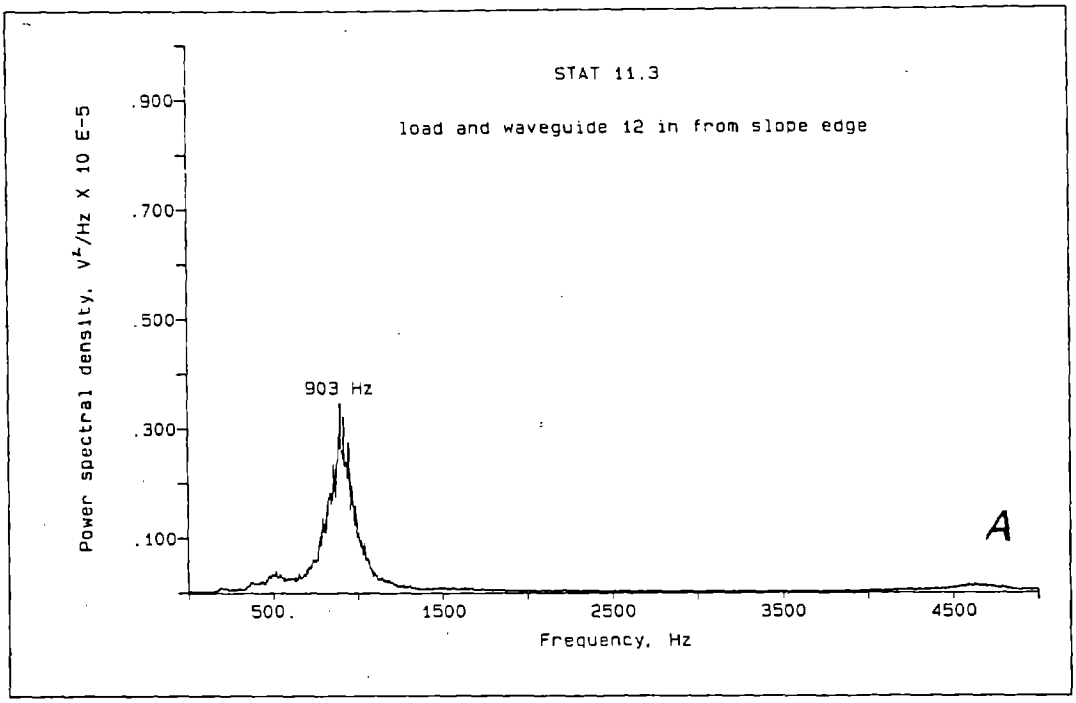

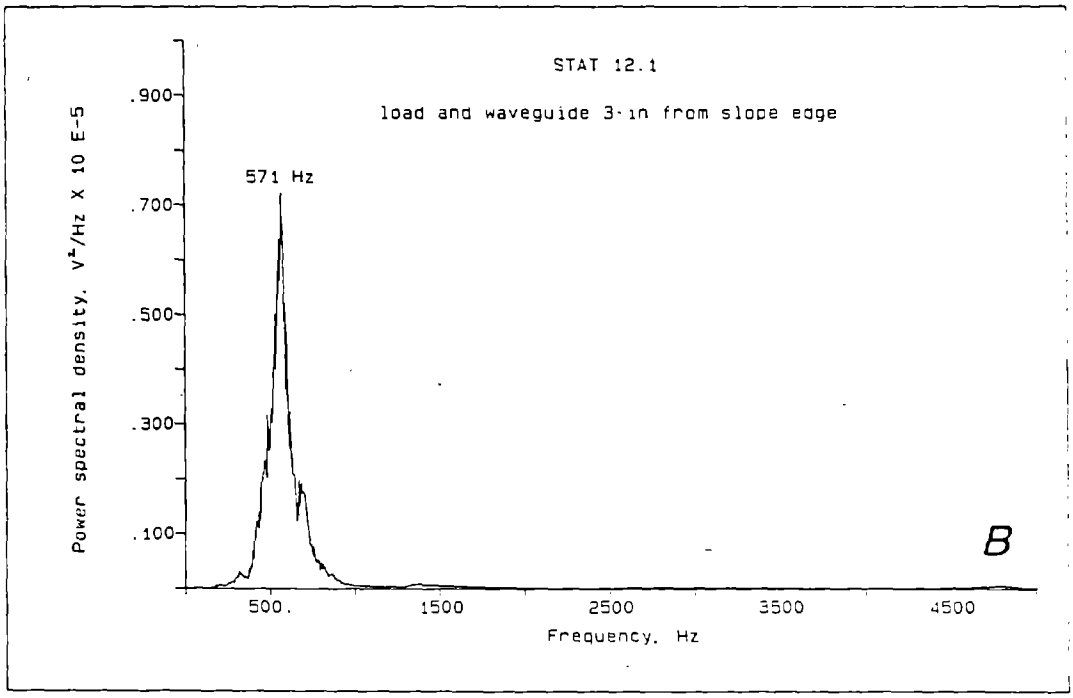

Figure 26.--Power spectral densities of stationary load tests STAT 11.3 (A) and STAT 12.1 (B), at 12 in and 3 in from slope edge, respectively.

Comparing the frequency between a stable and unstable slope by observing the average peak frequency (as described above), results in the frequency of the unstable load being higher about 50 pct of the time, compared to a lower frequency 44 pct of the time (the remainder being about equal). But, when comparing frequency based on the average frequency of the 100 largest PSD's, the results are quite different. When compared in this way, the frequency was lower near the slope edge 89 pct of the time. This may be a reflection of the increased response in the 4000 to 5000 Hz range for stable slope loadings, as discussed above in figures 25 and 26. Both of these methods of analyzing the average frequency for a test are given in table 2. Other researchers have reported a shift to lower frequencies as the stress placed on a material is increased or as the load increases as a percentage of the ultimate breaking load (*14,29,31*). This would tend to support a decreasing frequency near the edge of the slope.

Effect of Toe Removal

The purpose of these tests was to create an unstable slope in a slightly different manner than simply adjusting the load point to slope edge distance. Soil at the base of the slope was removed in an effort to create an unstable condition. Within a series of tests, the toe was progressively removed until the slope failed. The load was placed a little further back from the slope edge in these tests in order to prevent the slope from failing right away, before toe removal. Also, the load pressure was reduced, again to prevent a premature failure.

The data for the toe removal tests are shown in table 4. The rate and strength of AE was expected to increase as the toe of the slope was removed, but in many cases this did not happen. This is contrary to similar testing done by others (*13,14,27,30*). In general there was very little difference in the strength of the emissions as the toe was removed. The toe was removed one inch with each successive test. Most of the slopes were 9-in high, so each removal was about 11 pct of the slope height. Normally about 33 pct of the toe was removed before the slope failed. The data from tests TOE 5-7 show the signal strengths decreasing slightly as the toe was removed. This is the most typical result of these tests. In tests TOE 8-10 the amplitude and energy rates increased by a very small amount, but the ring-down count rate increased significantly with each removal of the toe.

There does appear to be an increase in the average frequency during the test that is run just before failure. For example, in tests TOE 5-7, test 7 has the highest average frequency (fig. 27). In this series of tests the slope failed after TOE 7, while the toe was being removed for the next test. This also happened in the series of tests TOE 11-14, where TOE 14 had the highest frequency (fig. 28) and was the last test before the slope failed.

Throughout these tests it was very difficult to capture data that included the failure of the slope. The slope often failed while the toe was being removed or immediately after, but before the data recorder was started. The slope did not fail until after data recording had stopped in some of the tests. Because of the limited memory, the length of data recording time was not long enough in these cases to capture that data.

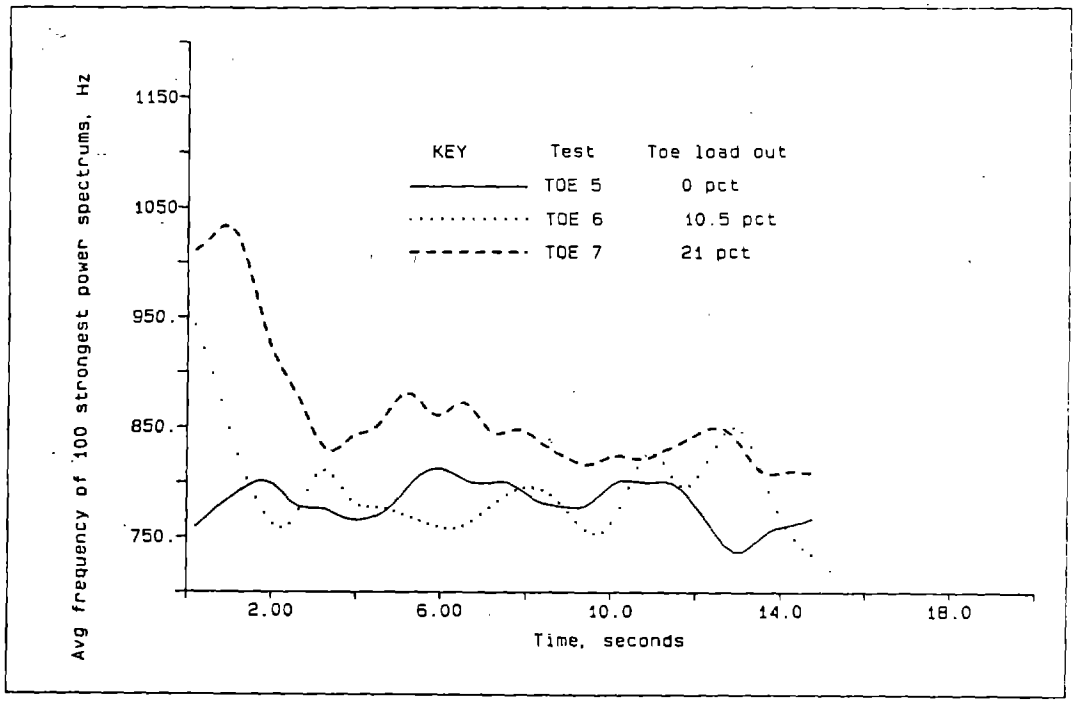

Figure 27.--Frequency trend with time for tests TOE 5-7.

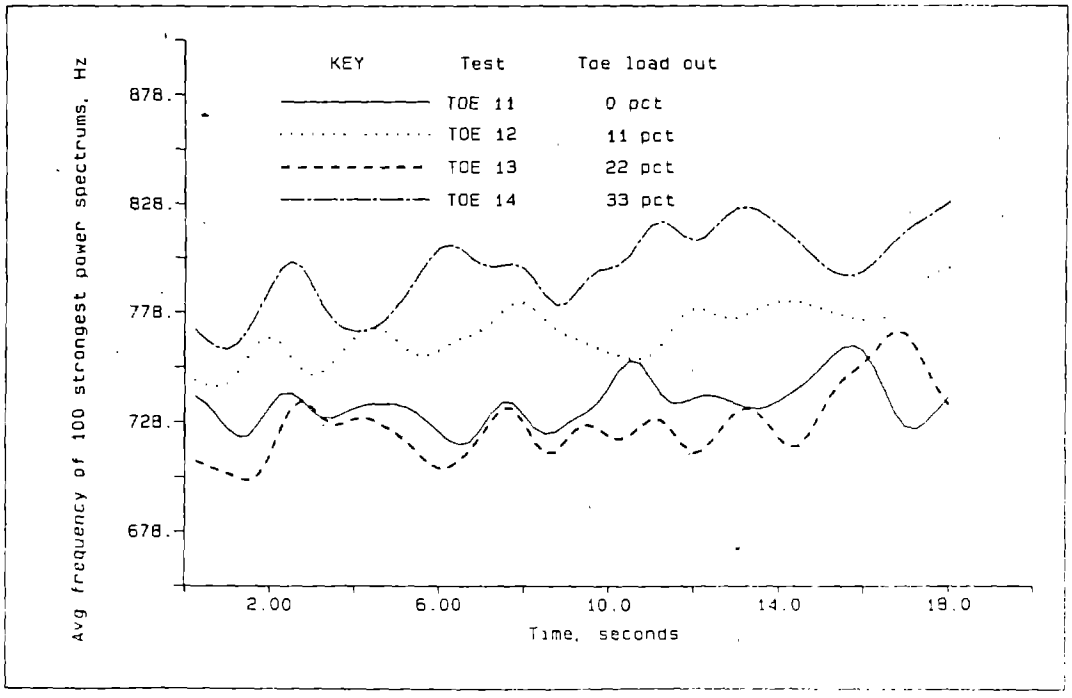

Figure 28.--Frequency trend with time for tests TOE 11-14.

In a few tests the toe was removed while the data recorder was running. Slope failure was captured on the data recorder, but the toe removal procedure produced sufficient noise that the slope failure AE signals were obscured. The average frequencies during the toe removal and slope failure periods were extremely erratic, varying by up to 700 Hz. In table 4, notice the high count rates of test TOE 4, which was loaded out while recording data. This is due to the digging and scraping noises created while removing the toe. Because of the erratic nature and noise of these tests, no further data analysis was performed.

Dynamic Load Tests

The small scale dynamic load tests were designed to simulate a haulage truck backing up to a dump point. Most tests were conducted with the tire starting 10 to 15 in from the slope crest and run until slope failure occurred. This generally provided 15 to 20 s of data. In the initial stages of testing, the soil was not strong enough for the wheel to ride over the soil surface. The wheel barely turned and tended to plow through the soil. As stated earlier, bentonite clay was added to the sand and gravel mixture to produce a stronger slope surface. This allowed a larger vertical load to be placed on the soil and thus made the slope failures larger and easier to detect. Without the clay in the soil, only small loads could be placed on the slope and essentially no slope failure occurred. Even with the extra clay, the load had to be monitored to prevent the tire from sinking and plowing into the soil. The single tire caster was used early in the study, but the dual tire caster was found to work better and was used for all subsequent testing.

In the early stages of testing the load pressure was increased manually as the tire moved toward the slope edge. This was done to make sure a slope failure occurred and to ensure that the tire would keep up with the moving slope as failure occurred. These tests are identified in table 5 by the "M" placed in front of the load rate value. The number given is the final load pressure (psig) reached at the end of the test. In most cases there would have been no slope failure if the pressure had not been increased. A few cracks would form at the edge of the slope, but no true slope failure. In later tests the initial load pressure was increased and the maximum flow rate used so that the load pressure could be kept constant throughout the test. This produced more reproducible tests and made test comparisons easier.

Signal Strength

Figure 29 is an example of an amplitude versus time plot of a dynamic load test (DYN 1.1, table 5), as displayed by the digital waveform recorder. The same test data is shown in figure 30 after averaging and plotting with Asystant. A trace of the load cell output was added to the plot to make interpretation of the data easier. The level of AE activity tended to increase as the load tire moved toward the slope edge and the slope began to weaken and fail. The time at which the load cell output dropped suddenly was when the failure

Table 5.--Dynamic load test data

Test number	Distance to Waveguide, in slope	tire	Tire/slope distance, in start	end	Slope failure time, s	Waveguide even with tire, s	Amplitude avg mV	max time, s	Count rate [1]c/s	Energy rate [2]V²/s	[3]Frequency avg Hz	max time	Soil moist [4]pct	comp [5]t/ft²	Vertical load [6]psig	[7]flow
DYN 1.1	6	6	10	2	13.6	6.4	16.7	13.3	114	8.7	724	3.7	0	>5	10	M48
DYN 1.3	6	12	10	2	13.6	6.4	11.9	13.3	181	3.1	651	2.5	0	>5	10	M48
DYN 2.1	6	6	10	2	15.9	6.9	15.4	11	96	6.9	677	3.6	0	>5	10	M62
DYN 2.3	6	6	10	2	15.9	6.9	13.4	8.5	92	4.5	865	0.4	0	>5	10	M62
DYN 3.1	6	6	10	2	NA	9.3	12.3	7.8	53	2.6	739	4.2	5.8	0.5	10	M40
DYN 3.2	12	6	10	2	NA	9.3	13.6	9.5	60	3.3	634	9.2	5.8	0.5	10	M40
DYN 4.1	6	12	10	2	NA	7.4	8.4	6.3	6.4	1.2	670	8.9	5.8	0.5	10	M35
DYN 5.1	6	6	12.5	0	15.5	12.7	13.8	14.2	163	4.7	1110	3.3	5.6	0.9	7	M40
DYN 5.2	12	6	12.5	0	15.5	0	8.5	5	46	1.7	1084	3.3	5.6	0.9	7	M40
DYN 6.1	8	6	12.5	0	20.6	7.8	12	10	88	3.6	1062	4.1	5.6	0.9	7	M35
DYN 6.2	8	12	12.5	0	20.6	7.8	5.5	11.2	2.4	0.52	868	25	5.6	0.9	7	M35
DYN 7.1	12	12	13	0	NA	0	8.6	3.2	14	1.5	745	0.8	5.6	0.9	7	M40
DYN 7.2	12	16	13	0	NA	0	11.3	4	98	3.3	1061	0.8	5.6	0.9	7	M40
DYN 8.1	6	6	14	8	NA	>15	14.4	6	68	3.6	558	2.4	3.6	0.5	10	5.9
DYN 8.3	12	6	14	8	NA	3.4	14.4	1.8	82	3.8	878	3.5	3.6	0.5	10	5.9
DYN 9.1	6	6	12	5	NA	11	12.9	5.3	62	3.2	632	2.5	3.6	0.5	10	5.9
DYN 9.3	12	6	12	5	NA	0	11.2	5	33	2.4	740	7.7	3.6	0.5	10	5.9
DYN 10.1	6	6	11	3	NA	NA	7.7	5.4	15	1.4	579	11.2	3.6	0.5	10	5.9
DYN 10.3	12	6	11	3	NA	NA	6.7	2.8	5.2	1.2	774	11.8	3.6	0.5	10	5.9
DYN 11.1	6	6	8	0	13.7	5.4	8.7	13.5	6	1.1	639	5.8	3.6	0.5	10	5.9
DYN 11.3	12	6	8	0	13.7	<0	8.1	0.25	5.6	0.8	704	0.6	3.6	0.5	10	5.9
DYN 12.1	14.5	6	16.5	8	NA	3.6	4.7	9	3.2	0.44	924	9	2	3.8	10	5.9
DYN 12.3	8.5	6	16.5	8	NA	>15	4	14.3	4	0.36	800	8.5	2	3.8	10	5.9
DYN 13.1	12.5	6	16.5	8	NA	7.8	4.8	14.3	2.8	0.44	859	9	2	3.8	10	5.9
DYN 13.3	18.5	6	16.5	8	NA	<0	4.2	14.3	1.2	0.32	654	2.8	2	3.8	10	5.9
DYN 14.1	14.5	6	16.5	8	NA	2.8	17.4	10	156	5.3	720	12.5	4.8	0.4	10	5.9
DYN 14.3	8.5	6	16.5	8	NA	14.5	14	3.5	124	3.4	833	2.5	4.8	0.4	10	5.9
DYN 15.1	11.5	6	15.5	7	NA	7	15.9	6.3	132	4.6	827	4.4	4.8	0.4	10	5.9
DYN 15.3	17.5	6	15.5	7	NA	<0	17.2	6.3	152	5.6	692	0.8	4.8	0.4	10	5.9
DYN 16.1	12	6	11.8	0	12	0	8.2	1.3	46	1.8	1111	1.3	5	0.9	8	M33
DYN 16.2	6	6	11.8	0	12	8.4	12.3	6.5	168	4.1	1094	1.3	5	0.9	8	M33
DYN 17.1	6	6	13.5	3.5	NA	15	20.5	5.8	264	8.4	822	12	5.8	<.2	8	5.9
DYN 17.2	12	6	13.5	3.5	NA	3.5	15.4	6.3	140	4.8	1037	1.8	5.8	<.2	8	5.9
DYN 18.1	6	6	13.5	3.5	NA	15.5	20.3	11	292	7.5	839	14.7	5.8	<.2	10	5.9
DYN 18.2	12	6	13.5	3.5	NA	3.5	14.9	3.5	136	4.2	1062	3.5	5.8	<.2	10	5.9
DYN 19.1	6	6	13.5	3.5	NA	15.5	22.9	11.8	352	9.8	852	12.7	5.8	<.2	12	5.9
DYN 19.2	12	6	13.5	3.5	NA	3.5	16.6	2.8	196	5.6	1078	4	5.8	<.2	12	5.9
DYN 20.1	6	6	13.5	3.5	NA	15	14	14	92	4.9	630	12.5	2.5	1.7	7	4
DYN 20.2	12	6	13.5	3.5	NA	1.5	10	5.8	44	2.6	879	5.1	2.5	1.7	7	4
DYN 21.1	6	6	13.5	3.5	20	15	17	10.5	144	6.7	639	12.6	2.5	1.7	11	4
DYN 21.2	12	6	13.5	3.5	20	2	13.5	2.8	96	4.1	890	1	2.5	1.7	11	4
DYN 22.1	6	6	13.5	3.5	NA	15	9.4	11.3	37	-2.4	749	17.3	2.5	1.7	6	5.9
DYN 22.2	12	6	13.5	3.5	NA	2	7.9	11.3	27	1.6	865	4	2.5	1.7	6	5.9
DYN 23.1	6	6	13.5	3.5	NA	15	11	11	42	2.4	674	14	2.5	1.7	8	5.9
DYN 23.2	12	6	13.5	3.5	NA	2	10	6.5	47	2.2	814	2.5	2.5	1.7	8	5.9
DYN 24.1	6	6	13.5	3.5	20	15	10.7	14.4	41	2.3	703	19.5	2.5	1.7	10	5.9
DYN 24.2	12	6	13.5	3.5	20	2	9.6	3.8	42	2.1	824	2.3	2.5	1.7	10	5.9

See footnotes at end of table.

Table 5.-Dynamic load test data-Continued

Test number	Distance to Waveguide, in slope	tire	Tire/slope distance, in start	end	Slope failure time, s	Waveguide even with tire, s	Amplitude avg mV	max time, s	Count rate [1] c/s	Energy rate [2] V^2/s	[3]Frequency avg Hz	max time	Soil moist [4] pct	comp [5] t/ft^2	Vertical load [6] psig	[7] flow
DYN 25.1	6	6	12.5	0	14.3	11.7	12.6	11.5	124	3.7	1092	2.5	5.3	1.1	8	M36
DYN 25.2	6	6	12.5	0	14.3	11.7	10.6	11.5	68	2.6	969	11.8	5.3	1.1	8	M36
DYN 26.1	6	6	12.5	0	16.2	9	7.4	11.8	15	1.1	1046	9.4	5.4	1.1	8	M36
DYN 26.2	12	6	12.5	0	16.2	0	5.3	1.2	6	0.6	1204	0.4	5.4	1.1	8	M36
DYN 27.1	6	6	12.3	0	15.6	9.5	7.5	13	7.6	1	913	5.1	5.2	1.1	8	M40
DYN 27.2	6	6	12.3	0	15.6	9.5	8	7.6	23	1.3	1029	8.6	5.2	1.1	8	M40
DYN 28.1	16	6	16.5	2.5	>25	0	12.1	2.5	80	3.1	1075	2.6	4.9	0.8	8	M35
DYN 28.2	12	6	16.5	2.5	>25	8.9	15	11.5	160	5	1156	11.4	4.9	0.8	8	M35
DYN 28.3	6	6	16.5	2.5	>25	22.3	18	20.1	216	6.5	913	14	4.9	0.8	8	M35
DYN 29.1	6	6	15.3	1.5	21	23.5	11	21	80	2.6	888	19	3.1	0.95	8	M36
DYN 29.2	12	6	15.3	1.5	21	8.8	8.9	2.6	36	1.7	1234	13.3	3.1	0.95	8	M36
DYN 29.3	16	6	15.3	1.5	21	0	7.9	2.6	28	1.4	1298	0.6	3.1	0.95	8	M36
DYN 30.1	6	6	14	2	NA	15	16	7.5	149	4.8	961	8.2	3.8	0.5	8	M35
DYN 30.2	6	[8]A	14	2	NA	15	21	14	288	8.5	841	7.6	3.8	0.5	8	M35
DYN 30.3	6	[9]H	14	2	NA	NA	12.3	11.2	72	2.8	955	6.3	3.8	0.5	8	M35
DYN 31.1	6	6	14.5	2.5	NA	14.6	19.7	9	252	7.3	929	6.8	3.8	0.5	8	M36
DYN 31.2	6	[10]A	14.5	2.5	NA	14.6	12.1	14.5	48	2.6	697	17	3.8	0.5	8	M36
DYN 31.3	6	H	14.5	2.5	NA	NA	13.2	9	104	3.2	903	1.3	3.8	0.5	8	M36
DYN 32.1	12	6	10.5	2	NA	<0	8.8	3.5	14	1.5	706	2.8	4.8	0.5	10	5.9
DYN 32.3	6	6	10.5	2	NA	7.2	9.7	2	28	2	783	5	4.8	0.5	10	5.9
DYN 33.1	12	6	10.5	2	NA	<0	10.5	3.5	31	2.1	655	1	4.8	0.5	10	5.9
DYN 33.3	6	6	10.5	2	NA	6.9	8.4	3.8	11	1.6	777	2.6	4.8	0.5	10	5.9
DYN 34.1	12	6	10.5	2	NA	<0	9	3.5	32	1.8	745	0.9	4.8	0.5	10	5.9
DYN 34.3	6	6	10.5	2	NA	7.8	13.3	3.8	89	3	793	3.7	4.8	0.5	10	5.9
DYN 35.1	6	6	10	2	NA	6.2	11	6.5	52	2.6	855	3.7	5.7	0.6	8	M28
DYN 35.3	12	6	10	2	NA	<0	12	6.5	15	2.2	741	13.9	5.7	0.6	8	M28
DYN 35.4	6	12	10	2	NA	6.2	7	5.8	4.4	0.92	566	5.5	5.7	0.6	8	M28
DYN 36.1	6	6	10	2	NA	7.1	8.5	6.5	19	1.3	830	2.5	5.7	0.6	8	M29
DYN 36.3	12	6	10	2	NA	<0	7.4	6.8	1.6	1.1	718	13.5	5.7	0.6	8	M29
DYN 36.4	6	12	10	2	NA	7.1	7.1	2.5	0.8	0.84	622	14.3	5.7	0.6	8	M29
DYN 37.1	6	6	10	2	NA	NA	8.5	3.8	8	1.2	588	5.8	5.7	0.6	8	M30
DYN 37.3	12	6	10	2	NA	<0	8	2.8	10	1	836	1.3	5.7	0.6	8	M30
DYN 37.4	6	12	10	2	NA	NA	7.1	4.3	1.6	0.84	740	1.4	5.7	0.6	8	M30

NA = Not available

[1]Ring-down count rate (40 mV threshold).
[2]Average energy rate.
[3]Average frequency of 100 largest power spectrums.
[4]Percent soil moisture.
[5]Compressive strength of soil from pocket penetrometer.
[6]Vertical cylinder air pressure.
[7]Number without M indicates vertical cylinder, micrometer flow control valve setting (5.9=max flow), number with M indicates final air pressure, which was increased manually during test.
[8]Waveguide entered soil at 30° angle 6 in from tire, parallel to slope edge.
[9]Wvaveguide was horizontal, perpendicular and 6 in from tire, 2.25-in deep.
[10]Waveguide entered soil at 30° angle 12 in from tire, parallel to slope edge.

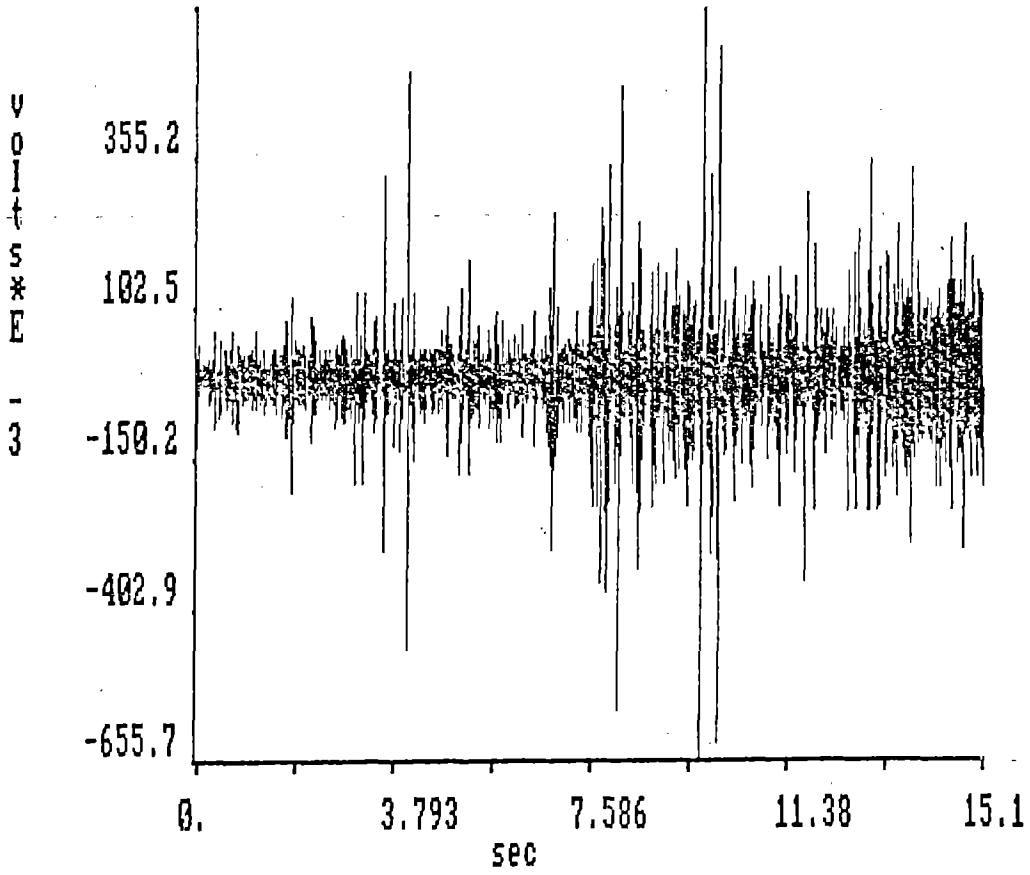

Figure 29.--Digital waveform recorder display of test DYN 1.1.

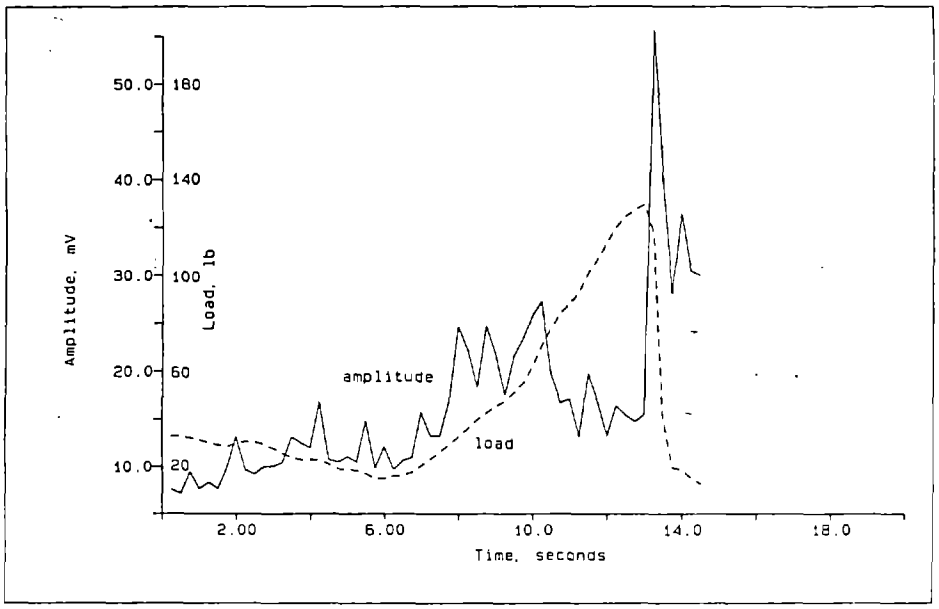

Figure 30.--Average amplitude and load cell output for dry, high compressive strength slope, test DYN 1.1.

occurred. The soil for this test was very dry and had a high compressive strength. A large wedge type failure occurred very suddenly, as evidenced by the large spike in average amplitude at the same time the load cell output was falling (fig. 30). This is not typical of most slopes, which were not as strong or dry. The weaker slopes form surface cracks before the actual failure as the tire approaches the edge of the slope. Test DYN 1.1 did not form any surface cracks, and failure occurred very suddenly.

A typical test with a moist and low compressive strength soil (test DYN 3.1, table 5) has an average amplitude and load cell output plot like that in figure 31. Notice that the amplitude and load increased initially, reached a peak and then dropped as the tire approached the slope edge and failure occurred. The load cell curve looks similar whether the load was increased manually during the test or the load pressure was kept constant. The amplitude plot generally peaks at the same time as the slope failed or immediately before failure. After the failure had started, the amplitude generally fell back down, even if the slope was still in the process of failing. This is probably due to the large decrease in the soil stress after the initial failure had begun. The timing of the peak in relation to the slope failure depended on the location of the waveguide. This will be discussed in more detail in a following section.

The average peak amplitude detected by the unamplified accelerometers in the dynamic load tests test was 2.2 mV or about 0.022 g. The maximum

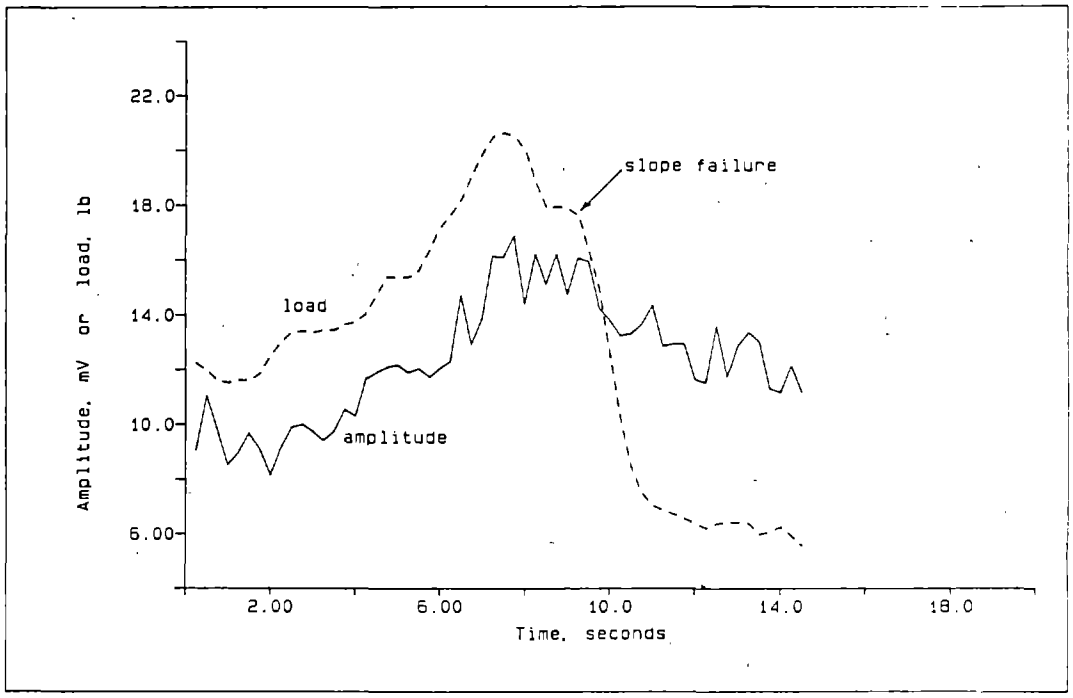

Figure 31.--Average amplitude and load cell output for moist, low compressive strength slope, test DYN 3.1.

peak amplitude obtained was 8.4 mV or 0.084 g. The accelerometers have an acceleration range of 0.005 g to 10,000 g. Only the low end of the accelerometers' range was utilized, and thus were not used to their full capabilities. The mean of the averaged amplitudes as output by the accelerometer, amplifier and filter was 13 mV, with a minimum of 4 mV and a maximum of 23 mV.

Koerner, et al. (*12*), report a maximum count rate of 7700 c/min for cut embankment tests in the field. The average count rate for the dynamic load tests in table 5 is 72 c/s or 4320 c/min. The average of the maximum count rates for all the tests in table 5 was 220 c/s or 13,200 c/min. A peak count rate of 43,440 c/min was recorded in test DYN 5.1. The count rates obtained here are significantly higher than those reported by others. This is probably the result of the high noise rates generated by the tire contacting the soil.

Soil Moisture/Compressive Strength

Some slopes were allowed to dry to increase the compressive strength of the slope. This allowed larger loads to be placed on the soil, produced larger slope failures, and stronger emissions. Drying the surface of the slope provided a hard loading surface which resulted in large wedge type slope failures. The internal moisture of the slope was nearly the same as the freshly made slope, just the surface had dried. The exceptions to this are tests DYN 1 and DYN 2, where the slope was dried completely for about a week. The objectives of these tests was to measure AE's from stronger slopes, not to evaluate the effects of soil moisture. But, some useful information on the effects of soil moisture and soil compressive strength was gained.

The effect of soil moisture alone, without a corresponding change in soil compressive strength, can be seen from tests DYN 10 and 32 (table 5). Both these tests had the same soil compressive strength (0.5 t/ft^2) but different soil moisture contents. Test DYN 10 had 3.6-pct water and test DYN 32 had 4.8-pct water in the soil. The AE signal levels can be seen to increase as the soil moisture increases. The change in frequency is different for the two waveguide positions and thus no trend can be noted.

Sixteen test pairs were found in table 5 which had different soil moistures and compressive strengths but similar loadings. These tests were analyzed to determine if any soil moisture/compressive strength trends were present. The average AE signal strengths increased with increasing soil moisture in eight of the sixteen cases. While the effect of soil moisture was split, the effect of soil compressive strength was more pronounced. Of the eight test pairs which showed a direct relationship between moisture and AE signal strength, seven had an inverse relation with compressive strength. Of the eight test pairs which showed an inverse relationship between moisture and AE signal strength, five of them had an inverse relation with compressive strength. Thus, three quarters of these tests showed an increase in AE strength as the soil compressive strength decreased. Compressive strength appears to have a greater affect on the AE signal strength than soil moisture does. This was true for all waveguide locations. This

seems reasonable because a compacted, more rigid soil will have less tendency to move and therefore produce fewer emissions.

The effect of soil moisture/compressive strength on the frequency was not significant. The average frequency of the 100 largest power spectrums, tended to increase slightly as the soil moisture increased and the compressive strength decreased.

Stable Slope Tests

A few tests were conducted with the load placed at least 15 in away from the edge of the slope and never approaching the slope edge to a distance less than 7 in (a stable condition). In these tests, the load cell output tended to rise slightly through a narrow range as the test progressed on a moist slope with a low compressive strength. The load continued to rise during the test because the tire sank into the soil as it moved, encountering more resistance. The amplitude followed the same general trend as the load curve. The average amplitude for these moist, stable slopes were higher than a comparable unstable slope test that produced a slope failure. It appears from this, that most of the emissions detected by the transducers for a moist slope are being generated by the tire rolling across the soil surface. The additional AE created by the failure of the slope are small in comparison.

For a dried, stable slope with a higher compressive strength, the load cell output also rose, but to a greater magnitude than the weaker slope. The resultant load on the soil is greater for the dry slope because the soil is strong enough to support the increased load. The average amplitude generally rose with the load cell output. With this hard and dry soil surface (test DYN 12.1, table 5), the average amplitude of the AE picked up by the accelerometers was three to four times smaller than those of the moist slope (DYN 14.1, fig. 32). Figure 33 shows the difference in amplitude distribution between a dry stable slope (DYN 13.1) and a moist stable slope (DYN 15.1). The counts for the dry slope (fig. 33 A) are skewed towards the low amplitudes while the moist slope counts (fig. 33 B) occur at higher amplitudes. In addition, the total counts for the moist slope were 12,580 compared to only 7173 counts at 10 dB for the dry slope. Thus the slope with the higher moisture and lower compressive strength is generating more, and stronger, tire noises than a drier and stronger slope, even though the resultant load on the soil is less.

With the hard dry slope, the tire was able to ride over the soil surface without causing the soil under the tire to move, i.e., the soil was strong enough to support the load. But with a moist, low compressive strength slope, the soil was continually moving and compacting under the tire as it rolled along. In effect the soil was under going a continuous local failure immediately below the tire. With this continuous failure taking place, it was difficult to determine when a larger, more significant slope failure was taking place in unstable slope tests. The tire would sink into the soil and plow through the soil instead of rolling over the surface when the load was too large for the strength of the slope. In these cases the AE signal levels tended to be higher than other tests.

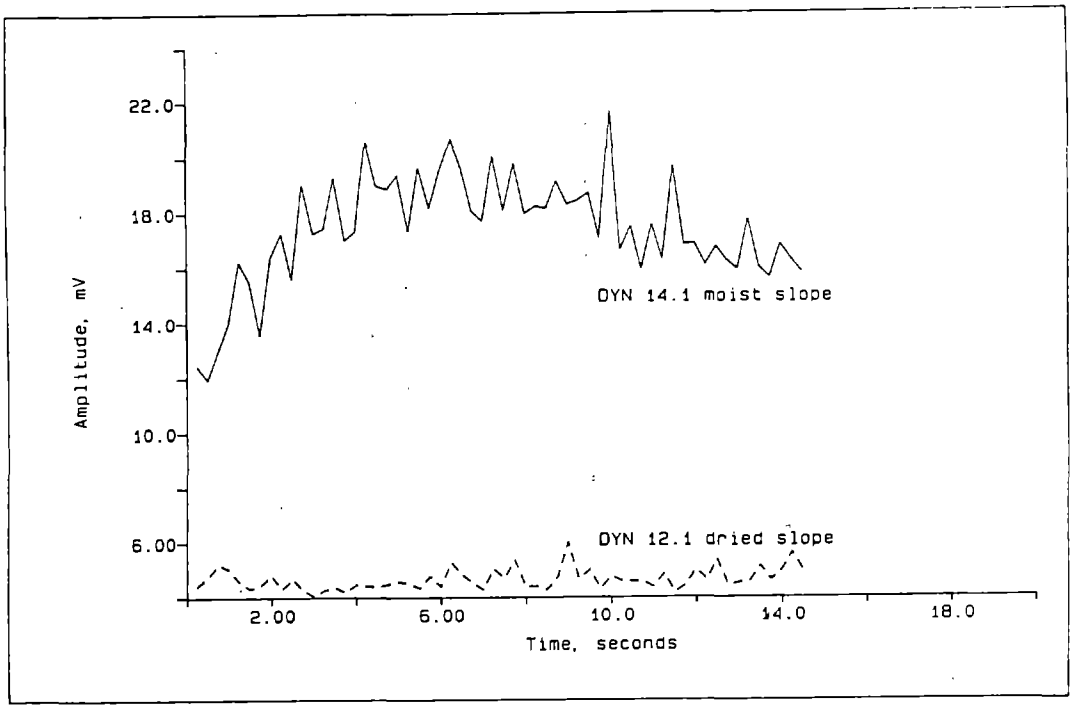

Figure 32.--Stable slope amplitudes of dried slope test DYN 12.1 versus moist slope test DYN 14.1.

Effect of Waveguide Placement

As stated in the previous section, waveguide position had a significant effect on the AE waves detected by the accelerometer. This was no surprise considering the high attenuation rates through the soil. Waveguide placement was not much of a factor in the stationary load tests, because the waveguides were usually placed at equal distances from the tire in every test, and the load point was not moving. This was different for the dynamic load tests, where the tire was continually moving. The distance between the tire and the waveguide was changing and therefore the attenuation of the noise created by the tire was changing. This made the analysis of the data much more difficult.

Waveguide placement for dynamic load tests was based on the distance of the waveguide from the edge of the slope and also from the tire. The diagram in figure 34 shows the layout of a typical test. The tire path during a test was always perpendicular to the crest of the slope. During the early stages of the study, the waveguides were placed as close as 4 in to the side of the tire. This was changed to 6 in later on. This distance was thought to be more realistic to a field test situation where it would be unsafe to get too close to a operating haulage truck. Distances out to 16 in were used, but 12 in was used most commonly for the waveguide furthest from the tire. Different waveguide to slope crest distances were also experimented with. The distance chosen for most testing was 6 or 12 in from the slope edge. Thus waveguides were usually set up on a 12-in by 12-in grid, divided

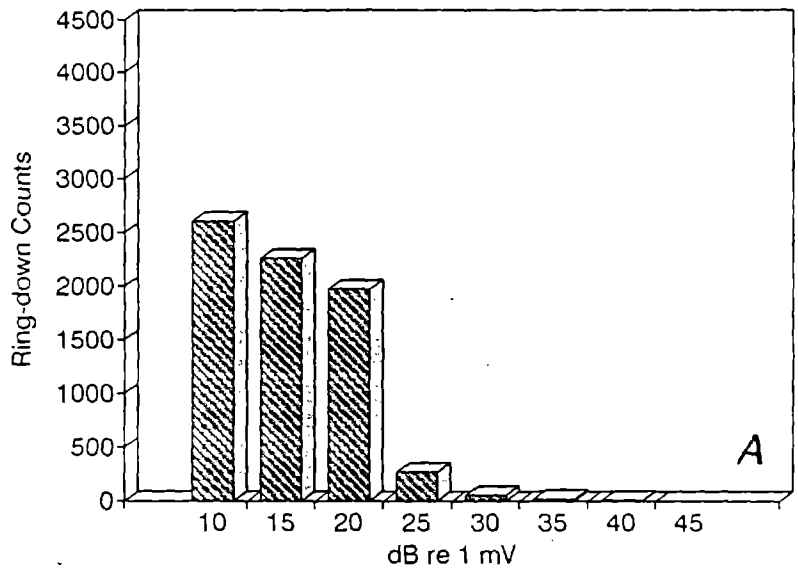

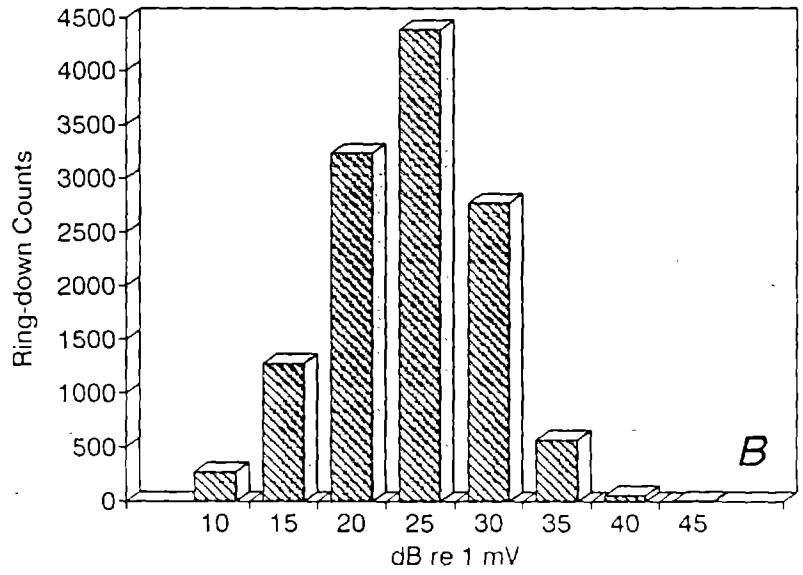

Figure 33.--Stable slope amplitude distributions of dried slope test DYN 13.1 (A) versus moist slope test DYN 15.1 (B).

into quarters, to the side of the tire and the edge of the slope (fig. 34). This pattern of waveguide placement provided up to four different positions to be chosen for each test. Only three accelerometers were available, so not all positions could be monitored in each test.

The method used to describe the position of a waveguide was to first list the distance from the edge of the slope, followed by the distance to the side of the tire. A waveguide 6 in from the slope and 6 in to the side of the tire was described as a 6 X 6 placement. A waveguide 12 in from the slope and 6 in to the side of the tire was described as a 12 X 6 placement, and so on. The waveguide positions are shown in the second and third columns of table 5.

Figure 35 is an example of how the AE signal strength changes with the waveguide location in test DYN 28. The waveguide for channel 2 was positioned 12 X 6 while channel 3 was located at 6 x 6. The peak amplitude for each channel occurs near the time when the tire was closest to the waveguide. These times are indicated in figure 35. When the tire was closest to the waveguide was often when the signal strength reached a maximum. The relationship between the time that the tire was even with the waveguide to the time that the average amplitude peaked is shown in figure 36. The data points tend to lie along the diagonal of the axis, indicating the time of maximum amplitude was close to the time that the tire was even with the waveguide. The same trend holds true for ring-down count rates and energy rates. This indicates that much of the signal received by the transducer was generated by the tire.

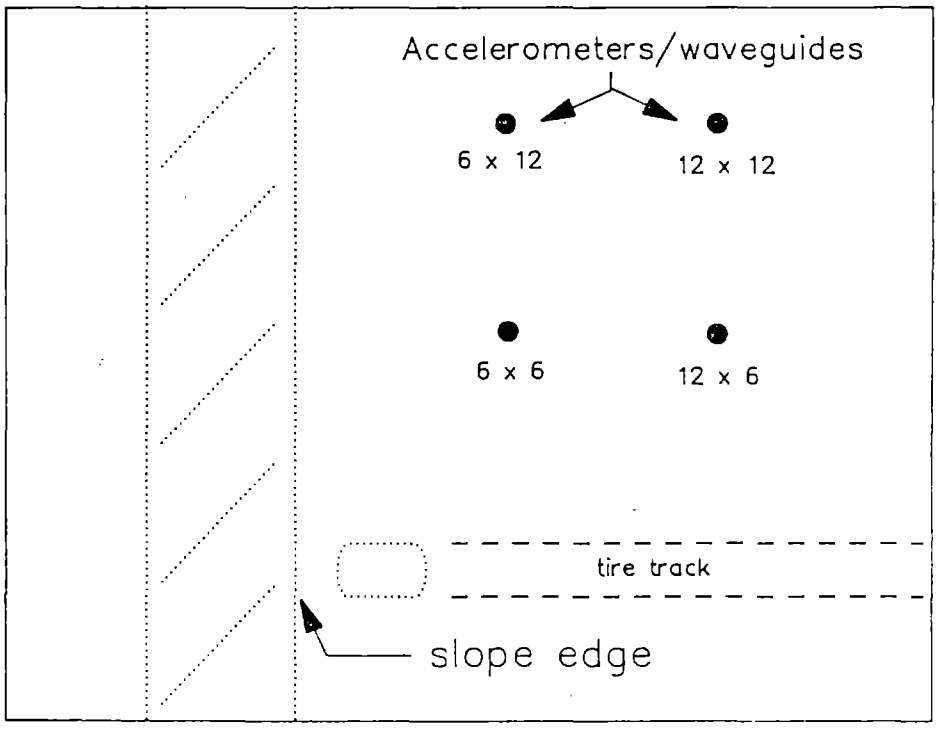

Figure 34.--Schematic diagram of dynamic load test layout.

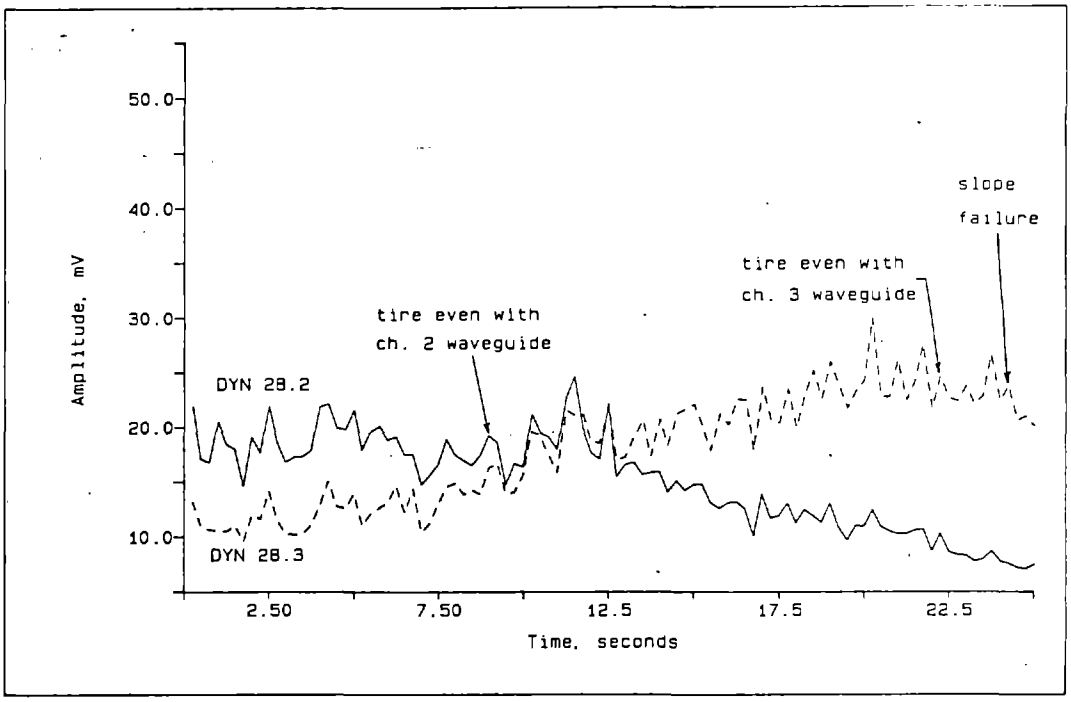

Figure 35.--Effect of waveguide location on amplitude, test DYN 28.

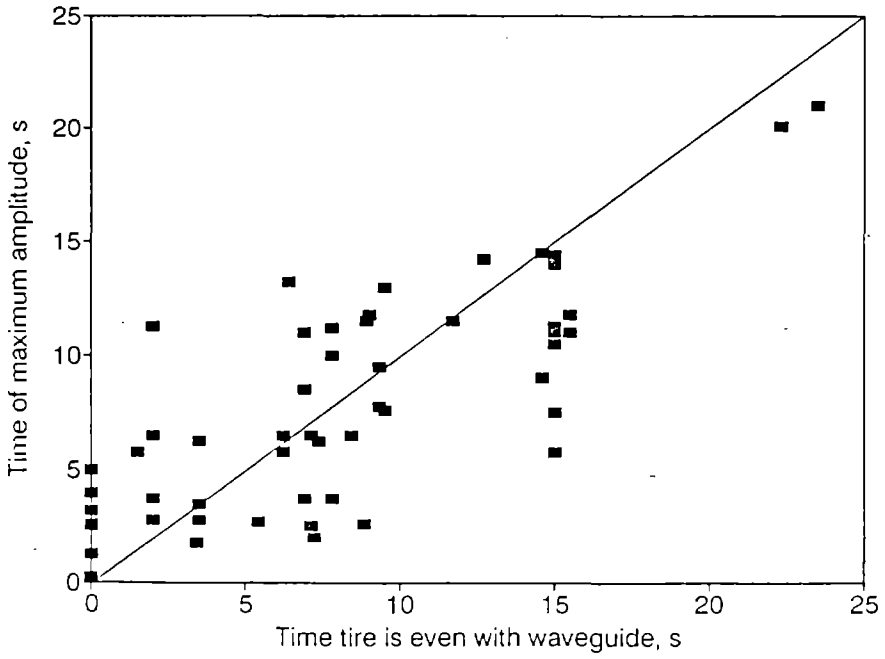

Figure 36.--Relationship of peak amplitude time to time tire was even with waveguide for dynamic load tests.

Because the peak AE signal strength is dependent on the waveguide location, the relationship between the peak signal strength and the time of slope failure will be affected by the waveguide location. From table 5 and figure 37, it can seen that the amplitude usually peaked before slope failure occurred (most points lie below the axis diagonal, added for visual reference). This does not necessarily indicate the AE signal strength was acting as a precursor to the slope failure. The same relationship is shown in figure 38 between the failure time and the time that the tire was even with the waveguide. Thus, the time of peak signal strength appears largely dependent on the waveguide location.

A waveguide positioned 6 in from the slope edge and 6 in to the side of the tire (6 X 6) was used in every test and was considered the baseline position for comparing the other positions. The 6 X 6 waveguide generally produced the highest output, but the difference was not that great when compared to a 12 X 6 waveguide. The 6 X 12 position generally produced an output significantly lower than the 6 X 6 or 12 X 6 waveguide. A 12 X 12 waveguide generally produced an output that was quite weak, and was thus not used very often. The 6 X 6 waveguide was not the best position for monitoring the stability of the slope. This is because the time that the tire was closest to the waveguide coincided with the time that slope failure was beginning. Thus it is difficult to determine whether the peaking signals are due to the instability of the slope or the location of the load tire.

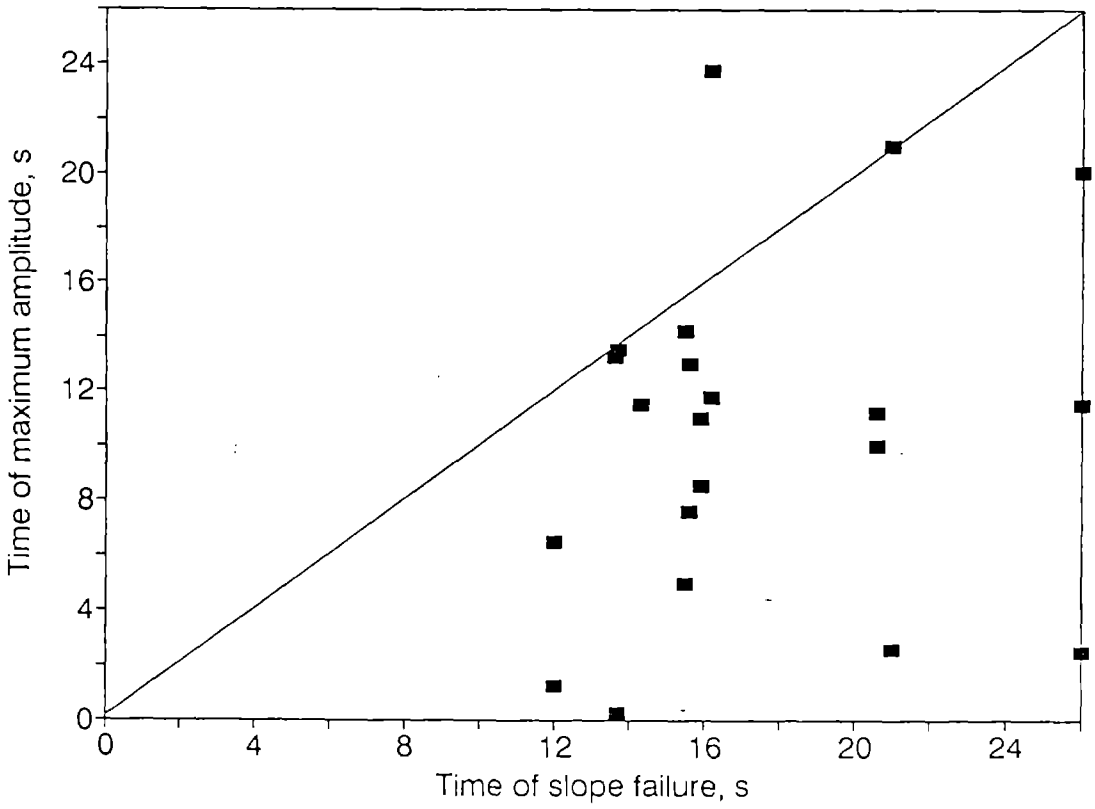

Figure 37.--Relationship of peak amplitude time to slope failure time for dynamic load tests.

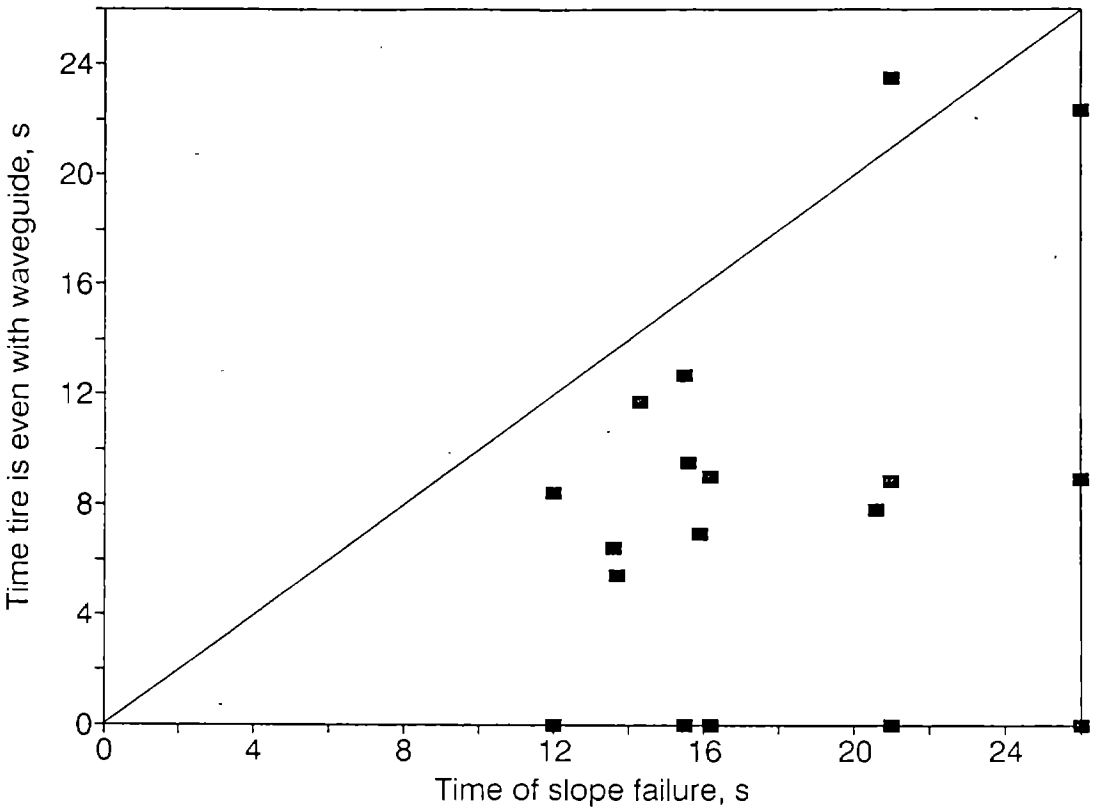

Figure 38.--Relationship of time tire was even with waveguide to slope failure time for dynamic load tests.

A waveguide positioned at 12 X 6 is thought to provide a better location from which to monitor the slope stability. This waveguide position does not have the tire coinciding with the location of the waveguide at the time of slope failure, as is the case for the 6 X 6 and 6 X 12 positions. For this reason the 12 X 6 position was used more often than the 6 X 12 position. The AE signal strength generally peaks early in the test with the 12 X 6 waveguide position. The signal strengths then tended to decrease as the tire moved away from the waveguide, towards the slope edge (fig. 39, test DYN 16, table 5). Any significant increase in signal strength occurring after the tire had passed the waveguide position may indicate slope instabilities.

Load Rate/Magnitude

The effect of load magnitude and rate of loading was not studied very extensively for the dynamic load tests. This is because the range of loadings that the soil will support was rather limited. As a result, the effect of load on the AE signal strength is not as clearly demonstrated with the dynamic load data as it was for the stationary loads. Tests DYN 17-24 were run specifically to determine the effect

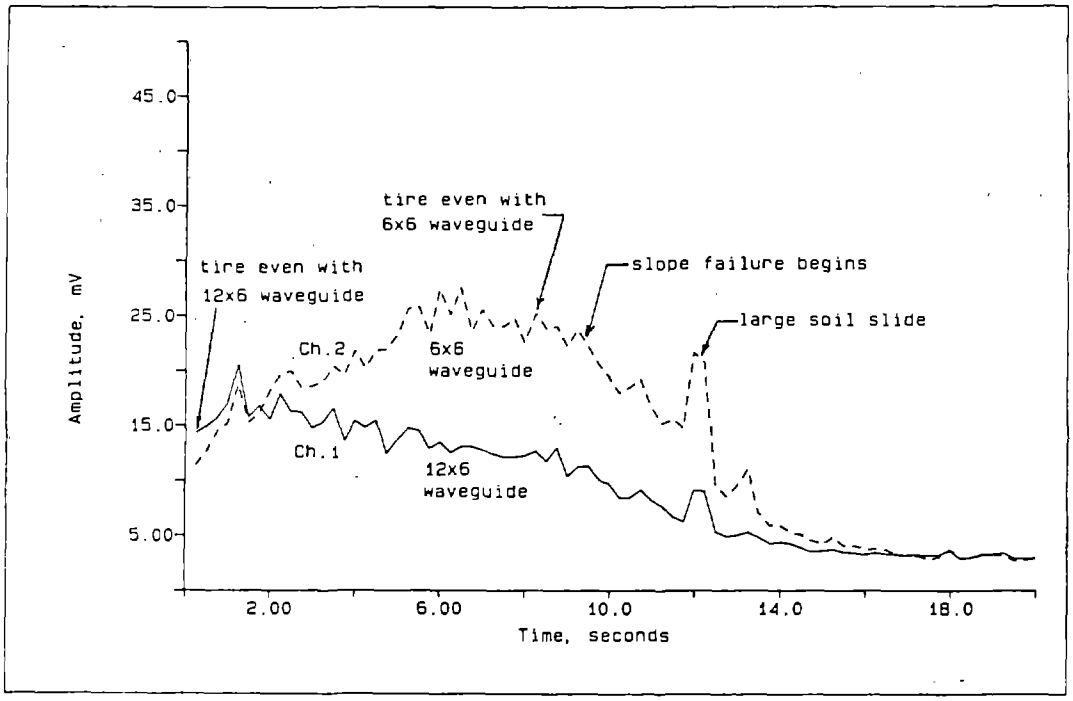

Figure 39.--Effect of waveguide location on amplitude peak for test DYN 16.

of vertical load pressure on the AE signal strength (table 5). In most cases the AE signal strength increased as the load pressure increased. In tests DYN 17-19, the flow rate was kept constant at a micrometer setting of 5.9 while the load pressure was increased by 2 psig each test. The soil was moist (5.8-pct water) and had a very low compressive strength. An increase in pressure from 8 to 10 psig resulted in slight decreases in the amplitudes and energies but a slight increase in the count rate. A further increase to 12 psig resulted in an increase in all three indices. The average frequency of the 100 largest power spectrums increased slightly throughout this series of tests.

In tests DYN 20 and 21 the flow was kept at a micrometer setting of 4.0 while the load pressure was increased from 7 psig to 11 psig (table 5). The soil was drier (2.5-pct water) and had a higher compressive strength (1.7 t/ft^2) in this series of tests. All AE signal strength indices increased as the vertical cylinder pressure increased. The average frequency of the 100 largest power spectrums also increased slightly as the pressure increased. Tests DYN 22-24 were conducted on a slope with the same soil moisture and compressive strength as tests DYN 20 and 21 (table 5). The flow valve was set at 5.9 while the cylinder pressure was increased by 2 psig for each test, from 6 psig to 10 psig. The first increase in pressure, from 6 psig to 8 psig, resulted in small increases in the AE signal strengths and decreases in the average frequency. An additional increase in the pressure to

10 psig resulted in slight decreases in the AE signal levels and increases in the average frequency.

Throughout all these tests there appeared to be a slight increase in the AE signal level as the load pressure increased. This trend was not strong, as expected from the small range of load pressures used. This agrees with similar tests conducted for stationary loads. The frequency also tended to increase with the load pressure for the dynamic load tests, though this was not a strong tendency. No clear pattern in frequency changes was found for the stationary load tests. Some other instances of the AE signal strength increasing with load pressure or flow rate can be found in the data of table 5.

The data were analyzed to compare changes in the load cell output to changes in the AE signal strength. In general, the AE signal strength trended with the load cell output, as shown in the example of test DYN 32, figure 40. This shows that the AE signal strength (as represented by the average amplitude) correlates closely to the load placed on the soil. This is a typical example, except for the stable slope loadings, where signal strength did not correlate as well to load.

No attempt was be made to compare the effect of load magnitude or load rate for tests where the load pressure was increased manually during the test. These tests are marked with an "M" in the load rate or flow column of table 5. The number after the "M" indicates the final load pressure at the conclusion of the test, expressed in psig. The manual adjustment of the pressure was not controlled and therefore can not be counted on to give consistent results between tests.

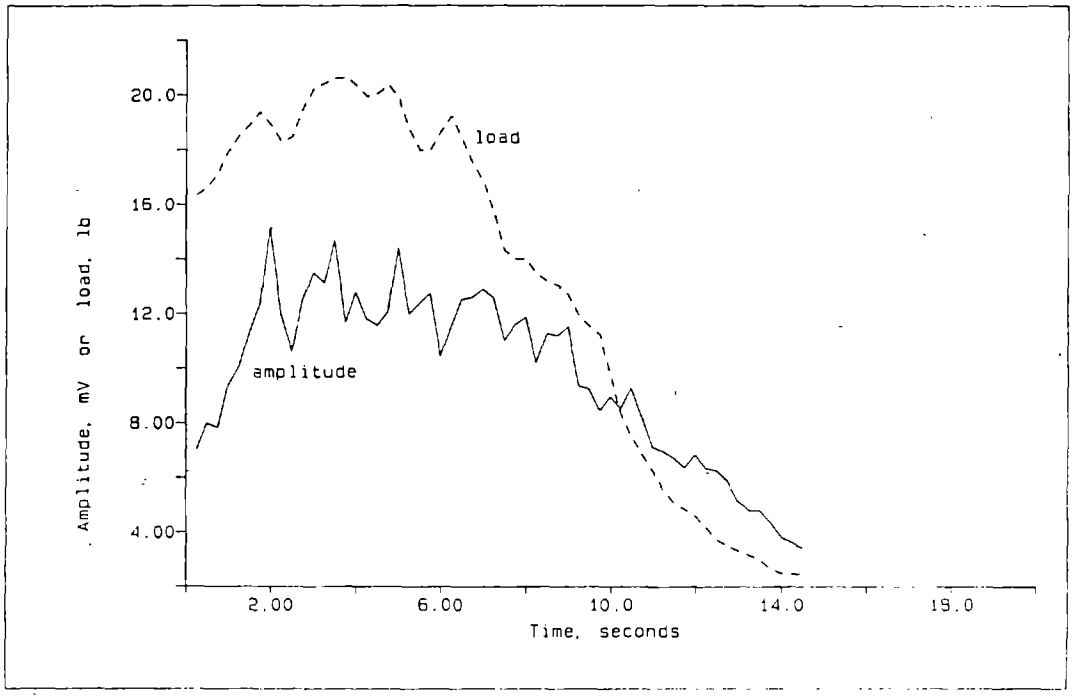

Figure 40.--Dependence of amplitude on load cell output, test DYN 32.

Frequency Spectra

Average amplitude plots for the dynamic load tests were compared to the plots of the average frequency of the 100 largest power spectrums. In general, the frequency followed the same trend as the amplitude. Figure 41 shows these two plots for test DYN 25.2. Not all tests produced as close a correlation between the amplitude and frequency, but the plots from most tests do follow similar trends. This correlation can be seen in figure 42, where the time of maximum average amplitude was plotted against the time of the maximum average frequency of the 100 strongest power spectrums. Notice that the points on the plot tend to lie near the diagonal of the axis, which was added for visual reference.

Figure 41 also illustrates that the frequency, like the average amplitudes, counts and energies, tends to peak near the time that the tire was even with the waveguide. This is expected because of the correlation between the frequency and AE signal strength and because the frequency attenuation changes with distance. Also shown in figure 41, and typical of most tests, is the drop in frequency at the time of slope failure. This corresponds to a similar drop in the AE signal strength. The release of stress when the slope began to fail appeared to cause a decrease in the AE signal strength and the frequency.

There is a slight change in average frequency as the severity of the slope failure changes. Table 6 is a condensed and sorted version of table 5. The stable slope tests and any tests with waveguides that were

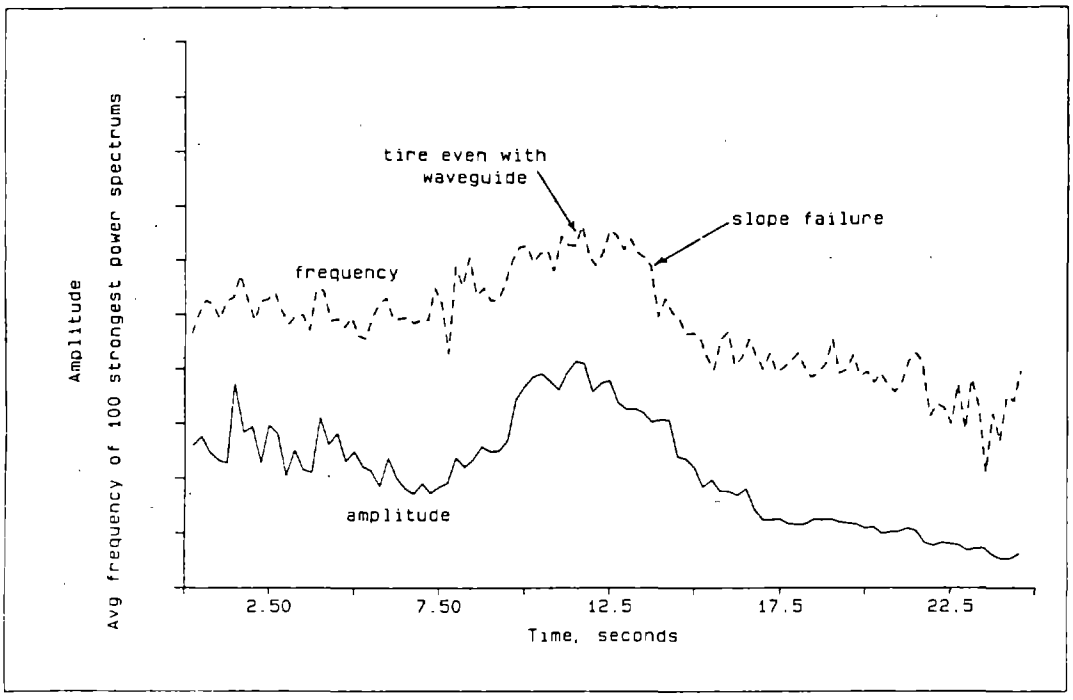

Figure 41.--Comparison of amplitude and frequency trends for test DYN 25.2.

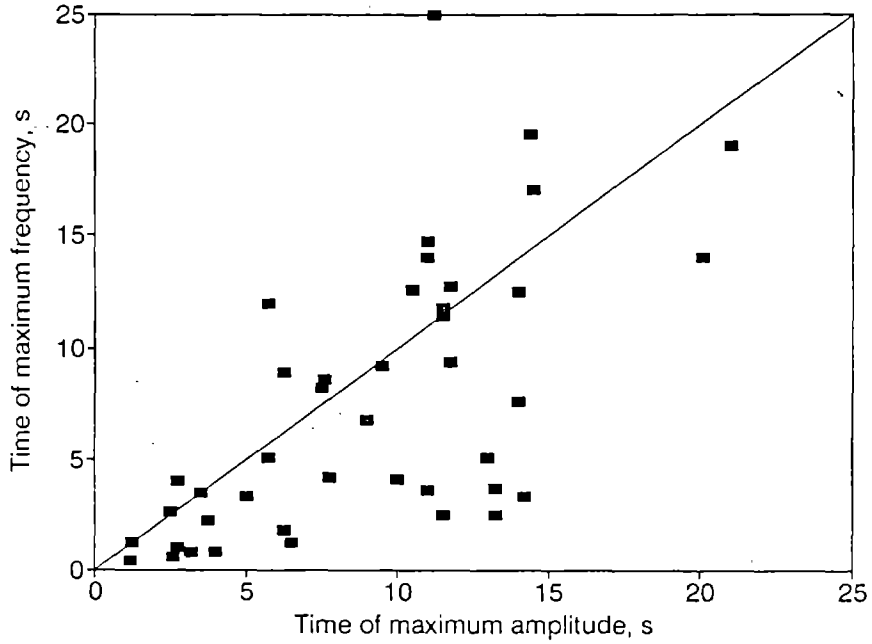

Figure 42.--Relationship of peak frequency time to peak amplitude time for dynamic load tests.

not positioned 6 X 6, 6 X 12, or 12 X 6 have been deleted. The tests were sorted by waveguide position and relative size or severity of the slope failure (columns 2-4, table 6). This table shows that the average frequency increased slightly as the size of the slope failure increased. For a 6 X 6 waveguide the average frequency changes from 678 Hz for no slope failure, to 806 Hz for a small failure, to 846 Hz for a medium failure, and 871 Hz for a large slope failure. This same trend holds somewhat for the 12 X 6 waveguide position, except that the frequency was higher for no slope failure than for a small failure.

The average frequency detected by the 12 X 6 waveguide was generally higher than at the 6 X 6 waveguide position (table 6). The average frequency when no slope failure occurred was 678 Hz for the 6 X 6 position and 880 Hz at the 12 X 6 position. For slope failures of all sizes, the frequency averaged 839 Hz at 6 X 6 and 893 Hz at 12 X 6. This general trend can also be seen from figure 43. This figure compares the average frequency at the 6 X 6 position to the average frequency at the 12 X 6 position for the same test. Most of the points lie above the axis diagonal, indicating that the 12 x 6 frequencies were higher than the 6 X 6 frequencies. The 6 X 12 waveguide position had the lowest average frequency of the three positions shown in table 6. The longer distance from the load to the waveguide in this position appears to have attenuated some of the higher frequencies.

Table 6 also lists average AE signal strengths. The average amplitude of the 6 X 6 waveguide position was stronger than the average

Table 6.--Selected dynamic load test data sorted by size of failure and amplitude

Test Number	Distance to waveguide, in slope	tire	Slope failure size	Avg Amplitude mV	Count [1]rate c/s	Energy [2]rate V^2/s	Avg [3]freq Hz
35.1	6	6	none	9.4	37.2	2.36	749
43.1	6	6	none	12.9	62	3.2	632
33.1	6	6	none	14	92	4.88	630
42.1	6	6	none	14.4	67.6	3.64	558
30.1	6	6	none	20.5	264	8.36	822
avg				14.2	104	4.4	678
44.1	6	6	small	7.7	14.8	1.44	579
47.3	6	6	small	8.4	10.4	1.56	777
40.1	6	6	small	8.5	19.2	1.32	830
46.3	6	6	small	9.7	27.6	1.96	783
36.1	6	6	small	11	42	2.44	674
39.1	6	6	small	11	52	2.56	855
4.1	6	6	small	12.3	53.2	2.64	739
48.3	6	6	small	13.3	88.8	3	793
27.1	6	6	small	16	149	4.8	961
25.3	6	6	small	18	216	6.52	913
28.1	6	6	small	19.7	252	7.32	929
31.1	6	6	small	20.3	292	7.52	839
22.1	6	6	med	7.5	7.6	1.04	913
22.2	6	6	med	8	23.2	1.32	1029
41.1	6	6	med	8.5	8	1.24	588
32.1	6	6	med	22.9	352	9.76	852
20.1	6	6	large	7.4	14.8	1.12	1046
45.1	6	6	large	8.7	6	1.08	639
21.2	6	6	large	10.6	78	2.64	969
37.1	6	6	large	10.7	40.4	2.28	703
26.1	6	6	large	11	80	2.64	888
23.2	6	6	large	12.3	168	4.12	1094
21.1	6	6	large	12.6	124	3.72	1092
2.3	6	6	large	13.4	92	4.48	865
18.1	6	6	large	13.8	163	4.68	1110
2.1	6	6	large	15.4	96	6.92	677
3.1	6	6	large	16.7	114	8.68	724
34.1	6	6	large	17	144	6.68	639
avg				12.6	97	3.6	839
39.4	6	12	small	7	4.4	0.92	566
40.4	6	12	small	7.1	0.8	0.84	622
5.1	6	12	small	8.4	6.4	1.2	670
41.4	6	12	med	7.1	1.6	0.84	740
3.3	6	12	large	11.9	181	3.12	651
avg				8.3	38.8	1.6	650

See footnotes at end of table.

Table 6.-Dynamic load test data sorted by size of failure and amplitude-Continued

Test Number	Distance to waveguide, in slope	tire	Slope failure size	Avg Amplitude mV	Count [1]rate c/s	Energy [2]rate V^2/s	Avg [3]freq Hz
35.2	12	6	none	7.9	27.2	1.6	865
33.2	12	6	none	10	44	2.56	879
43.3	12	6	none	11.2	32.8	2.4	740
42.3	12	6	none	14.4	82	3.76	878
30.2	12	6	none	15.4	140	4.84	1037
avg				11.8	65.2	3.2	880
44.3	12	6	small	6.7	5.2	1.16	774
40.3	12	6	small	7.4	1.6	1.08	718
46.1	12	6	small	8.8	14	1.52	706
48.1	12	6	small	9	31.6	1.84	745
36.2	12	6	small	10	46.8	2.2	814
47.1	12	6	small	10.5	31.2	2.12	655
39.3	12	6	small	12	14.8	2.24	741
4.3	12	6	small	13.6	60.4	3.28	634
31.2	12	6	small	14.9	136	4.2	1062
25.2	12	6	small	15	160	5	1156
41.3	12	6	med	8	10	1.04	836
32.2	12	6	med	16.6	196	5.64	1078
20.2	12	6	large	5.3	6	0.6	1204
45.3	12	6	large	8.1	5.6	0.8	704
23.1	12	6	large	8.2	45.6	1.8	1111
18.2	12	6	large	8.5	45.6	1.68	1084
26.2	12	6	large	8.9	36	1.72	1234
37.2	12	6	large	9.6	41.6	2.12	824
34.2	12	6	large	13.5	96	4.08	890
avg				10.2	51.6	2.4	893

[1]Average ring-down count rate (40 mV threshold).
[2]Average energy rate.
[3]Average frequency of 100 strongest power spectrums.

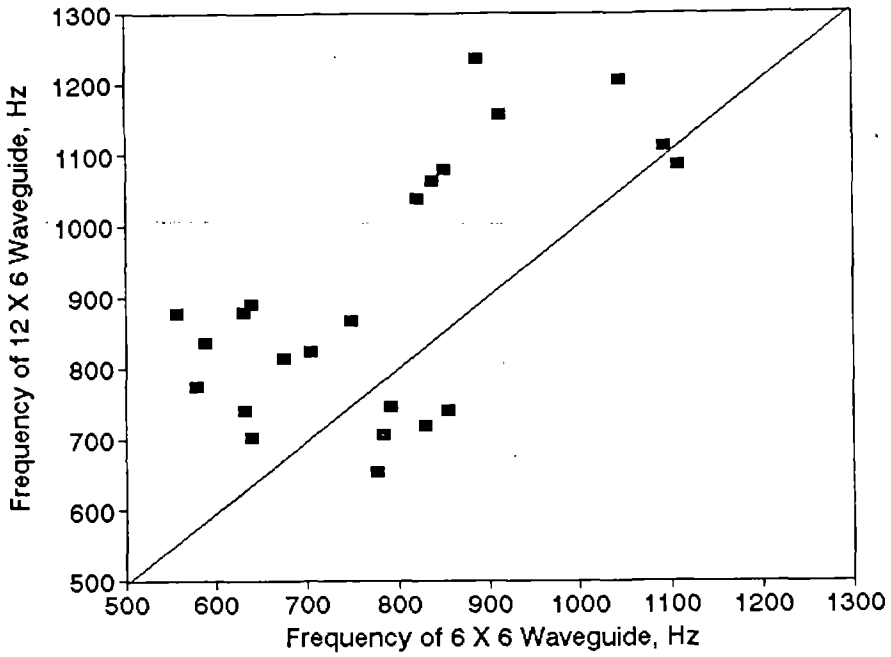

Figure 43.--Effect of waveguide location on average frequency for dynamic load tests.

amplitude of the 12 X 6 waveguide position. But the same trend in average amplitudes with increasing size of slope failure is not the same as it is with frequency, i.e., the amplitude did not increase as the size of the slope failure increased. The relationship between average frequency and average amplitude over the entire test appears to be random, as shown by the wide scatter of points in figure 44. Thus, this relationship is not helpful in determining the stability of the slope.

Effect of Toe Removal

Two series of dynamic load tests were run in which the toe of the slope was removed. One series was conducted with the load pressure increased manually (tests DYN 35-37, table 5) and another with the pressure kept constant throughout the test (tests DYN 32-34). In test DYN 35 the toe was not removed, test DYN 36 was loaded out 22 pct and test DYN 37, 33 pct. The 11-pct toe removal out was not used (the slope was still quite stable) to insure that a slope failure occurred in that series of tests without reconstructing the slope. The AE signal strengths decreased as the toe was removed from 0 to 22 pct. In both these tests small slope failures occurred as the tire plowed up to the edge of the slope. In test DYN 37 a larger sized failure occurred and the signal strengths were mixed, with some decreasing, some increasing and others staying the same. No consistent trend occurred with the frequencies in these tests.

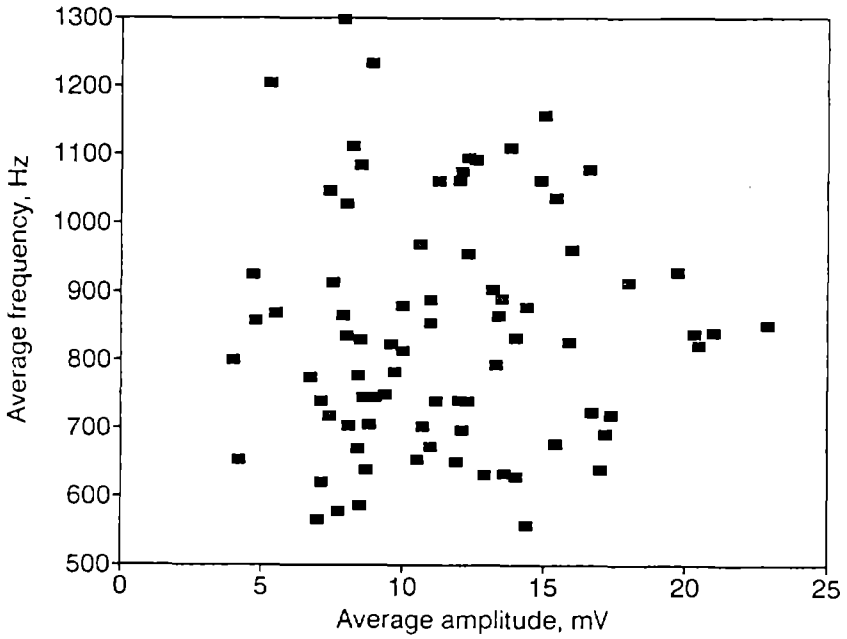

Figure 44.--Relationship of average frequency to average amplitude for dynamic load tests.

In the next series of tests (DYN 32-34, table 5), the toe was removed from 0 to 11 to 22 pct. The change in signal strength in this series of tests was mixed. In removing the toe from 0 to 11 pct, the signal strengths decreased for the 6 X 6 waveguide, but increased for the 12 X 6 waveguide. In removing the toe from 11 to 22 pct these trends were reversed. Again there was no consistent change in the frequency. No useful information could be gained from these tests and no further testing involving the removal of the toe was conducted.

FIELD TESTING

The background noise levels obtained with the AE field monitoring equipment were 7-8 mV with the accelerometer unprotected from the wind, and about 5 mV after being covered. The amplitude of the signals decreased as the waveguide to truck distance increased. With the truck just 5 ft from the waveguide, a 25-mV signal was obtained with the waveguide pounded into the top of the slope. At a distance of 36 ft the signal dropped to 8-9 mV. The signal strengths were greatest while the truck was dumping its load. While the truck was backing up, the signal amplitudes averaged 70 pct of the signal strength of the truck dumping, but ranged from 40 to 100 pct. The largest readings while backing were obtained when the truck hit the berm hard or the driver spun the wheels trying to back against the berm.

A waveguide placed in the outside of the berm resulted in slightlylower readings than a waveguide in the top of the slope. This may be due to the lower consolidation of the berm material, the indirect path between the waveguide and the truck or the lower level of airborne noise from the truck. It was not known what percentage of the signals received were being transmitted through the ground or were airborne noise from the truck. The complete waveguide and accelerometer were buried 3 or 4 in under the surface to try to answer this question. Before any readings were taken the oscilloscope batteries went dead and the no further testing could be completed to obtain the necessary data. Not knowing how much of the signal was from the truck noise makes it difficult to make any significant conclusions.

The stockpile these readings were taken on seemed to be very stable. It's doubtful that any significant soil movement was taking place to generate AE. The trucks were able to back very close to the edge of the slope. One side of the stockpile had a vertical face where the toe had been removed. This occurred with a crushed and washed limestone, which theoretically has no cohesion. Most of the signals being detected were probably from the truck, either engine noise transmitted through the air or the noise of the tires contacting the surface.

DISCUSSION OF RESULTS

The goal of this research was to determine whether AE monitoring could be used as a simple and practical method of determining the stability of mine stockpiles and waste dumps. Acoustic emission monitoring was not found to be a practical method of determining dump point stability given the simple methods and equipment employed in these tests.

Research done by others had shown that unstable slopes emit more AE than similar stable slopes (*8,9,12,13,14,30*). This research was performed to attempt to prove the hypothesis that, using inexpensive and easily deployed instruments and simple, straightforward analytical procedures, the AE generated by an unstable soil could be differentiated from and detected over the noises resulting from the trucks and mining environment. This was expected to be a difficult task given the dynamic and noisy environment encountered in active mines. This hypothesis was not proven, and thus, the project research in this area was terminated. Though beyond the scope of this research, more elaborate instrumentation systems and more complex analytical methods may enable slope failures to be predicted with AE.

The results reported here were generally inconclusive and inconsistent, and therefore few significant conclusions could be drawn from them. None of the findings were exclusive, that is, there were always conflicting results. A more controlled and detailed test sequence may clear up many of these inconsistencies. The goal in these tests was not to gain basic knowledge of AE generation and propagation in slopes, but to develop a simple and practical method of monitoring dump point stability. The approach taken here was simple, which was thought to be necessary for the successful utilization of this method by mine personnel in the field. However, there appear to be too many

variables involved in this type of soil monitoring to allow the simple techniques to work.

One of the most significant findings from the dynamic load testing was the strong effect that the waveguide position had on the AE signal level. The average amplitude generally peaked before or at the time of slope failure, but this was also the time that the load tire was closest to the waveguide. Average frequency also tended to peak at the same time, because frequency generally trended with the AE signal strength. This indicates that the signal strength and frequency were very dependent on the distance from the source, i.e. signal attenuation was a major factor.

A high proportion of the signals detected by the transducers appeared to be noise created by the tire contacting the soil surface. This was true for both stationary and dynamic loadings, but more so with the moving load. Stationary load test data indicated that most of the signals were being generated at the surface underneath the load tire. A vertical waveguide intersecting the surface produced stronger signals than a buried horizontal waveguide. Dynamic loads on a low compressive strength, stable slope had signal levels higher than a comparable load on an unstable slope. When the tire rolled across the soil, the soil was continually undergoing a localized failure directly below the tire. Thus the accelerometers were detecting a constant state of failure, even on a stable slope. The emissions from the tire and the soil instabilities are similar in signal content, but possibly of different magnitudes. This made it difficult to separate them to remove the effects of the tire. Another indication that the tire was creating a lot of noise was the stronger signal strengths compared to other published signal amplitudes. A highest count rate sighted in the literature was 7700 c/min (*12*), compared to the 43,440 c/min rate recorded in this study.

On a low compressive strength soil, the tire generated noises tended to be stronger, because the soil moved more as the tire rolled along. This appears to be why the low compressive strength soils generally produced stronger AE signal strengths. Because soil moisture and compressive strength tended to relate inversely, this also explains the slight tendency for low moisture soils to produce higher emissions.

Creating a more unstable slope by removing the toe did not result in any significant or consistent change in the AE signal strengths or frequencies. This also indicates that the emissions generated within the soil were being lost to the tire noises. The inability to separate the noise created by the load tire from the AE generated by an unstable slope was really the root of the problem. Finding a simple and practical method to do that would have went a long way towards making AE monitoring of mine dump points a feasible task.

One of the more consistent findings of this study was simply a confirmation of previous findings of others. For both stationary and dynamic load tests, the AE signal strength was found to increase as the load on the soil increased. Previous research had shown that the AE activity rates increased as the stress on the soil or rock increased. Acoustic emission signal strength was generally higher for a stationary load in an unstable location compared to a stable location. This was also expected from the previous work. This information was thought to

be important when advancing to the dynamic load tests. But the tire noises tended to obscure the AE produced by the slope during the dynamic load tests. Thus, the findings from the stationary load tests were of little value in the analysis of the dynamic load tests.

It was found to be very difficult to model a truck causing a slope failure on a dump point. The load system could not keep up with the failing soil block as the slope began to fail. Scaling appears to be a problem in these dump point model tests. A larger scale experiment would allow a smaller load to be placed on the soil, thus reducing the noise created by the load tire. A larger scale failure may produce more or stronger emissions prior to and during failure. Soil moisture and compaction were difficult to control. Often the slope had to be rebuilt between tests, which meant two slopes which may not be alike. This was especially true for the compaction or strength of the slope. The problems associated with accurately modeling a mine dump point were responsible for many of the difficulties encountered in this project.

Most AE studies dealing with slope stability have focused on static slopes with no load or a static load monitored over a long period of time (several days to years). In this study, the slope failures occurred quite quickly. The data of interest was compressed into a very short time period, thus, accepted AE data analysis procedures were of limited usefulness. Over such a small time period it was difficult to discern any consistent data patterns that could be used to characterize the emissions being generated.

Data recording equipment that would allow data acquisition over a longer period of time would enhance the capabilities of a study in this area. A longer record time would allow an analysis of the AE associated with the removal of the toe from a slope. Such information may be significant, because this practice accounts for many of the dump point accidents in the mining industry. Other research has shown this practice weakens the slope and increases the AE count rates (*12,13,30*). This could not be shown in this study because of the limited record lengths of the waveform recorder. Some AE monitoring systems are now available which have an automatic, floating threshold level, which would be useful for eliminating the effect of the tire generated noises (*27*). Expanding the range of frequencies to look at and using accelerometers of greater sensitivity may increase the success of future research efforts. The use of velocity gauge transducers may reduce the effect of the tire noise.

Vertical waveguides were used throughout most of the testing. Vertical waveguides gave stronger signals than horizontal waveguides and were a more convenient placement, especially for field monitoring. But, the analysis showed that vertical waveguides may be picking up too much noise from the tire contacting the soil surface. A buried waveguide may insulate the waveguide enough from the surface generated noises to increase the signal to noise ratio and provide meaningful data. But whether this is a practical method in the field is questionable. A waveguide shielded from the upper soil layers while still exposed at depth may provide the same benefits while still being practical.

Most mine dump points are stable when there is no external load, such as a haulage truck or front end loader. Monitoring the slope between dump cycles when equipment is not on the slope does not seem to

be an alternative. The slope must be monitored in the presence of the equipment, and this means dealing with the noise associated with that equipment. The harsh environment of a mine dump point was difficult to model in the lab. Even the relative quiet of the lab model was too noisy for the methods used in this study. The increased noise levels of an active dump point in the field provides a larger challenge to AE monitoring. For this reason, the field work done in this study was limited. If the method could not be used successfully in the lab, there was little use in attempting an elaborate field study.

The limited field testing completed indicated that AE are being detected in the vicinity of a backing or dumping truck. Signal attenuation is a major factor in field tests. It's not clear what percentage of the signals detected were transmitted through the ground or through the air. Most of these emissions were probably being generated by the truck and not soil instabilities. Problems with the equipment halted further testing to determine if the signals were coming from the truck. With incomplete data, no significant conclusions could be made. The high attenuation through soil may limit the use of AE monitoring on full scale dump points in the field.

SUMMARY

Acoustic emission (AE) monitoring was studied as a possible method for monitoring the stability of dump points on mine stock piles and waste dumps. A small scale test facility was built to simulate the dynamic surcharge loading represented by a haulage truck approaching the crest of a dump point. Tests were conducted with a sand and gravel mixture in a 2-ft by 3-ft by 2-ft plywood box. Loads were applied to the soil by a rubber caster mounted on a vertical shaft. Horizontal and vertical motions of the tire were provided by an air-over-oil hydraulic system. Accelerometers mounted on steel waveguides were pushed into the soil to detect the AE released by the soil. Accelerometer and load cell data were recorded and saved with a digital waveform recorder. Data was analyzed with a commercial data analysis program on a personal computer. Both stationary and dynamic loads were applied to the soil surface. Stationary but increasing loads were applied near the edge of the slope (unstable condition) and away from the edge (stable condition). Dynamic, moving loads, simulated a truck backing towards the edge of a dump point.

Stationary load tests were conducted to determine the difference in AE signals between a stable and unstable slope loading. This information was to have been used to help distinguish the difference between a stable and unstable slope for the dynamic loadings.

The results of the stationary load tests were generally inconsistent and not conclusive. There was a slight tendency for the signal strengths of an unstable slope to be stronger than a corresponding stable slope. Frequency tended to shift lower as the load moved toward the edge of the slope. Increasing the load on the soil generally resulted in increased AE signal strengths.

Dynamic load tests results were also generally inconclusive. The dynamic load tests results were largely dependent on the position of the

waveguide in relation to the load tire. The AE signal strength was dependent on the position of the waveguide. A waveguide near the slope edge produced peak signals at the same time that the slope was failing, but a waveguide further from the slope peaked before failure. Soil compressive strength appeared to have a larger influence on the data than soil moisture. Signal strength was dependent on the vertical load, which was difficult to maintain constant with the test apparatus. Frequency showed a fairly strong correlation to signal strength of individual tests.

In this study, given the techniques and research methods utilized, AE monitoring was not shown to be a feasible approach for mine dump point failure prediction. The method may be workable utilizing more sophisticated data recording and analysis techniques.

REFERENCES

1. Rybicki, S. Structure and Physicomechanical Properties of Dump Soils. Paper in Proc. 5th Int. IAEG Congress (Buenos Aires, Argentina, 1986). IAEG, 1986, pp. 1019-1027.

2. May, J. P. Analysis of Dump-Point Accidents Involving Mobile Mining Equipment. BuMines IC 9250, 1990, 19 pp.

3. Obert, L., and W. Duvall. Use of Subaudible Noises for the Prediction of Rock Bursts, Part II. BuMines RI 3654, 1942, 22 pp.

4. Lord, A.E. Jr. Acoustic Emission Ch. in Physical Acoustics, ed. by R.N. Thurston and W.P. Mason. Academic Press, v. II, Ch. 6, 1975, pp.289-353.

5. Stateham, R.M. and R.H. Merrill. Acoustic Emission Techniques Applied to Slope Stability Problems. Ch. in Rockslides and Avalanches, 2, ed. by B. Voight. Elsevier Scientific, 1979, pp. 577-593.

6. Rowell, G.A. and L.P. Yoder. The Effect of Geophone Emplacement on the Observed Frequency Content of Microseismic Signals. Paper in Proceedings Third Conference on Acoustic Emission/Microseismic Activity in Geologic Structures and Materials, ed. by H.R. Hardy and F.W. Leighton (Penn. St. Univ., Oct. 5-7, 1981). Trans Tech Publ., 1984, pp. 707-727.

7. Beard, F. D., Predicting Slides in Cut Slopes. Western Construction, v. 36, 1961, p 72.

8. Cadman, J. D., and R. E. Goodman. Landslide Noise. Science, v. 15, December 1, 1967, pp. 1182-1184.

9. Koerner, R. M., and A. E. Lord, Jr. Use of Acoustic Emissions to Predict Ground Stability. U.S. Dept. of Transportation, Report No. FHWA/RD-82/052, Dec., 1982, 155 pp.

10. Hardy, H. R., Jr. Applications of Acoustic Emission Techniques to Rock and Rock Structures: A State-of-the-Art Review. Paper in Acoustic Emissions in Geotechnical Engineering Practice, ed. by V. P. Drnevich and R. E. Gray. STP 750, ASTM, 1981, pp. 4-92.

11. Pollock, A.A. Metals and Rock: AE Physics and Technology in Common and in Contrast. Paper in Proceedings First Conference on Acoustic Emission/Microseismic Activity in Geologic Structures and Materials, ed. by H.R. Hardy, Jr. and F.W. Leighton (Penn. St. Univ., June 1975). Trans Tech Publ., 1977, pp.383-401.

12. Koerner, R. M., A. E. Lord, Jr., and W. M. McCabe. Acoustic Emission Monitoring of Soil Stability. Journal of the Geotechnical Engineering Division, ASCE, v. 104, No. GT5, Proc. Paper 13753, May, 1978, pp. 571-582.

13. Koerner, R. M., W. M. McCabe, and A. E. Lord, Jr. Acoustic Emission Behavior and Monitoring of Soils. Paper in Acoustic Emissions in Geotechnical Engineering Practice, ed. by V. P. Drnevich and R. E. Gray. ASTM STP 750, American Society for Testing and Materials, 1981. pp. 93-141.

14. Lord, A.E., and R.M. Koerner. Acoustic Emissions in Geological Materials. J. of Acoustic Emission, v. 2, No. 3, 1983, pp 195-219.

15. Koerner, R.M., A.E. Lord, Jr., W.M. McCabe, and J.J. McElroy. AE/MA Characteristics and Behavior of Mine Tailings. Paper in Proceedings Third Conference on Acoustic Emission/Microseismic Activity in Geologic Structures and Materials, ed. by H.R. Hardy and F.W. Leighton (Penn. St. Univ., Oct. 5-7, 1981). Trans Tech Publ., 1984, pp.437-447.

16. Lord, A.E., C.L. Fisk, and R.M. Koerner. Utilization of Steel Rods as AE Waveguides. Journal of the Geotechnical Engineering Division, ASCE, v. 108, No. GT2, Feb., 1982, pp. 300-305.

17. Hough, B. K. Basic Soils Engineering. The Ronald Press Company, 2nd ed., 1969, 634 pp.

18. Koerner, R. M., A. E. Lord, Jr., W. M. McCabe, and J. W. Curran. Acoustic Emission Behavior of Granular Soils. Journal of the Geotechnical Engineering Division, ASCE, v. 102, No. GT7, Proc. Paper 12239, July, 1976, pp. 761-773.

19. Koerner, R.M., A.E. Lord, Jr., and W.M. McCabe. Acoustic Emission Behavior of Cohesive Soils. Journal of the Geotechnical Engineering Division, ASCE, v. 103, No. GT8, Aug., 1977, pp. 837-850.

20. Beattie, A.G. Acoustic Emission, Principles and Instrumentation. J. of Acoustic Emission, v. 2, No. 1-2, 1983, pp. 95-128.

21. Asyst Software Technologies. Asystant Analysis Reference. Asyst Software Tech., Inc., 1988, 205 pp.

22. Randall, R.B. Frequency Analysis. Bruel & Kjaer, 1987, 344 pp.

23. Brindley, B.J., J. Holt and I.G. Palmer. Acoustic Emission - 3, The Use of Ring-Down Counting. Non-Destructive Testing, v. 6, No. 6, 1973, pp. 299-306.

24. Nakamura, Y. Detection and Analysis of Acoustic Emission Signals. Paper in Proceedings First Conference on Acoustic Emission/ Microseismic Activity in Geologic Structures and Materials, ed. by H.R. Hardy and F.W. Leighton (Penn St. Univ., June 1975). Trans Tech Publ., 1977, pp. 445-457.

25. Yamaguchi, K., H. Oyaizu, and N. Hamada. Acoustic Emission Source Location by Identification and Combination of Signals. Paper in Advances in Acoustic Emission, ed. by H.L. Dunegan and W.F. Hartman (Proc. Int. Conf. on Acoustic Emission, Anaheim, CA, Sept. 1979). Dunhart, 1981, pp. 49-64.

26. Harris, D.O. and R.L Bell. The Measurement and Significance of Energy in Acoustic-Emission Testing. Experimental Mechanics, v. 17, No. 9, 1977, pp. 347-353.

27. Leaird, J.D. Slope Stability Monitoring with Acoustic Emission. Paper in Advances in Acoustic Emission, ed. by H.L. Dunegan and W.F. Hartman (Proc. Int. Conf. on Acoustic Emission, Anaheim, CA, Sept. 1979). Dunhart, 1981, pp. 374-376.

28. Miller, R.K. and P. McIntire (ed.). Nondestructive Testing Handbook. Vol. 5 - Acoustic Emission Testing. Am. Soc. for Nondestructive Testing, 2nd ed., 1987, 603 pp.

29. Koerner, R.M., W.M. McCabe, and A.E. Lord, Jr. Overview of Acoustic Emission Monitoring of Rock Structures. Rock Mechanics 14, 27-35, Springer-Verlag, 1981, pp. 27-35.

30. Penning, A., H. van der Kogel, R.M. Koerner, and F.M. Schenkeveld. Acoustic Emissions During Slope Failure. Paper in Field Measurements in Geomechanics, ed. by K. Kovari (Proc. Int. Sym. Zurich, Switzerland, Sept. 5-8, 1983). A.A. Balkema, 1984, pp. 749-763.

31. McCabe, W.M. Acoustic Emission in Coal: A Laboratory Study. Paper in Proceedings Second Conference on Acoustic Emission/Microseismic Activity in Geologic Structures and Materials, ed. by H.R. Hardy, Jr. and F.W. Leighton (Penn. St. Univ., Nov. 13-15, 1978). Trans Tech Publ., 1980, pp. 35-53.

APPENDIX.-DATA ANALYSIS USER FUNCTIONS

Analysis of the AE data was done with Asystant software on a PC. The raw data was transferred to a floppy disk from the DSP Technology data acquisition system. DSP software converted the data into Asyst format, which was a format that Asystant would read. The data files were transferred to the PC's hard disk and then analyzed with the file processor of Asystant (*21*). User functions within the file processor converted the data to the desired form. The processed data was stored as an array in the variable memory.

To convert the data into voltage, the Asyst data had to be multiplied by 0.00245361 and then subtract 5.028 from that. The conversion figures depend on the calibration of the DSP data acquisition system. These figures show up in the first line of all the user functions. Asystant works most efficiently with Reverse Polish Notation, the syntax used for these user functions. The raw data was also offset from zero; this was corrected by subtracting the average from the data by the "DUP AVG -" commands. The "T" in the functions refers to the output variable of the file processor. For most functions T is an array, with each data set producing a new element as the data file is processed. An understanding of the operation and commands of Asystant is needed to completely understand these functions. A listing of the user functions utilized to analyze the AE data follows.

AVERAGE AMPLITUDE

```
1. 0.00245361 * -5.028 + DUP AVG -
2. ABS AVG T SWAP CAT
```

This function takes the absolute value of the voltage and then averages it.

ENERGY RATE

```
1. 0.00245361 * -5.028 + DUP AVG -
2. DUP * INTEG []MAX T SWAP CAT
```

The energy rate was calculated by squaring the voltage and then integrating it.

EVENT COUNT RATE

```
1. 0.00245361 * -5.028 + DUP AVG -
2. 0.040 >N:SEARCH 0 CAT DUP 1 N:ROT -
3. ABS 35 >N:SEARCH 0 CAT INDEX []MAX 2 -
4. T SWAP CAT
```

Events were counted similar to the ring-down counts, except only one count was taken for each series of threshold crossings. The function determines the number of data points greater than a 40-mV threshold, and

then eliminates all those that are not separated by more than 35 data points (3.5 ms). This spacing (and the voltage threshold) may have to be changed to fit the data being analyzed. This function was not used much in this study because overlapping events were occurring in many cases, making it difficult to separate and count them.

LOAD CELL OUTPUT

```
1. 0.00245361 * -5.028 +
2. AVG 62.46 * 61.85 - T SWAP CAT
```

The output from the load cell was recorded on one channel of the DSP waveform recorder, just as the accelerometer outputs were. The data was first converted into a +/-5 V signal, then averaged and converted to load in pounds. The conversion to pounds depends on the calibration of the load cell. The result was the average load per data set (0.25 s).

POWER SPECTRAL DENSITY

```
1. 0.00245361  -5.028 + DUP AVG - PWRSPEC
2. B 2 / DUP * / A B / /
3. < 2 , B 2 / > STORE Y
4. B N:RAMP 1 - B / A *
5. < 2 , B 2 / > STORE X
```

This function (lines 1-3) calculates the power spectrum and then converts it to a power spectral density, eliminating the dc voltage (21). The result was stored to variable Y. This function was used for calculating the power spectral density of individual data sets. Variable A is the sampling rate (10,000 Hz) and B is the data set size (2048 points). Lines 4 and 5 calculate the X-axis (frequency) for the power spectral density plot, storing the result in variable X.

POWER SPECTRUM AVERAGE VERSUS TIME

```
1. 0.00245361 * -5.028 + DUP AVG - PWRSPEC
2. < 42 , B 2 / 40 - > INDEX 40 +
3. < 885 , 100 > AVG 4.8828 * T SWAP CAT
```

As discussed in the text, this function produced a frequency versus time plot, where the frequency was the average of the 100 largest power spectrums in a data set. Averages of less than 100 power spectrums were also used on a limited basis, but 100 was used most often and found to produce a smoother curve. Frequencies from 0 to 200 Hz are not included in this average. The X-axis (time) is calculated doing an N:RAMP on the number of data sets processed and multiplying by the length of the data set. Running this function through the file processor takes about 12 minutes for a 15-s data file on a 286 microprocessor based PC.

RING-DOWN COUNT RATE

```
1. 0.00245361 * -5.028 + DUP AVG - 0.040
2. >N:SEARCH 0 CAT DUP DUP INDEX []MAX
3. STORE C DUP < 1 , 1 > SWAP CAT < 1 , C >
4. - DUP 1 <>N:SEARCH INDEX []MAX SWAP
5. 0 =N:SEARCH INDEX []MAX - T SWAP CAT
```

This function searches the data array for voltages greater than the 40-mV threshold. Any consecutive points are subtracted out to make sure only one count is obtained for each voltage spike. The parameter C is a variable temporarily stored in memory for later recall to complete the calculation. The result is an array, with each element being the number of ring-down counts per data set (0.25 s). Running the N:SEARCH command on our computer system uncovered a bug in the Asystant program. Before plotting the data, one must save the data and exit the program, and then return to the program, otherwise the program would lock up. The threshold of this function was varied to determine the amplitude distribution at increasing thresholds. The difference in total counts between successive threshold levels was then plotted against the threshold, expressed as dB referenced to 1 mV.